ENERGY AND EXERGY ANALYSIS OF AMMONIA-WATER DOUBLE EVAPORATOR VAPOUR ABSORPTION REFRIGERATION SYSTEM

A dissertation

Submitted in the partial fulfilment of requirement for the award of degree of

Master of Technology

In

Thermal Engineering

Submitted by:

DEEPAK PANWAR

2K17/THE/04

Under the supervision of

Dr. AKHILESH ARORA

MECHANICAL ENGINEERING DEPARTMENT

DELHI TECHNOLOGICAL UNIVERSITY

(formerly Delhi College of Engineering)

Bawana Road, Delhi- 110042

JUNE 2019

CANDIDATE'S DECLARATION

I **Deepak Panwar**, Roll no. **2k17/the/04** student of **M.TECH** with specialisation in **"Thermal Engineering"** hereby declare that the project dissertation titled **"Energy and Exergy analysis of ammonia-water double evaporator vapour vapour absorption refrigeration system (DE VARS)"** which is submitted by me to the Department of **Mechanical Engineering**, **Delhi Technological University, Delhi** in the fulfilment of the requirement of the award of the degree **of Master of Technology** is original and not copied from any source without proper citation. This work has not previously formed the basis of the award of any Degree, Diploma Associateship, Fellowship or other similar title or recognition.

Place: Delhi **DEEPAK PANWAR**

Date: **2K17/THE/04**

CERTIFICATE

I hereby certify that the project dissertation titled **"Energy and Exergy analysis of ammonia-water double evaporator vapour vapour absorption refrigeration system (DE VARS)"** which is submitted by **Deepak Panwar**, Roll No. **2k17/the/04** in the fulfilment of the requirement of the award of the degree of **Master of Technology** with specialisation in **"Thermal Engineering"** is a record of project work carried out by student under my supervision. To the best of my knowledge this work has not been submitted in part or full for any Degree, Diploma Associateship to this university or elsewhere.

Place: Delhi **DR. AKHILESH ARORA**

Date: **SUPERVISIOR**

ACKNOWLEDGEMENT

It is a matter of distinct pleasure for me to express deep sense of gratitude and indebtedness to my learned supervisor **Dr. Akhilesh Arora,** Associate professor in the department of Mechanical Engineering, Delhi Technological University, Delhi, for his invaluable expert guidance and patient review. His continuous inspiration has made me complete this major dissertation.

I am also thankful to my friends and classmates for their unconditional support and motivation during the project.

DEEPAK PANWAR

2K17/THE/04

ABSTRACT

The energy and exergy analysis of "ammonia-water double evaporator vapour absorption refrigeration system (NH_3-H_2O DE VARS)" have been done in this correspondence. The energy analysis of double-evaporator vapour absorption cycle involves the determination of coefficient of performance (COP) at various operating conditions and study the effect of the variation of both the evaporator temperature (i.e. T_{e1}& T_{e2}), generator temperature (i.e. T_{g1}& T_{g2}), absorber temperature (i.e. T_{a1}& T_{a2}), condenser temperature and other parameters on the COP. It is observed that by using double evaporator NH_3-H_2O VAR cycle instead of using simple NH_3-H_2O VAR cycle having cooling load (20 TR) at low temperature, there is an increase in 11.11% COP in comparison to when the load on both the evaporator is equal i.e. $Q_{e1} = Q_{e2} = 10$ TR and there is an increase of 22.22% in COP when the system is fully operated at high temperature evaporator i.e. $Q_{e1} = 20$ TR, $Q_{e2} = 0$. It is also observed that the optimum value of COP is obtained at the temperature of 363° K and 383° K and at the pressure of 11.5 bar & 12 bar in generator-1 & 2 respectively for equal loading of both evaporators i.e. 10 TR. The effect of variation of both the generator temperature (i.e. T_{g1}& T_{g2}), absorber temperature (i.e. T_{a1}& T_{a2}), evaporator temperature (i.e. T_{e1}& T_{e2}), condenser temperature and solution circulation ratio (SCR-1 & SCR-2) in high pressure and low pressure circuit on the exergetic efficiency (η_{ex}) are also discussed in this communication. Exergy analysis is also performed to calculate the total exergy destruction rate, thermal exergy loss rate and the destruction of exergy in each components of the system. It is observed that the maximum exergy destruction occurs in the solution heat exchanger (shx-1& shx-2) followed by absorbers (absorber-1& absorber-2), evaporators (evap-1& evap-2) and generators (gen-1& gen-2). The maximum exergetic efficiency (η_{ex}) occur at a temperature of 358° K and 378° K in generator-1 & 2 respectively. The study shows that NH_3-H_2O DE VAR systems are more promising than simple VAR systems in a wide operating range of evaporator temperature.

TABLE OF CONTENTS

LIST OF FIGURES

LIST OF TABLES

LIST OF SYMBOLS

COP	coefficient of performance (Non- dimensional)
DE VARS	double 0evaporator vapour absorption refrigeration
$\dot{E}_d$	exergy destruction rate
$\dot{E}_L$	thermal exergy loss rate
f_1(SCR-1)	solution circulation ratio in circuit-1 (Non- dimensional)
f_2(SCR-2)	solution circulation ratio in circuit-2 (Non- dimensional)
h	specific enthalpy (kJ kg^{-1})
$\dot{m}$	mass flow rate (kg s^{-1})
P_h	high pressure (bar)
P_l	low pressure (bar)
$\dot{Q}$	heat transfer rate (kW)
s	specific entropy (kJ $kg^{-1}K^{-1}$)
SEV	solution expansion valve
SHX	solution heat exchanger
T	temperature (K)
TV-1	throttle valve-1
TV-2	throttle valve-2
$\dot{W}$	work transfer rate (kW)
X	mass fraction of ammonia in solution (dimensionless)

Greek letters

$\in$	effectiveness of heat exchanger
ϑ	specific volume (m^3 kg^{-1})
$\sum$	represents sum of
η	efficiency
δ	efficiency defect

Subscripts

o	represent surrounding conditions
1,2,3	represents state points in the equations, components in the systems
a1	absorber-1
a2	absorber-2
c	condenser
e	evaporator, exit
e1	evaporator-1
e2	evaporator-2
ex	exergetic
g1	generator-1
g2	generator-2
h	high
i	inlet
l	low
p1	solution pump-1
p2	solution pump-2
r	refrigerant
rec1	rectifier-1
rec2	rectifier-2
ss1	strong solution in high pressure circuit
ss2	strong solution in low pressure circuit
ws1	weak solution in high pressure circuit
ws2	weak solution in low pressure circuit

CHAPTER-1
INTRODUCTION

The problem of environment pollution and global energy shortage have been increasing seriously. Most of the industries uses thermal energy by burning fossil fuels to produce heat or steam for its purpose. In this process only some percentage of the thermal energy is utilised and the remaining part of energy is going waste which is rejected to the surrounding and thus increase the environmental problems. This waste energy can be utilised to produce useful refrigeration in the industries for the purpose of air conditioning to give human comfort and also for the purpose of storing, manufacturing processes of some products which require proper refrigeration for its increased life and reliability. The use of heat operated VAR systems helps in reducing environmental problems such as global warming and ozone layer depletion. In this way consumption of electricity for conventional vapour compression refrigeration system (VCRS) is reduced and thus saves the extra expenditure incurred on consuming electricity.

Vapor absorption refrigeration system (VARS) with the utilization of natural inviting refrigerants have been given more consideration lately in light of the distinction in the working liquid utilized in the regular vapor compression refrigeration system (VCRS) and vapor absorption refrigeration system (VARS). The most regularly refrigerant utilized in vapor compression refrigeration system is chlorofluorocarbon refrigerants (CFCs), in light of their great thermo-physical properties however the utilization of CFCs is confined because it is responsible for the depletion of ozone layer which protects us from the sun ultraviolet rays. Although absorption refrigeration system provides many advantages but still vapour compression systems dominated in the market due to its design, cost and suitability. So as to advance the utilization of absorption systems, further advancements are required to improve their exhibition, structure and decrease cost.

Besides, absorption refrigeration systems have been given more consideration since they can likewise utilize non-conventional sources of energy such as sun oriented, geothermal, biomass and waste heat from thermal systems as a heating capacity for these frameworks. Because of this favourable position, these systems can challenge the VCR systems disregarding their low COPs. Likewise, the working liquid utilized in absorption systems are condition amicable.

The history of the development of the absorption cycles had been started approx. 300 years earlier as in 1700's at the time when the generation of ice should be possible by evaporation of unadulterated (pure) water from a vessel which would be contained in an emptied holder within the sight of sulfuric acid. In the time of 1810, the generation of ice should be possible from water in a vessel, which was associated to another vessel containing sulfuric acid. In this procedure water vapor assimilated in the acid, which would cause a decrease in the temperature and on the outside of water ice were framed as layers. Erosion and spillage of air into the vacuum vessel were the serious issues looked by this framework. In the time of 1859, Ferdinand Carre built up a novel machine utilizing ammonia/water as the working liquid. In 1860, US patent would be taken out by this machine. Machines were utilized to make ice and store sustenance which depended on this patent. It was utilized as a fundamental structure in the early time of Refrigeration advancement. During the long stretches of 1926-1933, hands were joined by Szilárd and Einstein in the zone of household refrigeration to improve the advancements and development.

In the time of 1950's, a framework was presented for modern applications which utilized lithium bromide/water as the working liquid. A couple of years after the fact, a twofold absorption system was presented which has been widely utilized as a mechanical standard for an elite heat worked refrigeration cycle. In 1960's, the absorption innovation returned with application in cooling.

The greatest advantage of using absorption refrigeration systems is found in reducing electricity consumption by using waste energy from the heat source, industries to increase the system efficiency, environmental protection and economic benefits to the users. Now a days, the cost of systems operating on absorption refrigeration is much higher than the mechanical vapour compression refrigeration system (VCRS) of the same capacity. Also, the operation costs are not enough to compensate the difference in between the two refrigeration systems. So great commercial success is only possible by developing small refrigeration units.

Principle of VARS

In both the refrigeration systems i.e. VARS and VCRS, refrigerant having low boiling point (B.P.) is used where refrigerant evaporates (boils) in the evaporator which takes away some heat providing the cooling effect on the system or space. The main difference between the VCRS and VARS refrigeration systems is the way of refrigerant going back

into a liquid state and pass through the evaporator again to operate the cycle continuously. An absorption system changes the gas into the liquid using a method which needs heat and very less electrical energy to pump the liquid from low pressure to high pressure which is very less because specific volume (ϑ_l) of liquid is very small in comparison to the vapour (ϑ_v) but in VCRS system gas after evaporator section is compressed in compressor to increase the temperature of gas so that it can rejects the heat into surrounding in the condenser.

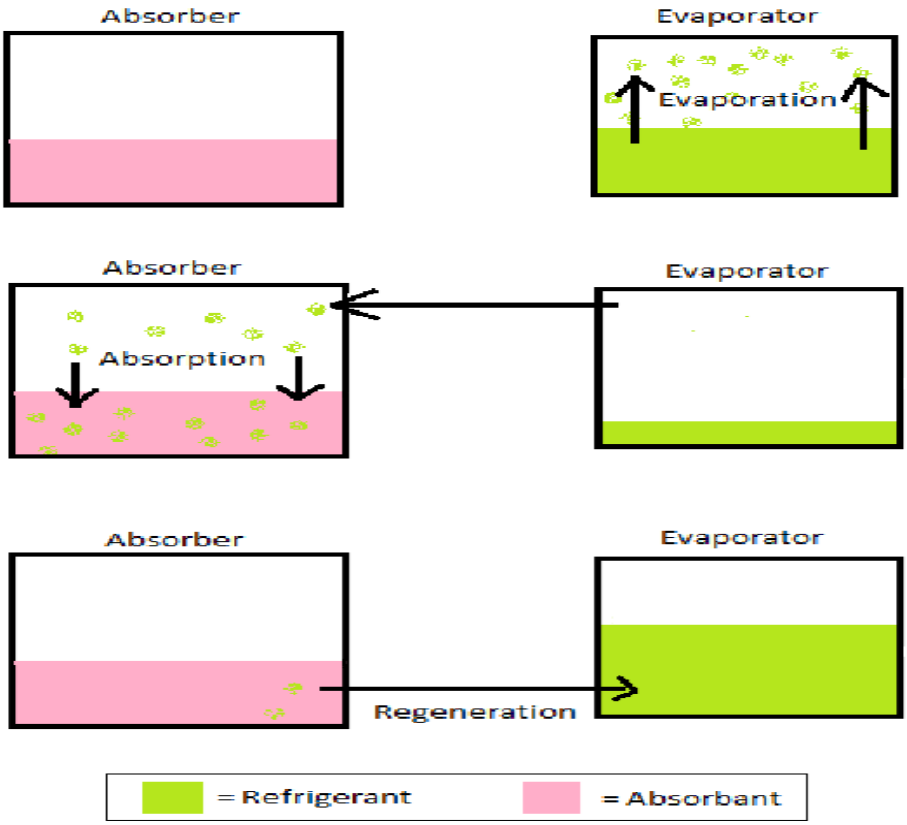

Fig.1.1 Principle of VARS cycle

Fig.1.1 shows how the refrigerant passes through the different phases which can be described in three phases namely:

1. **Evaporation**: A fluid refrigerant evaporates in a low partial pressure condition in the evaporator, in this manner extricating heat from its environment (space to be cooled or framework). Due to the low partial pressure, the temperature required for evaporation is likewise low so heat transfer happens from surrounding to evaporator. At least 5 – 10° C temperature required for heat transfer to happens.

2. **Absorption**: Now the refrigerant in gaseous stage is absorbed by another liquid to form solution mixture (e.g. a salt solution). Now this solution mixture is pumped at high pressure in the generator for regeneration of refrigerant to takes place.
3. **Regeneration**: The refrigerant-fluid blend present in the generator is then warmed, making the refrigerant evaporate out from the arrangement. The hot vaporous refrigerant goes through a heat exchanger (for example condenser), moving its heat outside the framework, (for example, to surrounding ambient-temperature air), and consolidates. The condensed (fluid) refrigerant supplies to the evaporator for the evaporation phase.

Another distinction between the two kinds of refrigeration systems is the sort of refrigerant utilized in the system. VCRS commonly utilize a HCFC or HFC, while VARS regularly use ammonia-water and Li-Br/H_2O mixes where one fluid is utilized as an absorbant and other utilized as a refrigerant.

Some of the advantages of using absorption systems are as follows:

1. There are no moving parts in VARS with the exception of pump so that wear and tear losses are less.
2. Systems is quite in operation as there is no moving parts.
3. Maintenance expenses of the system are very less.
4. Systems can work only with low grade energy as input.
5. These systems can be built for huge working capacities.

Scope

In this communication, the analysis of simple VARS systems have been extended to the double- evaporator ammonia water vapour absorption refrigeration systems. This can be done by using the two evaporators in the system instead of using single evaporator in simple VARS. The purpose of using two evaporators is to avail the effect of using cooling load at wide range of temperatures. The program is developed in engineering equation solver (EES) software to analyse the system.

CHAPTER-2
LITERATURE REVIEW

2.1 Summarization of various authors work

A number of researchers had studied the performance of the VARS which is presented below:

Wang et al. [1] provides onboard refrigeration of fishing vessels from high-temperature waste heat source which is generated from diesel engines. To do so, he proposed molecular simulations (the Monte Carlo method) dynamic modelling method of the double-effect vapour absorption cycles to reduce the complexity of the system by preventing the use of rectifier in the system. In this proposed cycle, the COP of 1.1 is accomplished at a temperature of −5 °C by utilizing best working liquid, which is somewhat higher than that is gotten with the mix of generator-absorber cycles. When it is coordinated with the waste exhaust gas that ways out from diesel engines, the system cooling limit is adequate to work with the two seawater refrigeration plants for the majority of the engines working modes in high-latitude zones

Liang et al. [2] added Li-Br in NH_3-H_2O absorption refrigeration system to improve the system performance. It can likewise expand the concentration of ammonia in the vapor stream, in this manner it diminishes the utilization of energy during rectification, However the negative impact on the absorber is seen on the presence of Li-Br. By incorporation of electrodialysis process in this system, which isolates Li-Br from the arrangement entering the absorber with the goal that the vast majority of the Li-Br is held in the generator. By executing this, the working generator temperature is altogether decreased and the COP of the system is improved contrasted with the basic NH_3-H_2O VAR.

Vasudev et al. [3] propose a technique wherein he utilizes a latent heat storage substance called as ethylene glycol, which is introduced in the Evaporator area of an Ammonia/Water absorber system model to consider the transient impacts of ethylene glycol on the temperature. It is tentatively demonstrated that Ethylene Glycol decreases

the rate essentially, in this manner it secures the nature of sustenance which is put away inside.

Aprile et al. [4] investigates a completely stacked NH_3-H_2O heat pump driven by gas by changing the temperatures of heated water and halfway stacked system is broke down by diminishing the contribution of the gas down to half of the completely stacked worth. The exactness in estimations improves by utilizing numerical simulations and this gives comprehension of the COP variety and Gas Utilization Efficiency (GUE) in view of the calorific value. The estimation of GUE of about 1.5 (steady) is found for the temperature of high temp water lower than 50°C. It relentlessly diminishes to 1.33 from 50°C to 60°C. The estimation of COP diminishes all the more easily from 1.73 to 1.60 in the temperature ranges from 45°C to 60°C. The decrease in GUE and COP at half of the nominal gas input is 6.8% and 6.4% respectively. It is additionally seen from simulations that the performance of the system at halfway loads can be improved if dynamic control in the mass stream rate of arrangement is executed.

Swarnkar et al. [5] works the system with the refrigerant as ammonia and distinctive ionic fluids & water utilized as a solvent and cosolvent separately. The outcome demonstrates that there is an enormous reduction in the circulation ratio when water is utilized as a cosolvent and thus the equipment size, while it is additionally decline in coefficient of performance marginally.

Jia et al. [6] proposes a solitary stage and balanced-type ammonia-water absorption-resorption heat pump (ARHP) cycle which depends on the uneven ARHP cycle by removing the utilization of the rectifier in the absorption system and it relies upon just a single solute on circulation pump. By changing the fixation contrast of NH_3-H_2O arrangement at various pressure levels, cycle moderates the interior mass and species. A model acquired the sets of achievable high pressure/low pressure (P_h/P_l) to empower the cycle. The most extreme estimation of COP is 1.51 and it is gotten at the corresponding heat supply temperature of 43.4°C when (P_h/P_l) esteem is 1.50/0.48 MPa and the temperature of heat source is 95°C.

Jawahar et al. [7] proposed a framework where he recuperates greatest interior heat from the streams utilizing the pinch point examination in the ammonia-water absorption cooling system, subsequently increments in system performance. The system is worked in the temperature scope of generator somewhere in the range of 120°C and 150°C, sink temperature somewhere in the range of 25°C and 45°C and evaporator temperatures between - 10°C to 10°C. In view of the recouping of the greatest conceivable internal heat

from this methodology, the cycle is changed with no further need of rectification and the exhibition of this system is analysed. The estimation of coefficient of performance of this proposed cycle is observed to be increments from 17% to 56% than that of an ordinary cycle at same working conditions.

Horuz [8] concluded that VAR system using Li-Br/H_2O as a refrigerant provide better performance than ammonia water VARS but water- lithium bromide has the limitations of crystallisations problems and also it is impossible to operate the system in a very low temperatures because of the use of water as a refrigerant in Li-Br/H_2O vapour absorption refrigeration system.

Toppi et al. [9] numerically assessed semi-GAX cycle at the working conditions which is appropriate for the low temperature cooling application. The estimation of COP is unequivocally affected by the split ratio, which is utilized to decide the intermediate pressure and to accomplish the likelihood of GAX impact. The most extreme air temperature is 40°C to permits a circulation ratio underneath 15, chilled water at 7/12°C and 90°C of driving temperature.

Wu et al. [10] investigations that at the gulf temperature of 130 °C of generator, as the inlet temperature of evaporator diminishes from −5 °C to −25 °C, the estimation of COP of warmth siphon drops from 1.513 to 1.372, while the heating capacity of the system weakens from the estimation of 77.26 kW to 47.11 kW, Also the examinations between compressor assisted absorption heat pump (CAHP) and normal absorption heat pump (AHP) demonstrated that by utilizing CAHP in the framework can expand the lower limit reaches the inlet temperature of evaporator from −10 °C to −25 °C and it can likewise upgrade the heating capacity by roughly from 55.5%–85.0% even under the typical working states of AHP.

Dixit et al. [11] had done analysis of aqua-ammonia generator-absorber heat exchanger (GAX) and hybrid GAX (HGAX) absorption cycles and determined the worked conditions to think about the impact of temperature of evaporator, condenser and generator and furthermore seen that absorber and desorber represents most elevated energy demolition.

2.2 Conclusion of literature survey

On the basis of literature survey, it is concluded that lot of research work has been done on the NH_3-H_2O VARS cycle to increase performance of the system by using molecular simulations to reduce complexity [1], recovering waste by using GAX and HGAX [8] and [11], recovering internal heat from using pinch point analysis [7] . It is concluded From Horuz [8] that Water-Lithium bromide refrigerant is not suitable for sub- zero temperature and from Wu et al. [10], it is also concluded that COP of VARS system decreases as the evaporator temperature decreases. It is also a known fact that exergy analysis provides more substantial information in terms of useful energy than energy analysis performed on the system. Second law analysis is useful in identifying the magnitude and sources of irreversibility in energy conversion systems.

2.3 Research gaps

Since various researches have been done to increase the performance of the system whatever work has been done is restricted only to increase performance by recovering waste heat and reducing generator heat by adding another material to the refrigerant etc but no efforts have been done to work in areas given below

1. From the literature survey, it is found that no work has been done on the double or multi evaporator ammonia-water vapour absorption refrigeration system (VARS) which is used as to increase the performance, if cooling load is available at different temperature. With two evaporators in which one is at low temperature and others is at high temperature.
2. Further the energy and exergy analysis are also not carried out in order to analyse the double or multi evaporator in vapour absorption refrigeration system (VARS).

2.4 Objective of present work

1. A detailed energy and exergy analysis of ammonia-water double evaporator vapour absorption refrigeration system (DE VARS) have been carried out in this communication.
2. The value of coefficient of performance (COP) and exergetic efficiency (η_{ex}) are calculated at various conditions by varying temperature and pressure of the components.

3. The effect of cooling load of the evaporator-1&2, effect of the temperature of generator-1&2, temperature of absorber-1&2 and temperature of condenser and the effect of pressure in absorber-1&2 and generator-1&2 on the COP and η_{ex} are also analysed.
4. The analysis of the effects of ammonia mass fraction on the COP and η_{ex} are also carried out.
5. Exergy destruction and efficiency defect in the components of the system are also calculated to observe the irreversibility within the systems.

CHAPTER-3
THERMODYNAMIC ANALYSES

3.1 System description

The main components of Double Evaporator Vapour Absorption Refrigeration System (DE VARS) are divided into two circuits namely high pressure circuit and low pressure circuit illustrated in Fig.3.1 are as follows. The subscript 1 and 2 denotes the components of high pressure and low pressure circuit respectively.

- Condenser
- Throttle valve (TV-1 &TV-2)
- High and low pressure evaporator i.e. (Evaporator-1 & Evaporator-2)
- High and low pressure absorber i.e. (Absorber-1 & Absorber-2)
- Solution pump (Pump-1 & Pump-2)
- Solution expansion valve (SEV-1 & SEV-2)
- Solution heat exchanger (SHX-1 & SHX-2)
- High and low pressure generator i.e. (Generator-1 & generator-2)

In the high pressure circuit, The saturated strong solution (strong in ammonia) is pumped to high pressure (2) and then passed through a solution heat exchanger (SHX) to recover the heat internally. In the generator, external heat is supplied which boils off the refrigerant and the remaining saturated weak solution (4) after giving its heat to the strong solution by using SHX, expanded to low pressure in solution expansion valve flows back to the absorber. The vapours leaving the generator (7) consists of ammonia and water vapours, At the end of throttling process, water presents in the ammonia chokes the system, which hampers the performance of the system so it is to be rectified in the rectifier after leaving the generator. The vapours at the exit of rectifier (9) consists of almost 99.9% pure ammonia vapours and remaining condensed water in the rectifier flows back to the generator.

In the low pressure circuit, all the process occurs in same manners as that of high pressure circuit. The ammonia vapours leaving from low pressure circuit i.e. rectifier-2 (18) mixes with ammonia vapours from (9) passes through the condenser gives heat to

the surrounding (20). The temperature at inlet of evaporator 1 is controlled by the amount of pressure reduced in the throttling valve-1 (TV-1). The liquid refrigerant takes heat from high temperature cooling space converts into saturated vapour and this saturated vapour mixes with the weak solution in the absorber-1. This completes the high pressure cycle.

The remaining saturated liquid (22) reduced to low pressure (23) in throttle valve-2 (TV-2) depending upon the design temperature of refrigerated space temperature. The liquid refrigerant gets heated in evaporator-2 converts to vapour mixes with weak solution in absorber-2. This completes the cycle in low pressure circuit.

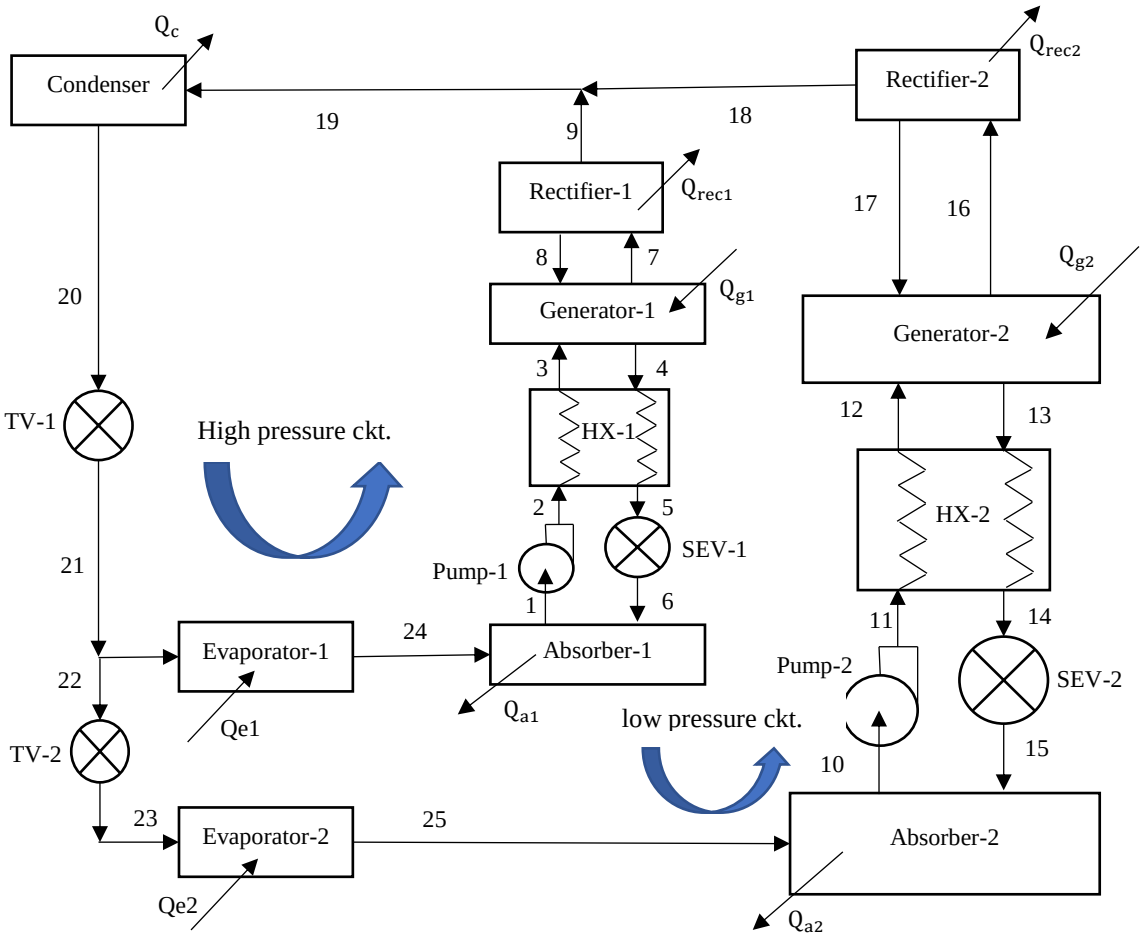

Fig.3.1 Schematic diagram of double evaporator NH_3-H_2O vapour absorption refrigeration system

3.2 System analysis

3.2.1 Introduction

The theoretical analysis of the system involves mass balance, material balance for ammonia, first and second laws of thermodynamic for energy and exergy balance to each component of the system. To carry out these balances, each component is considered as a control volume.

3.2.2 Mass and Material balances for Each Component

Mass balance involves the principle of conservation of mass in the control volume (C.V.) i.e. the mass flow rate that is entering into the C.V. is equal to the mass flow rate leaving out of the C.V. (1) and material balance involves the fraction of mass of ammonia in the solution or refrigerant entering into the C.V. is equal to the fraction of mass of ammonia in the solution leaving out of the control volume (2).

$$\sum \dot{m}_i - \sum \dot{m}_e = 0 \quad (1)$$

$$\sum \dot{m}_i X_i - \sum \dot{m}_e X_e = 0 \quad (2)$$

Mass and material balance of the components of double evaporator NH_3-H_2O VARS are as follows

Evaporator-1

$$m_{21} = m_{24} = m_{r1} \quad (3)$$

Evaporator-2

$$m_{23} = m_{25} = m_{r2} \quad (4)$$

Absorber-1

$$m_{ss1} = m_1 \;\&\; m_{ws1} = m_6 \quad (5)$$

$$m_{r1} + m_{ws1} = m_{ss1} \quad (6)$$

$$m_{r1}X_{r1} + m_{ws1}X_{ws1} = m_{ss1}X_{ss1} \quad (7)$$

Absorber-2

$$m_{ss2} = m_{10} \;\&\; m_{ws2} = m_{15} \quad (8)$$

$$m_{r2} + m_{ws2} = m_{ss2} \quad (9)$$

$$m_{r2}X_{r2} + m_{ws2}X_{ws2} = m_{ss2}X_{ss2} \quad (10)$$

Pump-1

$$m_1 = m_2 = m_{ss1} \quad (11)$$

$$X_1 = X_2 = X_{ss1} \quad (12)$$

Pump-2

$$m_{10} = m_{11} = m_{ss2} \quad (13)$$

$$X_{10} = X_{11} = X_{ss2} \quad (14)$$

SHX-1

$$m_{ss1} = m_2 = m_3 \;\&\; m_{ws1} = m_4 = m_5 \quad (15)$$

$$X_{ss1} = X_2 = X_3 \;\&\; X_4 = X_5 = X_{ws1} \quad (16)$$

SHX-2

$$m_{ss2} = m_{11} = m_{12} \;\&\; m_{ws2} = m_{13} = m_{14} \quad (17)$$

$$\&\; X_{ws2} = X_{13} = X_{14} \quad (18)$$

SEV-1

$$m_5 = m_6 = m_{ws1} \quad (18)$$

$$X_5 = X_6 = X_{ws1} \quad (19)$$

SEV-2

$$m_{14} = m_{15} = m_{ws2} \quad (20)$$

$$X_{14} = X_{15} = X_{ws2}$$

Generator-1

$$m_{ss1} + m_8 = m_{ws1} + m_7 \quad (21)$$

$$m_{ss1}X_{ss1} + m_8X_8 = m_{ws1}X_{ws1} + m_7X_7 \quad (22)$$

Generator-2

$$m_{ss2} + m_{17} = m_{ws2} + m_{16} \quad (23)$$

$$m_{ss2}X_{ss2} + m_{17}X_{17} = m_{ws2}X_{ws2} + m_{16}X_{16} \quad (24)$$

Rectifier-1

$$m_8 + m_9 = m_7 \quad (25)$$

$$m_8X_8 + m_9X_9 = m_7X_7 \quad (26)$$

Rectifier-2

$$m_{17} + m_{18} = m_{16} \quad (27)$$

$$m_{17}X_{17} + m_{18}X_{18} = m_{16}X_{16} \quad (28)$$

The refrigerant mixture after coming out of the both rectifier mixes and passes through the condenser. The equation of mass and material at the exit of both rectifiers are as follows

$$m_9 = m_{r1} \,\&\, m_{18} = m_{r2} \,\&\, m_{19} = m_r \quad (29)$$

$$m_{r1} + m_{r2} = m_r \quad (30)$$

Condenser

$$m_{19} = m_{20} = m_r \quad (31)$$

$$X_{19} = X_{20} = X_r \quad (32)$$

TV-1

$$m_{20} = m_{21} = m_r \quad (33)$$

$$X_{20} = X_{21} = X_r \quad (34)$$

TV-2

$$m_{22} = m_{23} = m_{r2} \quad (35)$$

$$X_{22} = X_{23} = X_{r2} \quad (36)$$

3.2.3 Energy balances for each component

Energy balance involves the principle of conservation of energy in the control volume (C.V.) which is evaluated from the steady flow energy equation (S.F.E.E.) as given in equation (37)

$$\sum \dot{W} - \sum \dot{Q} = \sum \dot{m}_i h_i - \sum \dot{m}_e h_e \quad (37)$$

Energy balance for the components of double evaporator NH_3-H_2O VARS are as follows

Evaporator-1

$$Q_{e1} = m_{r1}(h_{24} - h_{21}) \quad (38)$$

Evaporator-2

$$Q_{e2} = m_{r2}(h_{25} - h_{23}) \quad (39)$$

Absorber-1

$$Q_{a1} + m_{ss1}h_1 = m_{r1}h_{24} + m_{ws1}h_6 \quad (40)$$

Absorber-2

$$Q_{a2} + m_{ss2}h_{10} = m_{r2}h_{25} + m_{ws2}h_{15} \quad (41)$$

SHX-1

Consider effectiveness of heat exchanger SHX-1 is $\in_1$. The enthalpy at state point (5) is calculated by the relation

$$\in_1 = (h_4 - h_5)/(h_4 - h_{m5}) \quad (42)$$

Where h_{m5} is the minimum enthalpy reached at state point (5) when temperature at state point (5) is equal to the temperature at state point (2).

The enthalpy at state point (5) is calculated by the following relation

$$(f_1 - 1)(h_4 - h_5) = f_1(h_3 - h_2) \quad (43)$$

Where f_1 is the solution circulation ratio in high pressure circuit

Which is calculated by the following relation

$$f_1 = m_{ss1}/m_{r1} = (X_r - X_{ws1})/(X_{ss1} - X_{ws1}) \quad (44)$$

SHX-2

Consider effectiveness of heat exchanger SHX-2 is $\in_2$. The enthalpy at (14) is calculated by the relation

$$\in_2 = (h_{13} - h_{14})/(h_{13} - h_{m14}) \quad (45)$$

Where h_{m14} is the minimum enthalpy reached at state point (14) when temperature at state point (14) is equal to the temperature at state point (11).

The enthalpy at state point (12) is calculated by the following relation

$$(f_2 - 1)(h_{13} - h_{14}) = f_2(h_{12} - h_{11}) \quad (46)$$

Where f_2 is the solution circulation ratio in low pressure circuit

Which is calculated by the following relation

$$f_2 = m_{ss2}/m_{r2} = (X_r - X_{ws2})/(X_{ss2} - X_{ws2}) \quad (47)$$

Pump-1

$$W_{p1} = m_{ss1}(h_2 - h_1) \quad (48)$$

Pump-2

$$W_{p2} = m_{ss2}(h_{11} - h_{10}) \quad (49)$$

SEV-1

$$h_5 = h_6 \quad (50)$$

SEV-2

$$h_{14} = h_{15} \quad (51)$$

Generator-1

$$Q_{g1} + m_{ss1}h_3 + m_8h_8 = m_7h_7 + m_{ws1}h_4 \quad (52)$$

Generator-2

$$Q_{g2} + m_{ss2}h_{12} + m_{17}h_{17} = m_{16}h_{16} + m_{ws2}h_{13} \quad (53)$$

Rectifier-1

$$Q_{r1} + m_8h_8 + m_9h_9 = m_7h_7 \quad (54)$$

Rectifier-2

$$Q_{r2} + m_{17}h_{17} + m_{18}h_{18} = m_{16}h_{16} \quad (55)$$

Condenser

$$Q_c = m_r(h_{19} - h_{20}) \quad (56)$$

TV-1

$$h_{20} = h_{21} \quad (57)$$

TV-2

$$h_{22} = h_{23} \quad (58)$$

Coefficient of Performance (COP) of this system is defined as the ratio of useful heat (i.e. $\dot{Q}_{e1}$ & $\dot{Q}_{e2}$) to the work input to the system. Here useful heat is the cooling load in both the evaporator of the system and input work is the summation of heat given to both the generator and work input to both the pump, which is expressed as follows:

$$COP_{ME\ VARS} = \frac{\dot{Q}_{e1} + \dot{Q}_{e2}}{(\dot{Q}_{g1} + \dot{Q}_{g2} + W_{p1} + W_{p2})} \quad (59)$$

Where $\dot{Q}_{e1}$ & $\dot{Q}_{e2}$ are cooling load in evaporator-1 and evaporator-2 respectively, $\dot{Q}_{g1}$ & $\dot{Q}_{g2}$ are the heat given to generator-1 and generator-2 respectively and W_{p1} & W_{p2} are the work required to pump the solution form absorber to generator in high pressure and low pressure circuit respectively.

3.2.4 <u>Exergy analysis of the components of the system:</u>

The exergy of a system is assessed by the second law of thermodynamics and it is defined as the measure of usefulness, quality or capability of a stream to cause change and an effective measure of the potential of a substance to impact the environment. The exergy balance for a control volume undergoing steady-state process is expressed as:

$$\dot{E}_{d,i} = \sum \dot{m}_i e_i - \sum \dot{m}_e e_e + \left[\sum \left(\dot{Q} \left| \left(1 - \frac{T_o}{T}\right) \right| \right)_i - \sum \left(\dot{Q} \left| \left(1 - \frac{T_o}{T}\right) \right| \right)_e \right] \pm W \quad (60)$$

Where $\dot{E}_{d,i}$ represents the destruction rate of exergy occurring in the process of the component under consideration. $\sum \dot{m}_i e_i$ & $\sum \dot{m}_e e_e$ represent the exergy of streams entering and leaving the control volume in the components of the system. $\left[\sum \left(\dot{Q} \left| \left(1 - \frac{T_o}{T}\right) \right| \right)_I$ & $\sum \left(\dot{Q} \left| \left(1 - \frac{T_o}{T}\right) \right| \right)_e \right]$ represents the exergy associated with heat transfer $\dot{Q}$ from the source maintained at a constant temperature T and is equal to the maximum work obtained i.e. by the Carnot engine operating between T and T_o, and therefore it is equal

to the maximum reversible work obtained from heat energy $\dot{Q}$ and W is the mechanical work transferred to or from the control volume in the components of the system.

Thermal exergy loss rate ($\dot{E}_L$) [13] is identified with external irreversibility related with the parts of the system, which happens because of temperature difference (ΔT) between the components control volume (CV) and the environment. It relies on the choice of the system limit. In the event that surrounding environment incorporate into the system, at that point the warm framework limit is at a similar temperature as that of the surroundings temperature and thus thermal system misfortune ends up being zero. In any case, on the off chance that prompt surroundings does exclude in the system, at that point there is a temperature difference between the system boundary and the surrounding environment. For the last case, the rate of thermal exergy loss is given by

$$\dot{E}_{L,i} = \dot{Q}_l \left(1 - \frac{T_o}{T}\right)_i \tag{61}$$

Efficiency defect (δ_i) of a particular component is defined as the ratio of exergy destruction in i_{th} component to the exergy of the fuel given to the system i.e.

$$\delta_i = \frac{\dot{E}_{d,i} + \dot{E}_{L,i}}{\dot{E}F} \tag{62}$$

Where $\dot{E}F$ is equal to

$$\left(Q_{g1} * \left(1 - \frac{T_o}{T_{g1}}\right)\right) + \left(Q_{g2} * \left(1 - \frac{T_o}{T_{g2}}\right)\right) + W_{p1} + W_{p2} \tag{63}$$

Exergy analysis of various components are as follows:

Evaporator-1

$$T_{r1} = \left(\frac{T_{ei1} + T_{eo1}}{2}\right) + \Delta T \tag{64}$$

$$\dot{E}_{d,eva1} = m_{r1} * \left((h_{21} - T_o * s_{21}) - (h_{24} - T_o * s_{24})\right) + Q_{e1} * \left|\left(1 - \frac{T_o}{T_{r1}}\right)\right| \tag{65}$$

$$\delta_{eva1} = \frac{ED_{eva1}}{\dot{E}F} \tag{66}$$

Evaporator-2

$$T_{r2} = \left(\frac{T_{ei2} + T_{eo2}}{2}\right) + \Delta T \tag{67}$$

$$\dot{E}_{d,eva2} = m_{r2} * \left((h_{23} - T_o * s_{23}) - (h_{25} - T_o * s_{25})\right) + Q_{e2} * \left|\left(1 - \frac{T_o}{T_{r2}}\right)\right| \tag{68}$$

$$\delta_{eva2} = \frac{E_{d,eva2}}{\dot{E}F} \tag{69}$$

Absorber-1

$$\dot{E}_{d,a1} = m_{ws1} * (h_6 - T_o * s_6) + m_{r1} * (h_{24} - T_o * s_{24}) - m_{ss1} * (h_1 - T_o * s_1) - Q_{a1} * \left(1 - \frac{T_o}{T_{a1}}\right) \tag{70}$$

$$\delta_{a1} = \frac{\dot{E}_{d,a1} + \dot{E}_{L,a1}}{\dot{E}F} \tag{71}$$

Absorber-2

$$\dot{E}_{d,a2} = m_{ws2} * (h_{15} - T_o * s_{15}) + m_{r2} * (h_{25} - T_o * s_{25}) - m_{ss2} * (h_{10} - T_o * s_{10}) - Q_{a2} * \left(1 - \frac{T_o}{T_{a2}}\right) \tag{72}$$

$$\delta_{a2} = \frac{\dot{E}_{d,a2} + \dot{E}_{L,a2}}{\dot{E}F} \tag{73}$$

SHX-1

$$\dot{E}_{d,shx1} = m_{ss1} * \left((h_2 - T_o * s_2) - (h_3 - T_o * s_3)\right) + m_{ws1} * \left((h_4 - T_o * s_4) - (h_5 - T_o * s_5)\right) \tag{74}$$

$$\delta_{shx1} = \frac{\dot{E}_{d,shx1}}{\dot{E}F} \tag{75}$$

SHX-2

$$\dot{E}_{d,shx2} = m_{ss2} * \left((h_{11} - T_o * s_{11}) - (h_{12} - T_o * s_{12})\right) + m_{ws2} * \left((h_{13} - T_o * s_{13}) - (h_{14} - T_o * s_{14})\right) \tag{76}$$

$$\delta_{shx2} = \frac{\dot{E}_{d,shx2}}{\dot{E}F} \tag{77}$$

Pump-1

$$\dot{E}_{d,solpump1} = m_{ss1} * \left((h_1 - T_o * s_1) - (h_2 - T_o * s_2)\right) + W_{p1} \tag{78}$$

$$\delta_{solpump2} = \frac{\dot{E}_{d,solpump1}}{\dot{E}F} \tag{79}$$

Pump-2

$$\dot{E}_{d,solpump2} = m_{ss2} * \left((h_{10} - T_o * s_{10}) - (h_{11} - T_o * s_{11})\right) + W_{p2} \quad (80)$$

$$\delta_{solpump2} = \frac{\dot{E}_{d,solpump2}}{\dot{EF}} \quad (81)$$

SEV-1

$$\dot{E}_{d,sev1} = m_{ws1} * T_o * (s_6 - s_5) \quad (82)$$

$$\delta_{sev1} = \frac{\dot{E}_{d,sev1}}{\dot{EF}} \quad (83)$$

SEV-2

$$\dot{E}_{d,sev2} = m_{ws14} * T_o * (s_{15} - s_{14}) \quad (84)$$

$$\delta_{sev2} = \frac{\dot{E}_{d,sev2}}{\dot{EF}} \quad (85)$$

Generator-1

$$\dot{E}_{d,g1} = m_{ss1} * (h_3 - T_o * s_3) + m_8 * (h_8 - T_o * s_8) - m_7 * (h_7 - T_o * s_7) - m_{ws1} * (h_4 - T_o * s_4) + Q_{g1} * \left(1 - \frac{T_o}{T_{g1}}\right) \quad (86)$$

$$\delta_{g1} = \frac{\dot{E}_{d,g1}}{\dot{EF}} \quad (87)$$

Generator-2

$$\dot{E}_{d,g2} = m_{ss2} * (h_{12} - T_o * s_{12}) + m_{17} * (h_{17} - T_o * s_{17}) - m_{16} * (h_{16} - T_o * s_{16}) - m_{ws2} * (h_{13} - T_o * s_{13}) + Q_{g2} * \left(1 - \frac{T_o}{T_{g2}}\right) \quad (88)$$

$$\delta_{g2} = \frac{\dot{E}_{d,g2}}{\dot{EF}} \quad (89)$$

Rectifier-1

$$\dot{E}_{d,rec1} = m_7 * (h_7 - T_o * s_7) - m_8 * (h_8 - T_o * s_8) - m_9 * (h_9 - T_o * s_9) - Q_{rec1}\left(1 - \frac{T_o}{T_{rec1}}\right) \quad (90)$$

$$\delta_{rec1} = \frac{\dot{E}_{d,rec1} + \dot{E}_{L,rec1}}{\dot{E}F} \quad (91)$$

Rectifier-2

$$\dot{E}_{d,rec2} = m_{16} * (h_{16} - T_o * s_{16}) - m_{17} * (h_{17} - T_o * s_{17}) - m_{18} * (h_{18} - T_o * s_{18}) - Q_{rec2}\left(1 - \frac{T_o}{T_{rec2}}\right) \quad (92)$$

$$\delta_{rec2} = \frac{\dot{E}_{d,rec2} + \dot{E}_{L,rec2}}{\dot{E}F} \quad (93)$$

Condenser

$$\dot{E}_{d,con} = m_r * \left((h_{19} - T_o * s_{19}) - (h_{20} - T_o * s_{20})\right) - Q_c * \left(1 - \frac{T_o}{T_c}\right) \quad (94)$$

$$\delta_{con} = \frac{\dot{E}_{d,con} + \dot{E}_{L,con}}{\dot{E}F} \quad (95)$$

TV-1

$$\dot{E}_{d,tv1} = m_r * \left((h_{20} - T_o * s_{20}) - (h_{21} - T_o * s_{21})\right) \quad (96)$$

$$\delta_{tv1} = \frac{\dot{E}_{d,tv1}}{\dot{E}F} \quad (97)$$

TV-2

$$\dot{E}_{d,tv2} = m_{r2} * \left((h_{22} - T_o * s_{22}) - (h_{23} - T_o * s_{23})\right) \quad (98)$$

$$\delta_{tv2} = \frac{\dot{E}_{d,tv2}}{\dot{E}F} \quad (99)$$

Exergetic Efficiency (η_{II} or η_{ex})

It is defined as the ratio of the exergy rate of the product ($\dot{E}P$) to the exergy rate of fuel ($\dot{E}F$). In steady state condition of system. In terms of exergy, $\dot{E}F$ and $\dot{E}P$ are the rates at which the fuel is supplied and generation of product respectively i.e.

$$\eta_{II} = \dot{E}P/\dot{E}F \quad (100)$$

$$\eta_{ex} = \frac{\left(Qe_1 * \left(\frac{T_o}{T_{r1}} - 1\right)\right) + \left(Qe_2 * \left(\frac{T_o}{T_{r2}} - 1\right)\right)}{\left(Q_{g1} * \left(1 - \frac{T_o}{T_{g1}}\right)\right) + \left(Q_{g2} * \left(1 - \frac{T_o}{T_{g2}}\right)\right) + W_{p1} + W_{p2}} \quad (101)$$

Exergetic efficiency also defined as the

$$\eta_{ex} = 1 - \frac{\dot{E}_{d,i} + \dot{E}_{L,i}}{\dot{E}F} \quad (102)$$

It is also defined as the

$$\eta_{ex} = 1 - \sum \delta_i \quad (103)$$

Where δ_i is the efficiency defect in a particular component of the system

3.3 Assumptions

Following are the assumptions taken to analyse the system.

1. The system operated in steady state conditions.
2. The refrigerant exits at saturated state in rectifier and condenser.
3. Except through the expansion valves, pressure drops in the system components are neglected.
4. Efficiency of solution pump is 100%.
5. Effectiveness of solution heat exchanger (SHX) is 0.8.

3.4 Input parameters

1. Cooling load taken in both the evaporator i.e. evaporator-1 and evaporator-2 is 35.17 kW or 10 ton of refrigeration.
2. The temperature is varied from 245^oK to 263^oK and 278^oK to 290^oK in Evaporator-1 and evaporator-2 respectively.
3. The temperature in both the evaporator is varied from 293^oK to 313^oK.
4. The temperature in generator-1 and generator-2 is varied from 353^oK - 373^oK and 373^oK - 403^oK respectively.

3.5 Model validation

So as to validate the present model, the simulation consequences of energy analysis of present work have been contrasted and the accessible numerical information determined by Herold [13] for the simple vars cycle in the present work when the heat transfer from the evaporator-2 is put to zero and the comparison of heat transfer in various components

is shown in table.3.1. Heat transfer rate in all the components are within $\pm$1% when compared to Herold et. al [13] as shown in table.3.1. The values of COP and solution circulation ratio in the present case are 0.442 and 7.034 respectively and these values also matches with the results of Herold [13].

Table.3.1 Comparison of the results of the energy analysis of present work with the numerical data given in Herold [13]

Parameters: $\mathbf{T_{eo} = -10^oC}$, $\mathbf{T_c = T_a = 40^oC}$, $\mathbf{X_r}$= 0.999634, $\mathbf{M_{ss}}$=1 kg/s, difference in mass fraction of two solution stream= 0.10, fluid leaving evaporator at vapor quality= 0.975, effectiveness of solution heat exchanger =0.8, $\mathbf{Q_{e2} = 0.}$

Components	**Herold [13]**	**Present work**	**Difference**
	$\dot{Q}$(kW)	$\dot{Q}$(kW)	%
Generator	329.2	330.2	0.303
Absorber	275.8	275.7	-0.036
Condenser	157.2	158.6	0.88
Evaporator	147.2	147.3	0.03
Rectifier	45.0	45.33	0.727
Solution heat exchanger	256.0	257.0	0.389
Pump	1.5	1.489	-0.728
Solution circulation ratio (dimensionless)	7.025	7.034	0.127
COP (dimensionless)	0.445	0.442	-0.678

3.6 Properties value at different points

The values of various properties i.e. temperature, pressure, enthalpy, entropy, specific volume and ammonia mass fraction are calculated at different state points in the ammonia-water DE VAR system as shown in fig.3.1. The values are shown in table 3.1

Table.3.2 Various properties at different state points of ammonia-water DE VAR cycle at $P_{h1} = 12$ bar, $P_{h2} = 12$ bar, $T_{g1} = 363$ K, $T_{g2} = 383$ K, $T_{a1} = 313$ K and $T_{a2} = 303$ K

State point	h [kJ/k]	P [kPa]	q	s	T [K]	u [kJ/k]	v [m^3/kg]	X
1	-61.23	5	0	0.4357	313	-61.84	0.001227	0.4993
2	-60.37	12	-0.001	0.4357	313.1	-61.84	0.001226	0.4993
3	88.83	12	0.003944	0.8887	344.7	86.69	0.001783	0.4993
4	173.3	12	0	1.12	363	171.8	0.001249	0.3994
5	-5.651	12	-0.001	0.5983	323.2	-7.073	0.001185	0.3994
6	-5.651	5	-0.001	0.6009	323.3	-6.244	0.001185	0.3994
7	1491	12	1.001	4.861	363	1325	0.1377	0.9678
8	173.3	12	0	1.12	363	171.8	0.001249	0.3994
9	1296	12	1	4.284	309.9	1166	0.1086	0.9996
10	-90.21	1.8	0	0.3243	303	-90.42	0.001156	0.3797
11	-89.03	12	-0.001	0.3243	303.1	-90.42	0.001155	0.3797
12	162.7	12	-0.001	1.085	359.9	161.2	0.00123	0.3797
13	288.5	12	0	1.391	383	287	0.00123	0.3067
14	7.184	12	-0.001	0.5881	319.3	5.82	0.001137	0.3067
15	7.184	1.8	0.005765	0.5917	317.2	6.105	0.005996	0.3067
16	1599	12	1.001	5.129	383	1424	0.1459	0.9149
17	288.5	12	0	1.391	383	287	0.00123	0.3067
18	1296	12	1	4.284	309.9	1166	0.1086	0.9996
19	1313	11.66	1	4.357	309.9	1179	0.1167	0.9996
20	140.8	11.62	0	0.4979	303	138.8	0.001683	0.9996
21	140.8	5	0.09724	0.519	277.3	127.9	0.02576	0.9996
22	18.72	5	0	0.08207	277.3	17.93	0.001575	0.9996
23	18.72	1.8	0.08617	0.1022	251.9	8.297	0.0579	0.9996

24	1298	5	0.9995	4.671	287.3	1167	0.2622	0.9996
25	1264	1.8	0.999	5.019	261.9	1140	0.6858	0.9996

Table.3.3 COP, heat transfer rate, exergetic efficiency and exergy destruction at states corresponding to table 3.1

Q_{a1} [kW]	Q_{a2} [kW]	Q_{g1} [kW]	Q_{g2} [kW]	Q_{rec1} [kW]	Q_{rec2} [kW]	Q_{e1} [kW]	Q_{e2} [kW]	COP
49.77	61.62	57.71	75.92	8.144	13.69	35.17	35.17	
Q_{con} [kW]	W_{p1} [kW]	W_{p2} [kW]	η_{ex} [%]	δ_{tot} [%]	$\dot{E}_{d,tot}$ [kW]	$\dot{E}P$ [kW]	$\dot{E}F$ [kW]	0.5245
68.75	0.1568	0.3162	17.45	82.55	15.45	4.779	27.66	

Table.3.4 Various properties at different state points of ammonia-water DE VAR cycle at $P_{h1} = 12$ bar, $P_{h2} = 12$ bar, $T_{g1} = 373$ K, $T_{g2} = 393$ K, $T_{a1} = 313$ K and $T_{a2} = 303$ K

State point	h [kJ/k]	P [kPa]	q	s	T [K]	u [kJ/k]	v [m^3/kg]	X
1	-61.23	5	0	0.4357	313	-61.84	0.001227	0.4993
2	-60.37	12	-0.001	0.4357	313.1	-61.84	0.001226	0.4993
3	104.2	12	0.01298	0.933	345.5	100.7	0.002942	0.4993
4	229.3	12	0	1.256	373	227.8	0.001238	0.3517
5	16.14	12	-0.001	0.6452	325.2	14.74	0.001164	0.3517
6	16.14	5	-0.001	0.6477	325.4	15.56	0.001164	0.3517
7	1539	12	1.001	4.987	373	1369	0.1419	0.9462
8	229.3	12	0	1.256	373	227.8	0.001238	0.3517
9	1296	12	1	4.284	309.9	1166	0.1086	0.9996
10	-90.21	1.8	0	0.3243	303	-90.42	0.001156	0.3797
11	-89.03	12	-0.001	0.3243	303.1	-90.42	0.001155	0.3797
12	175.9	12	-0.001	1.122	362.8	174.4	0.001236	0.3797
13	350.3	12	0	1.522	393	348.9	0.001223	0.2638
14	35.87	12	-0.001	0.6401	321.4	34.53	0.001121	0.2638

15	35.87	1.8	-0.001	0.6437	321.6	35.67	0.001122	0.2638
16	1671	12	1.001	5.289	393	1492	0.1495	0.8712
17	350.3	12	0	1.522	393	348.9	0.001223	0.2638
18	1296	12	1	4.284	309.9	1166	0.1086	0.9996
19	1313	11.66	1	4.357	309.9	1179	0.1167	0.9996
20	140.8	11.62	0	0.4979	303	138.8	0.001683	0.9996
21	140.8	5	0.09724	0.519	277.3	127.9	0.02576	0.9996
22	18.72	5	0	0.08207	277.3	17.93	0.001575	0.9996
23	18.72	1.8	0.08617	0.1022	251.9	8.297	0.0579	0.9996
24	1298	5	0.9995	4.671	287.3	1167	0.2622	0.9996
25	1264	1.8	0.999	5.019	261.9	1140	0.6858	0.9996

Table.3.5 COP, heat transfer rate, exergetic efficiency and exergy destruction at states corresponding to table 3.3

Q_{a1} [kW]	Q_{a2} [kW]	Q_{g1} [kW]	Q_{g2} [kW]	Q_{rec1} [kW]	Q_{rec2} [kW]	Q_{e1} [kW]	Q_{e2} [kW]	COP
49.28	57.3	60.08	76.49	10.96	18.48	35.17	35.17	
Q_{con} [kW]	W_{p1} [kW]	W_{p2} [kW]	η_{ex} [%]	δ_{tot} [%]	$\dot{E}_{d,tot}$ [kW]	$\dot{E}P$ [kW]	$\dot{E}F$ [kW]	0.5138
68.75	0.1146	0.2114	15.47	84.38	17.42	4.779	30.9	

Table.3.6 Various properties at different state points of ammonia-water DE VAR cycle at $P_{h1} = 12$ bar, $P_{h2} = 12$ bar, $T_{g1} = 373$ K, $T_{g2} = 393$ K, $T_{a1} = 308$ K and $T_{a2} = 313$ K

State point	h [kJ/k]	P [kPa]	q	s	T [K]	u [kJ/k]	v [m^3/kg]	X
1	-61.23	5	0	0.4357	313	-61.84	0.001227	0.4993
2	-60.37	12	-0.001	0.4357	313.1	-61.84	0.001226	0.4993
3	88.83	12	0.003944	0.8887	344.7	86.69	0.001783	0.4993
4	173.3	12	0	1.12	363	171.8	0.001249	0.3994
5	-5.651	12	-0.001	0.5983	323.2	-7.073	0.001185	0.3994

6	-5.651	5	-0.001	0.6009	323.3	-6.244	0.001185	0.3994
7	1491	12	1.001	4.861	363	1325	0.1377	0.9678
8	173.3	12	0	1.12	363	171.8	0.001249	0.3994
9	1296	12	1	4.284	309.9	1166	0.1086	0.9996
10	-59.84	1.8	0	0.409	308	-60.05	0.001147	0.3519
11	-58.67	12	-0.001	0.409	308.1	-60.05	0.001147	0.3519
12	188.2	12	-0.001	1.145	364	186.8	0.001221	0.3519
13	288.5	12	0	1.391	383	287	0.00123	0.3067
14	24.42	12	-0.001	0.6418	323.3	23.05	0.001141	0.3067
15	24.42	1.8	0.01333	0.6457	318.2	22.19	0.01241	0.3067
16	1599	12	1.001	5.129	383	1424	0.1459	0.9149
17	288.5	12	0	1.391	383	287	0.00123	0.3067
18	1296	12	1	4.284	309.9	1166	0.1086	0.9996
19	1313	11.66	1	4.357	309.9	1179	0.1167	0.9996
20	140.8	11.62	0	0.4979	303	138.8	0.001683	0.9996
21	140.8	5	0.09724	0.519	277.3	127.9	0.02576	0.9996
22	18.72	5	0	0.08207	277.3	17.93	0.001575	0.9996
23	18.72	1.8	0.08617	0.1022	251.9	8.297	0.0579	0.9996
24	1298	5	0.9995	4.671	287.3	1167	0.2622	0.9996
25	1264	1.8	0.999	5.019	261.9	1140	0.6858	0.9996

Table.3.7 COP, heat transfer rate, exergetic efficiency and exergy destruction at states corresponding to table 3.5

Q_{a1} [kW]	Q_{a2} [kW]	Q_{g1} [kW]	Q_{g2} [kW]	Q_{rec1} [kW]	Q_{rec2} [kW]	Q_{e1} [kW]	Q_{e2} [kW]	COP
49.77	71.55	57.71	85.66	8.144	13.69	35.17	35.17	
Q_{con} [kW]	W_{p1} [kW]	W_{p2} [kW]	η_{ex} [%]	δ_{tot} [%]	$\dot{E}_{d,tot}$ [kW]	$\dot{E}P$ [kW]	$\dot{E}F$ [kW]	0.4883
68.75	0.1568	0.5076	16.08	83.92	16.49	4.779	30.01	

CHAPTER- 4

RESULTS AND DISCUSSIONS

4.1 Introduction

A computer program has been developed using Engineering Equation Solver (EES) software [14] for carrying out energy and exergy analysis of double evaporator NH_3-H_2O VARS. The thermodynamic properties of saturated and superheated NH_3-H_2O solutions is calculated based on correlations Patek and klomfar [15] by generating a computer program.

4.2 Energy analysis

4.2.1 Heat duty in various components of the system

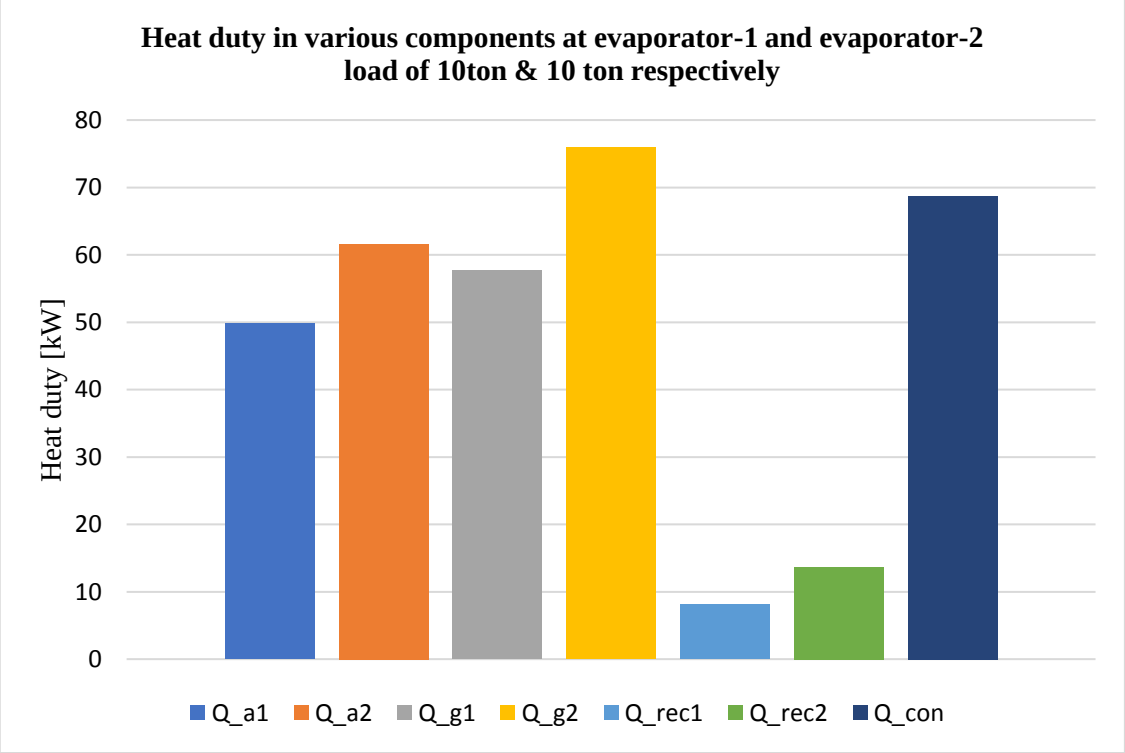

Fig.4.1 Heat duty in components at cooling load in $Q_{e1} = 10$ ton, $Q_{e2} = 10$ ton

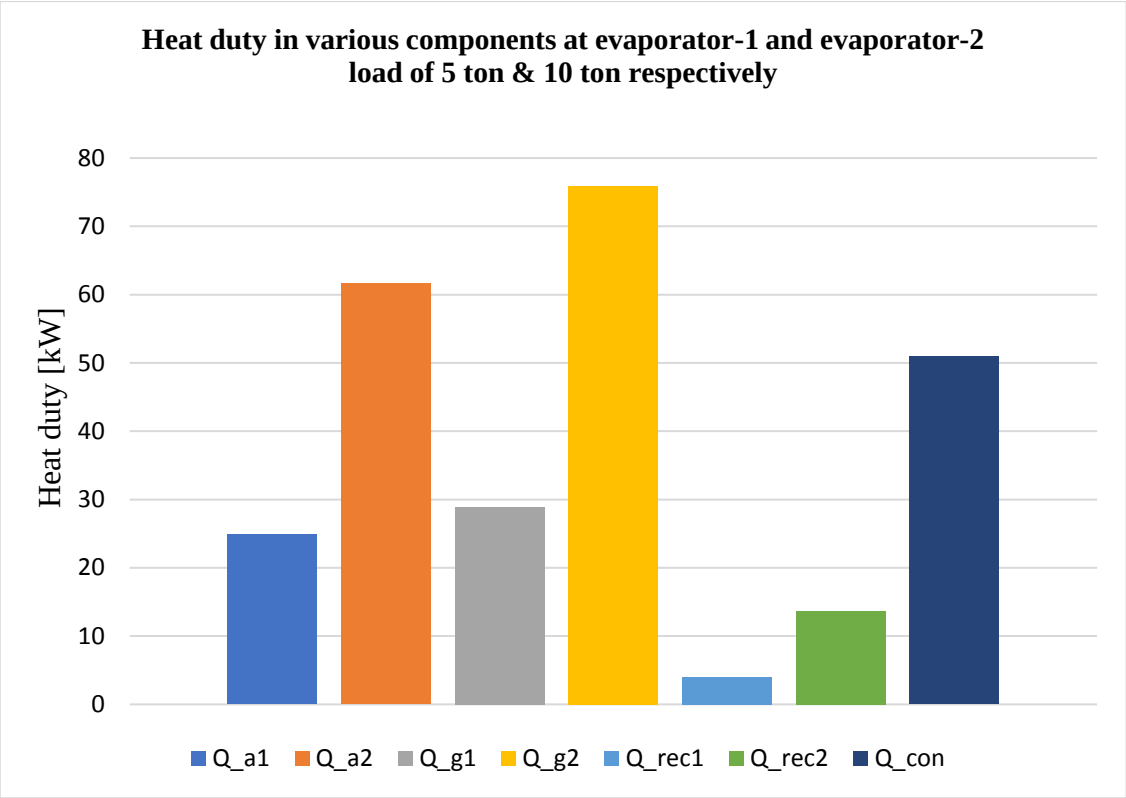

Fig.4.2 Heat duty in components at cooling load in $Q_{e1} = 5$ ton, $Q_{e2} = 10$ ton

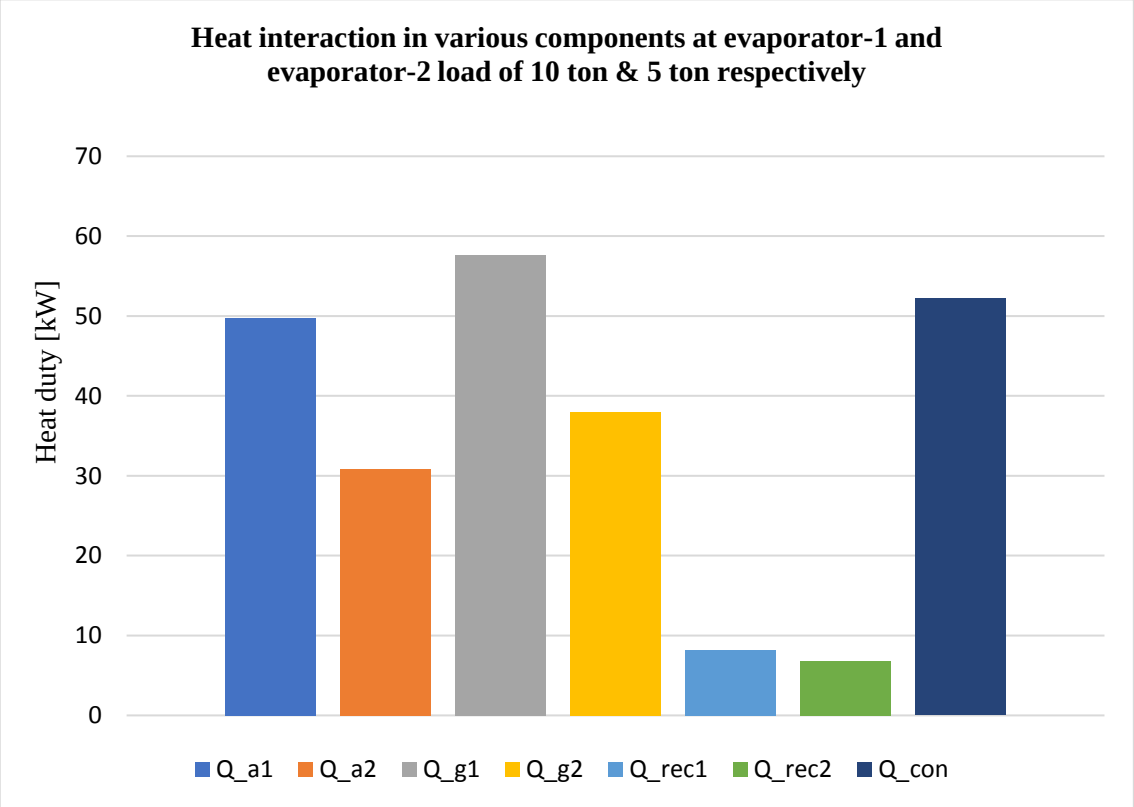

Fig.4.3 Heat duty in components at cooling load in $Q_{e1} = 10$ ton, $Q_{e2} = 5$ ton

Fig.4.1 to 4.3 shows the heat duty in the components of the system at different cooling load in evaporator-1 and evaporator-2. At cooling load of 10 ton in both the evaporator, heat duty is highest in generator-2 (approx. 75 kW) followed by condenser and absorber-2. Fig.4.2 depicts that decrease in cooling load in evaporator-1 decreases the heat duty in high pressure circuit i.e. absorber-1, generator-1 and rectifier-1 but doesn't affect the heat duty in low pressure circuit i.e. generaror-2, absorber-2 and rectifier-2 similarly by decreasing cooling load in evaporator-2 decreases the heat duty in low pressure circuit not affecting heat duty in high pressure circuit as shown in Fig.4.3.

The decrease in the heat duty with the decrease in evaporator load in the corresponding circuit is due to decrease in the mass flow rate in the corresponding circuit which correspondingly decrease the heat duty in the components of the corresponding circuit.

4.2.2 Effect of generator-1 and generator-2 temperature on the COP and solution circulation ratio in high pressure and low pressure circuit

Fig.4.4 to 4.6 shows the effect of variation of temperature of generator-1 and generator-2 on the coefficient of performance (COP) and solution circulation ratio (SCR) of the system. It is observed that at constant temperature of generator-2 (110^oC), as the generator-1 temperature increases, the coefficient of performance(COP) of the system first increases reaching maximum value of 0.53 at generator-1 temperature of approx. 85^oC and then COP decreases as the temperature further increases, similarly at constant temperature of generator-1 (90^oC), as the generator-2 temperature increases, the value of COP increases up to a value of 0.515 at a temperature of 110^oC, then COP decreases as the temperature increases further. At others temperature of generator which is kept to be constant, there is low value of COP.

The reason for increasing COP up to some temperature is due to generation of more ammonia vapours which increases refrigeration effects in comparison to increase in heat transfer to generator and it is also due to decrease in solution circulation ratio which decreases heat duty in generator. But after certain temperature, increase in generator temperature increases the average temperature of condenser, rectifier and absorber in the particular circuit which increase the irreversibility of these components as discussed in exergy analysis thus increase in COP due to increase in temperature is offset by the decrease in COP due to increase in irreversibility of components but the variation of COP of system is more pronounced of changing in generator-2 temperature i.e. T_{g2} than T_{g1}. This is due to the higher temperature of the generator-2 in comparison to generator-1 which brings higher irreversibility in components in comparison to generator-1 as the temperature is varied.

The value of solution circulation ratio (f_1&f_2) defined in equation 29&30 for high pressure and low pressure circuit respectively decreases as the generator temperature increases as shown in fig.4.6. This happens because, as the generator temperature increases, the ammonia mass fraction of weak solution increases so for constant absorber temperature, difference in mass fraction of strong and weak solution decreases, therefore SCR decreases as shown in fig.4.6. SCR affects the heat duty in the components of the system like generator-1&2, absorber-1&2.

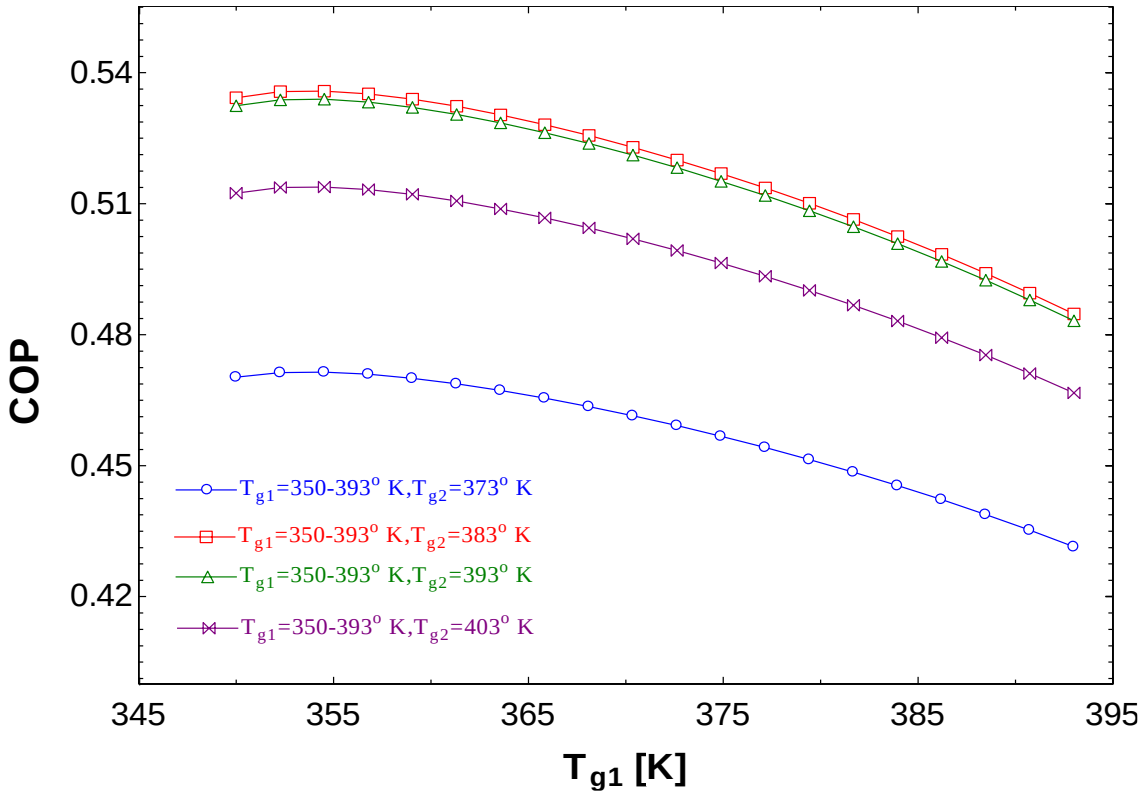

Fig.4.4 Variation of COP with T_{g1} at different T_{g2}

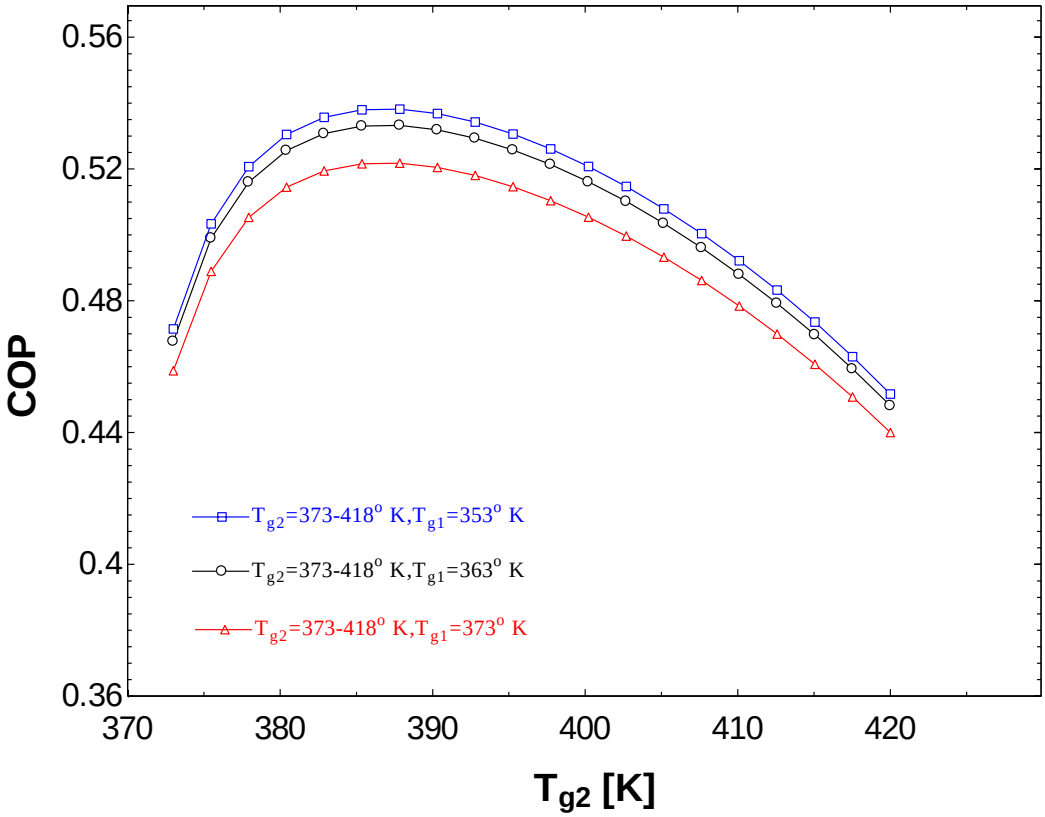

Fig.4.5 Variation of COP with T_{g2} at different T_{g1}

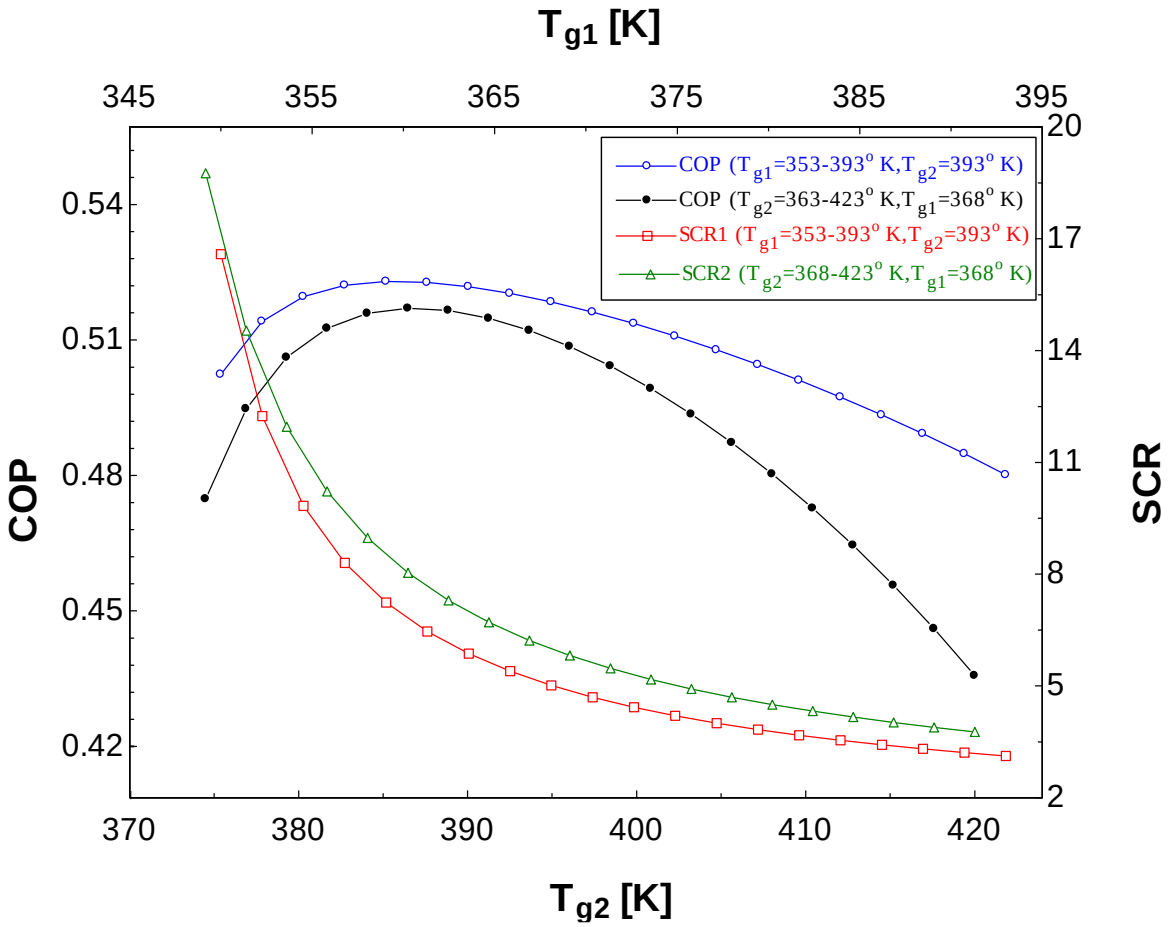

Fig.4.6 Variation of COP and SCR with T_{g1} and T_{g2}

4.2.3 Effect of generator-1 and generator-2 pressure on COP

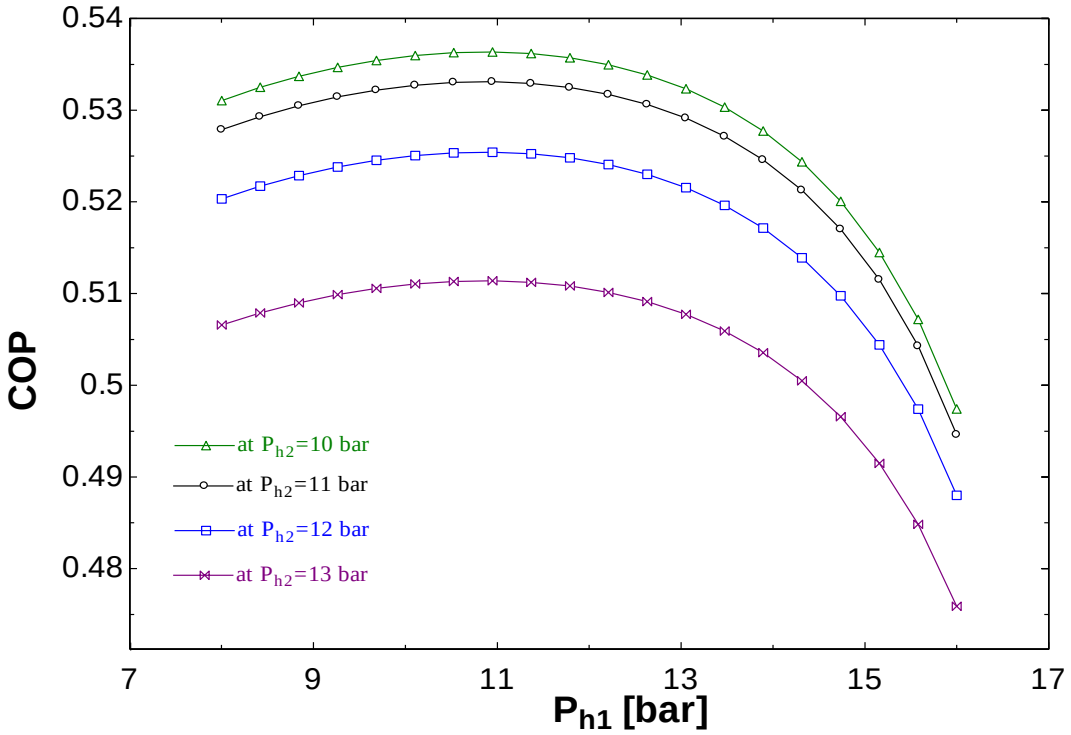

Fig.4.7 Variation of COP with P_{h1} at different P_{h2}

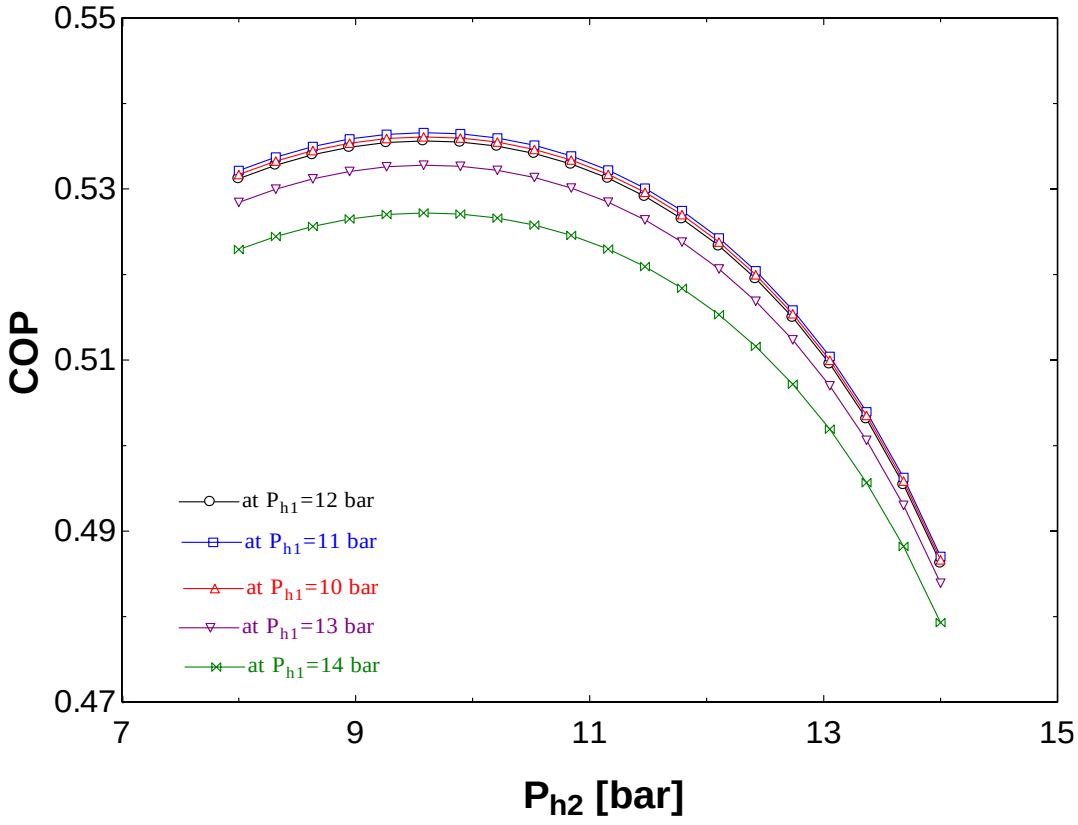

Fig.4.8 Variation of COP with P_{h2} at different P_{h1}

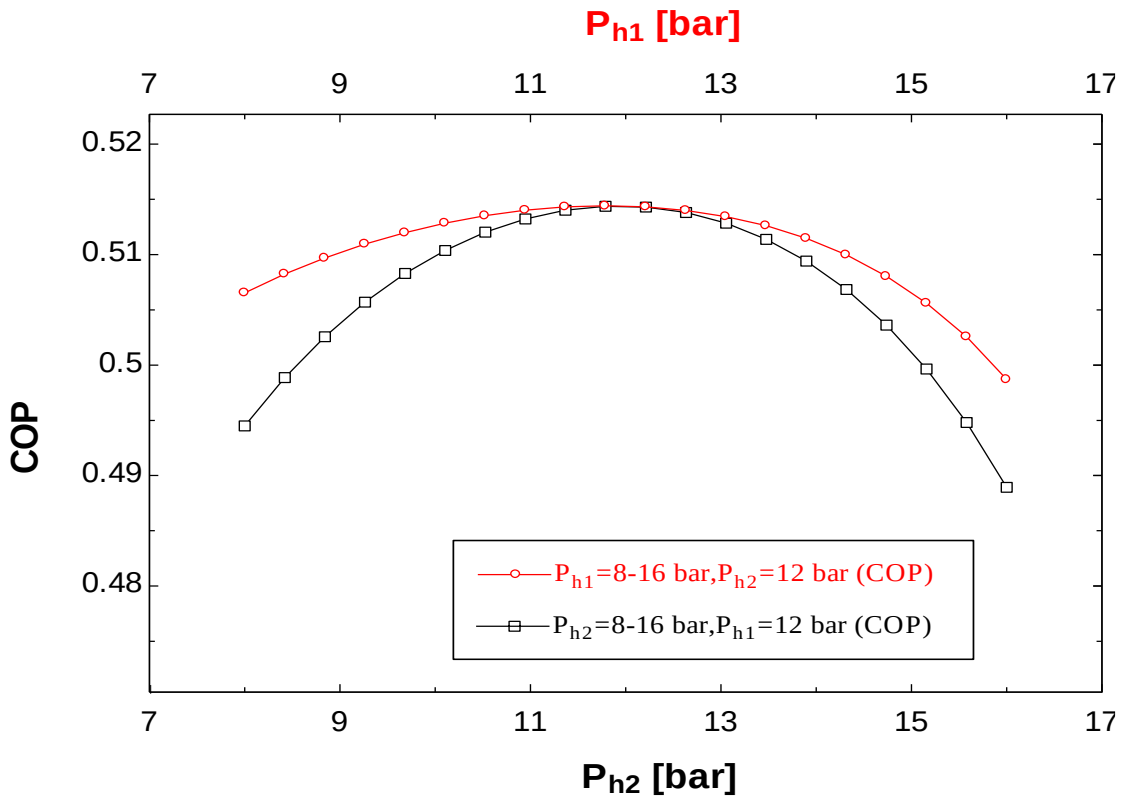

Fig.4.9 Variation of COP with P_{h1} and P_{h2} together

Fig.4.7 to 4.9 shows the variation of both the generator pressure i.e. P_{h1} & P_{h2} on the COP of system. It is observed from Fig.4.7 that at constant generator-2 pressure, As generator-1 pressure vary, the COP of system first increase up to some pressure and then it starts decreasing and maximum value is obtained at the pressure of approximately 11.5 bar in generator-1 and maximum value of COP is obtained at constant generator-2 pressure of 10 bar and COP decreases with increases in generator-2 pressure similarly from Fig.4.8 it is observed that at constant generator-1 pressure, As the generator-2 pressure increases, the COP of the system first increases and then it decreases with further increase in P_{h2}. This is due to the fact that as generator pressure increases, the temperature of the corresponding generator also increases, so the variation of COP with generator pressure is likely to behave in same manner as that of the generator temperature which explained in detail in section 4.2.1, but the effect of varying generator-2 pressure is more on the COP of the system than varying the generator-1 pressure because temperature in generator-2 is more corresponding to that of the generator-1, so varying of generator-2 pressure causes more irreversibility in the system due to which COP of system decreases. This is also due to the fact that generator-2 temperature has more effect on COP than generator-1 as discussed in section 4.2.1.

4.2.4 Effect of evaporator-1 and evaporator-2 temperature on the COP

Fig.4.10 shows the effect of temperature of the evaporator-1 & 2 on the coefficient of performance (COP) of system. The value of COP of the system increases by 5 % as the inlet temperature of the evaporator-1 increases from 273° K to 290° K at constant inlet temperature of 263° K in evaporator-2 and the value of COP of the system increases by 10.75 % as the inlet temperature of the evaporator-2 increases from 243° K to 253° K at constant inlet temperature of 277° K in evaporator-1.

This is due to the fact that as temperature of both evaporator increases, the lower pressure in evaporator and absorber increases so difference between high and low pressure decreases which reduces irreversibility in the generator and absorber due to decrease in difference of temperature of strong and weak solution going to absorber & generator and coming out of them as discussed in section 4.2.5. in detail.

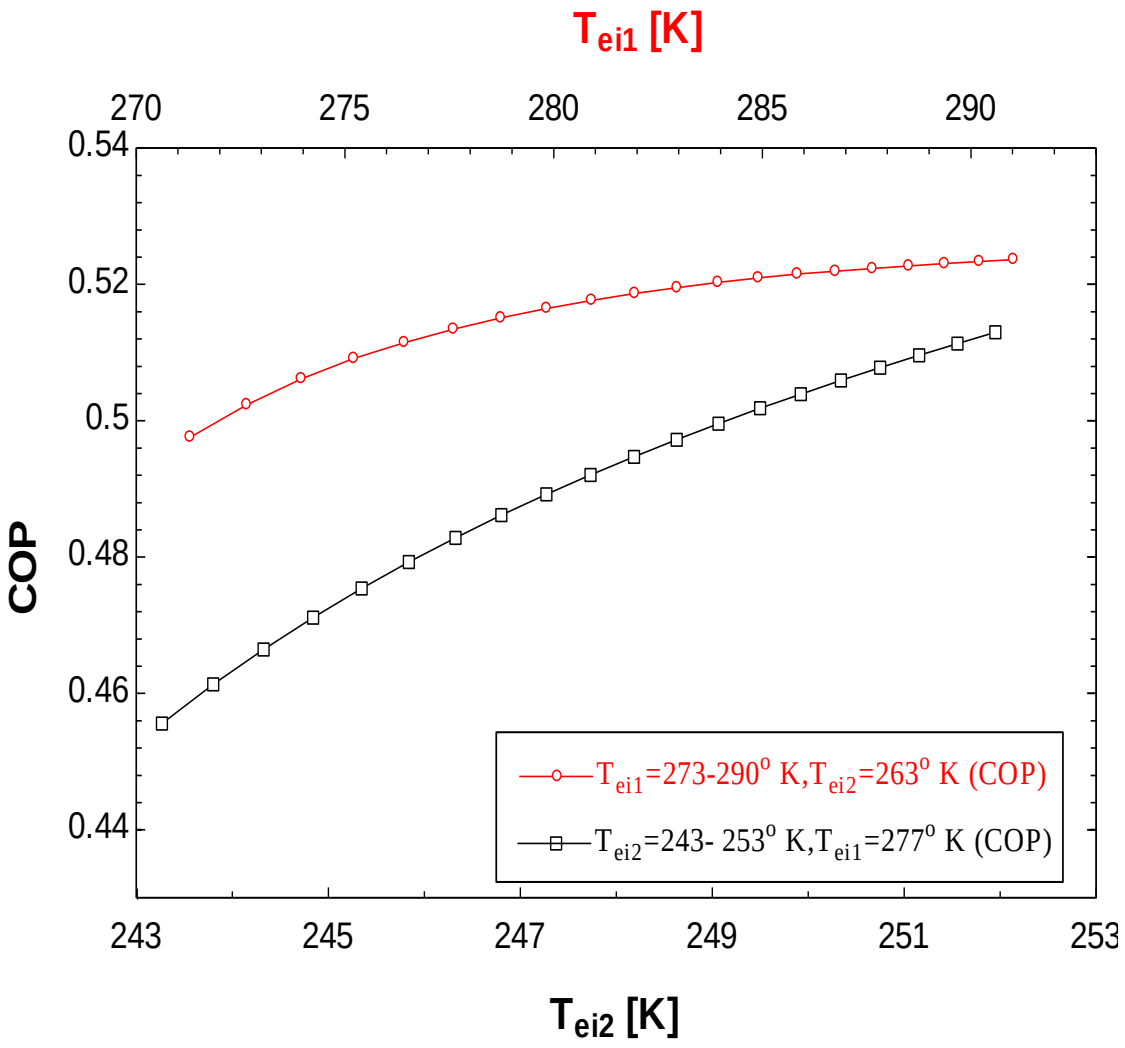

Fig.4.10 Variation of COP with T_{ei1} and T_{ei2}

4.2.5 Effect of condenser temperature on the COP of system

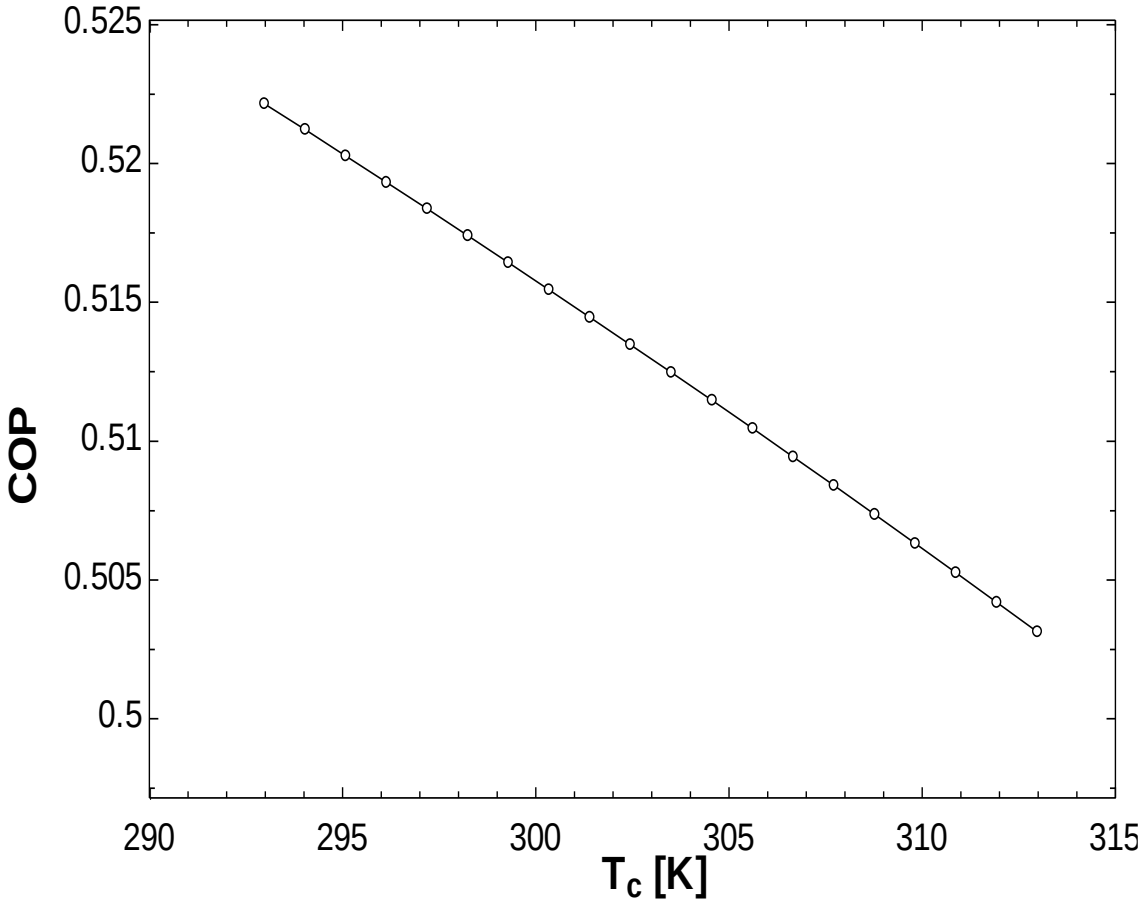

Fig.4.11 Variation of COP with T_c

Fig.4.11 shows the effect of condenser temperature on the COP of the system. The value of the COP of the system decreases by 3.8 % as the condenser temperature increases from 293° K to 313° K. this is because of the fact that temperature of the absorber-1 and absorber-2 remains doesn't change, hence 'X_{ss1}' & 'X_{ss2}' remains constant, whereas 'X_{ws1}' and 'X_{ws2}' decreases since the T_{g1} and T_{g2} is constant but the P_{h1} and P_{h2} increases due to increase in condenser temperature. This also causes an increase in solution circulation ratio, so increase in circulation losses and increase in irreversibility in components and thus reduction in COP.

4.2.6 Effect of absorber-1 and absorber-2 temperature on the COP of system

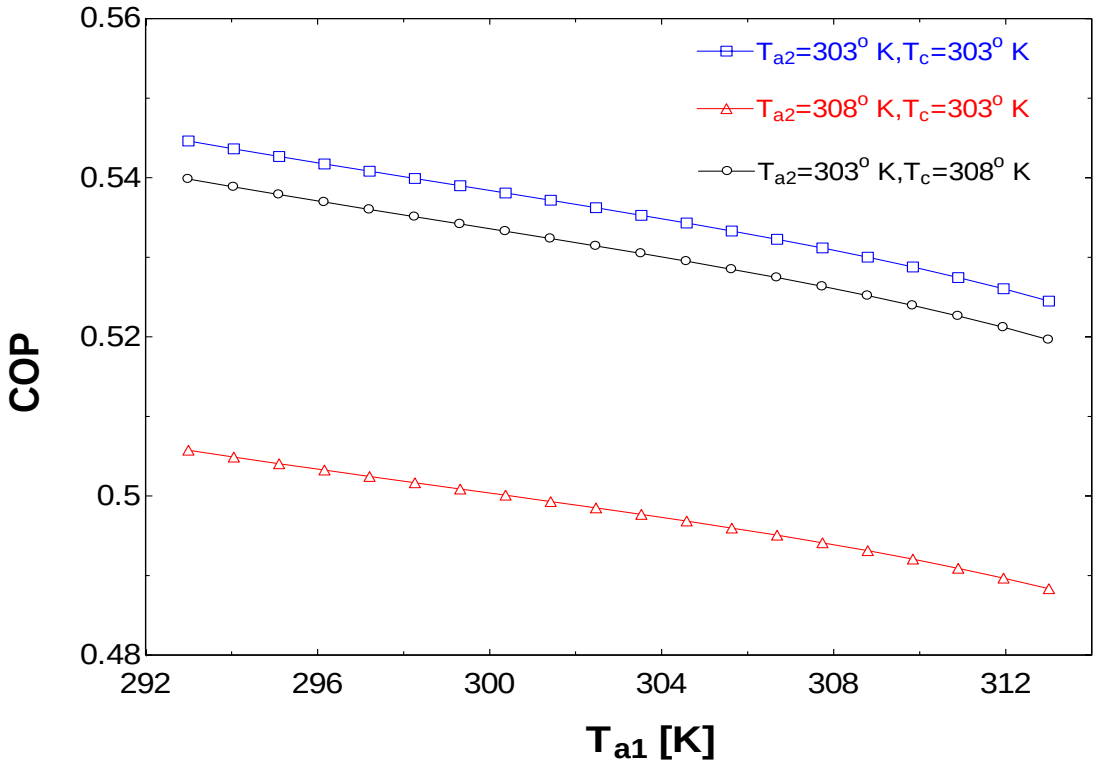

Fig.4.12 Variation of COP with T_{a1} at different T_{a2}

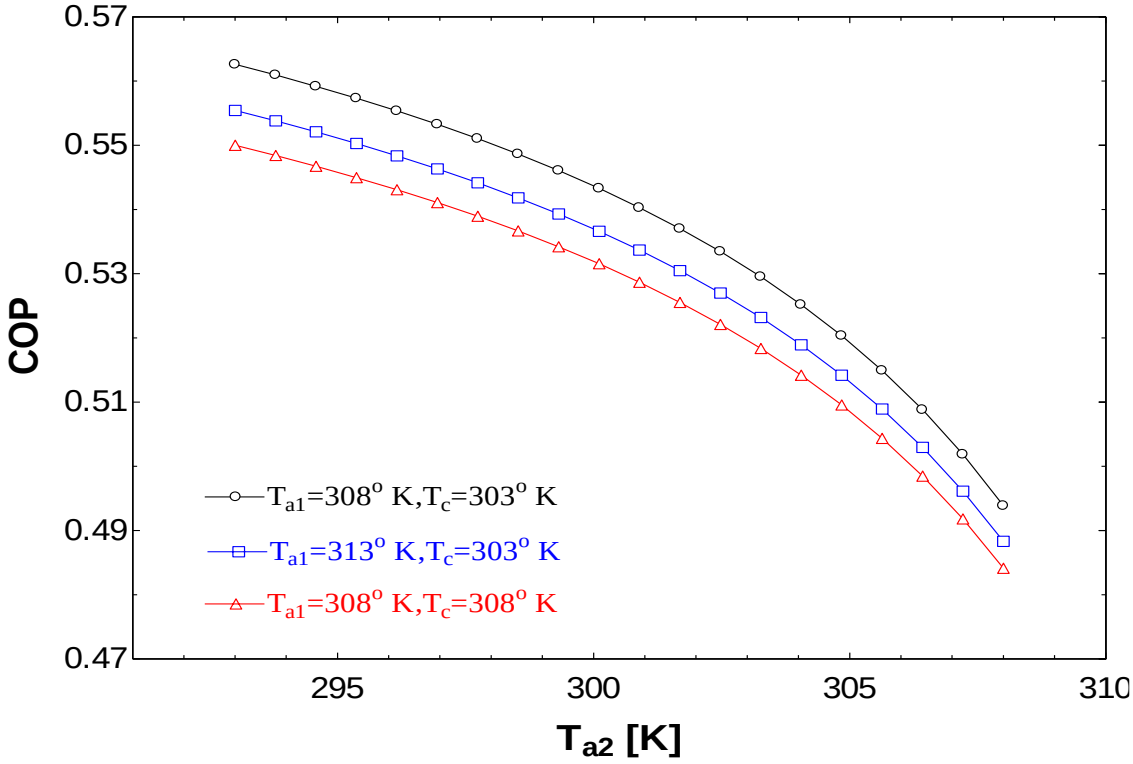

Fig.4.13 Variation of COP with T_{a2} at different T_{a1}

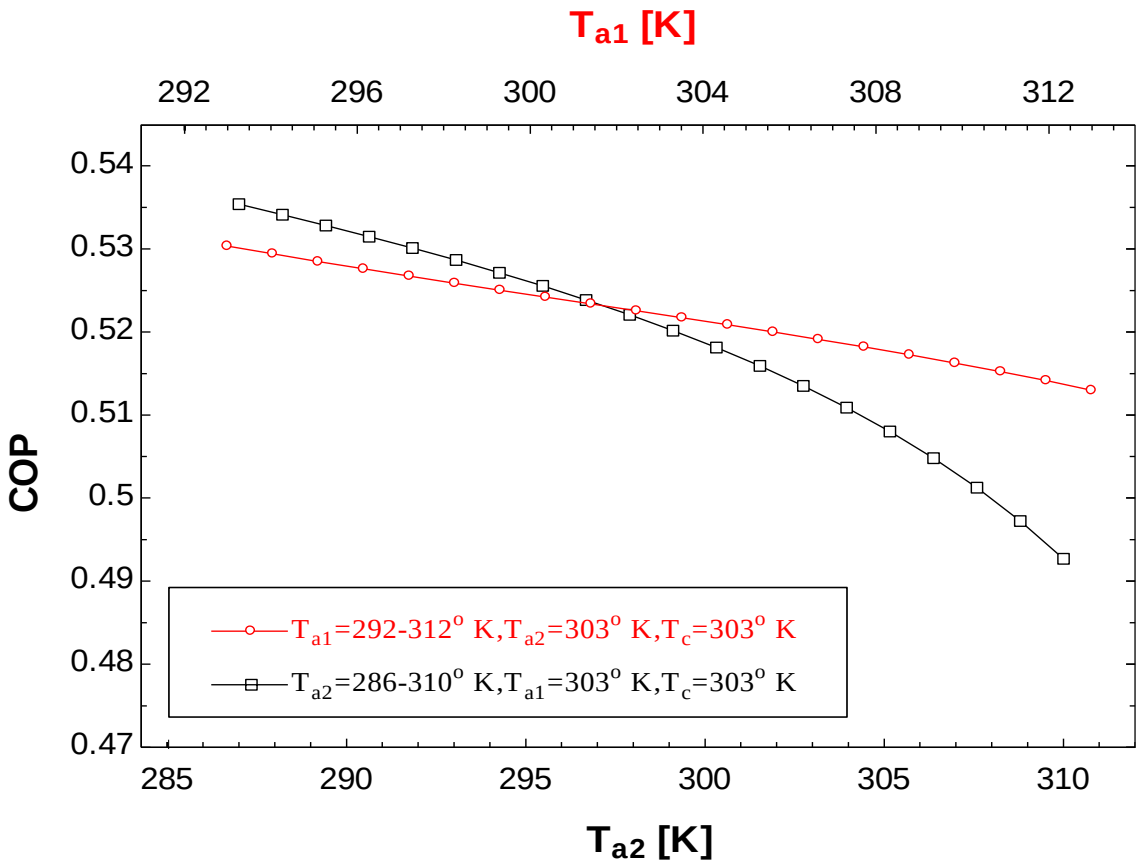

Fig.4.14 Variation of COP with T_{a1} and T_{a2}

Fig.4.12 to 4.14 shows the effect of absorber-1 and absorber-2 temperature on the coefficient of performance (COP) of the system. As the temperature of either of the absorber increases, the COP of the system decreases. This is due to the fact that as the absorber temperature increases, the SCR (Equation 44&47) in the solution circuit increases because ammonia mass fraction of strong solution (SS) decreases so difference between ammonia mass fraction between strong and weak solution decreases which will increase SCR. As SCR increases, mass of strong and weak solution increases which increase heat duty of generator or heat transfer to generator so at constant cooling load in evaporator, the COP of the system decreases. But the effect of temperature of absorber-2 has been more pronounced on the performance of the system as that of temperature of absorber-1 as shown in fig. 13 since the value of COP decreases by 3.8 % and 8.4 % when temperature in absorbe-1&2 varies from 293° K to 313° K. this is because pressure in absorber-2 is lower in comparison to absorber-1 so difference in pressure in generator-2 and absorber-2 is more and as discussed in section 4.2, the effect of high temperature of generator is more So variation in COP is more in absorber-2 in comparison to absorber-1.

4.2.7 Effect of cooling load of evaporator-1 and evaporator-2 on COP of system

Fig.4.15 shows the variation of evaporator load on the coefficient of performance (COP) of the system. As the cooling load on evaporator-1 increases keeping load on evaporator-2 constant, the value of COP increases but the COP decreases when the load on the evaporator-2 increases keeping load on evaporator-1 constant so it can be concluded that the performance or COP of the system increases as the load is distributed on both the evaporator instead of working on single evaporator-2. The reason for this is that by distributing load on both the evaporator-1 and evaporator-2, the mass flow rate of refrigerant is distributed to low and high pressure circuit and for total constant load on evaporator, the total heat transfer to generator-1 and generator-2 decreases because low heat is required to evaporate ammonia vapour in generator-1 i.e. in high pressure circuit as discussed in detail in section 4.2 .

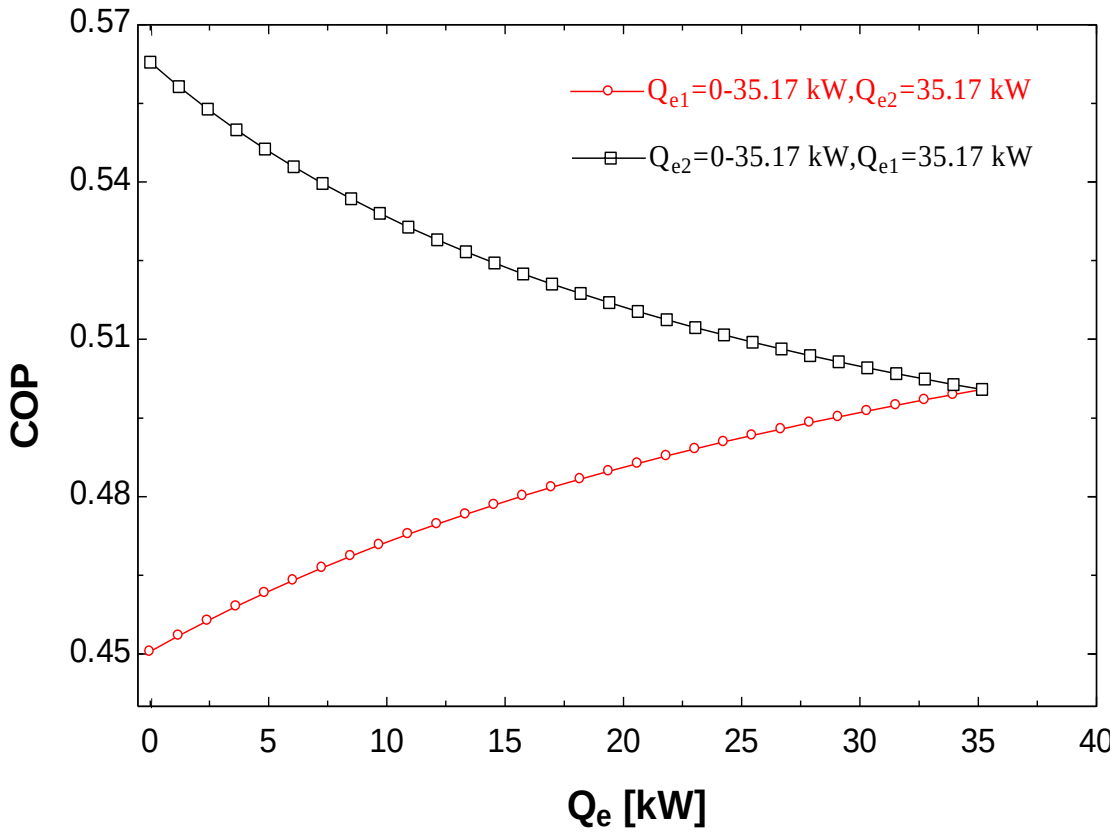

Fig.4.15 Variation of COP with cooling load on the Q_{e1} and Q_{e2}

4.2.8 Effect of SHX-1 and SHX-2 on the COP of system

Fig.4.16 represents the variation of effectiveness of heat exchanger (∈) on the coefficient of performance (COP) of the system. The value of COP increases by 22.7 % and 52.6 %, as the ∈ of both heat exchanger increase from 0.1-1.0. The increase in COP with increase in ∈ is due to the fact that as ∈ increases, more waste heat is utilised in heat exchanger so heat transfer to generator decreases so COP increases. But the variation of COP is more in case of the $\in_{shx2}$ than $\in_{shx1}$ because temperature of weak solution coming out from generator-2 is more as generator-2 temperature is more so more heat is utilised in HX-2 therefore effect of $\in_{shx2}$ is more than the $\in_{shx1}$ as shown in fig.4.16.

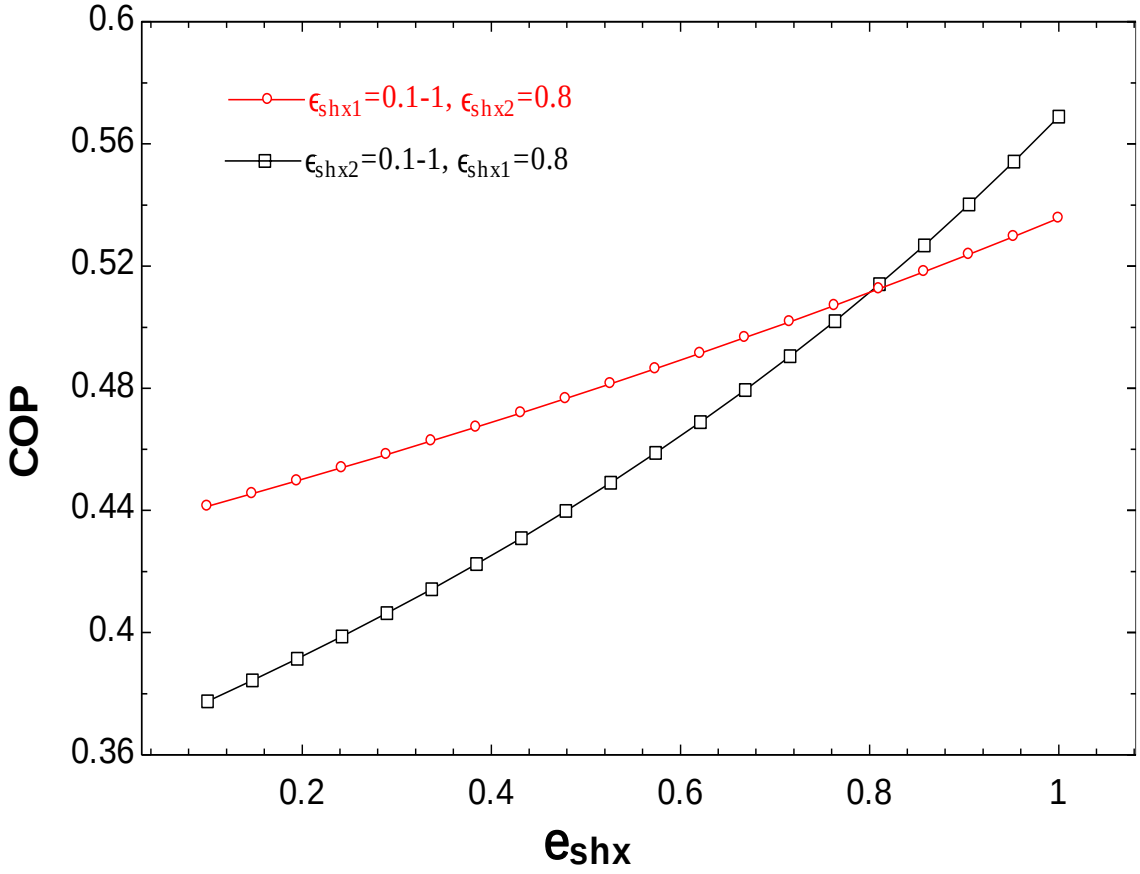

Fig.4.16 Variation of COP with $\in_{shx1}$ and $\in_{shx2}$

4.2.9 Effect of difference in absorber-1, absorber-2 and condenser temperature on COP

Fig.4.17 shows the effect of $T_{a1} \geq T_{a2} = T_c$, $T_{a2} > T_{a1} = T_c$, $T_{a2} \geq T_{a1} > T_c$, $T_{a1} > T_{a2} \geq T_c$, $T_c \geq T_{a1} = T_{a2}$, $T_{a1} \geq T_c \geq T_{a2}$, $T_{a2} = T_{a1} \geq T_c$ and $T_c \geq T_{a1} = T_{a2}$ on the coefficient of performance (COP) of the system. With the increase in T_{a1}, T_{a2} or T_c, a decrease in COP of the system is observed. For the case $T_c \geq T_{a1} = T_{a2}$, the value of COP decreases by 1.5 % when the condenser temperature changes varies from 303° K to 313° K at $T_{a1} = T_{a2} = 303°$ K but the overall value of COP is maximum in this case because condenser temperature has less effect on the COP than absorber temperature as discussed in above section 4.2.4. For the case $T_{a1} = T_{a2} = 313°$ K $\geq T_c$, the value of COP decreases by 1.5 % as the condenser temperature changes from 303° K to 313° K but the overall value of COP is lowest in this case because absorber temperature has more effect on the system especially the temperature of absorber-2 as discussed in section 4.2.4. For the case $T_{a1} > T_{a2} \geq T_c$, the value of COP decreases by almost same value by 1.5% as the condenser temperature changes from 303° K to 313° K but the overall value of COP is higher than the previous case. For the case $T_{a2} > T_{a1} = T_c$, the value of COP decreases by 3.9% as the absorber temperature-2 temperature varies from 303° K to 313° K. For the case $T_{a2} \geq T_{a1} > T_c$, the value of COP decrease by almost same value of 3.9 % but the overall value of COP is lower than the previous case due to higher temperature of absorber-1. For the case $T_{a1} \geq T_{a2} = T_c$, the value of COP decrease by 1.5 % as the temperature of absorber-1 varies from 303° K to 313° K, but the overall value of COP is highest as it coincide with the case $T_c \geq T_{a1} = T_{a2}$ So It is concluded from the results that at constant temperature of 303^oK in other components, the variation in COP is almost same when we vary absorber-1 and condenser temperature between 303^oK to 313^oK. It is also concluded from fig.4.17 that effect of varying absorber-2 temperature has more effect on the COP of system than varying absorber-1 and condenser temperature.

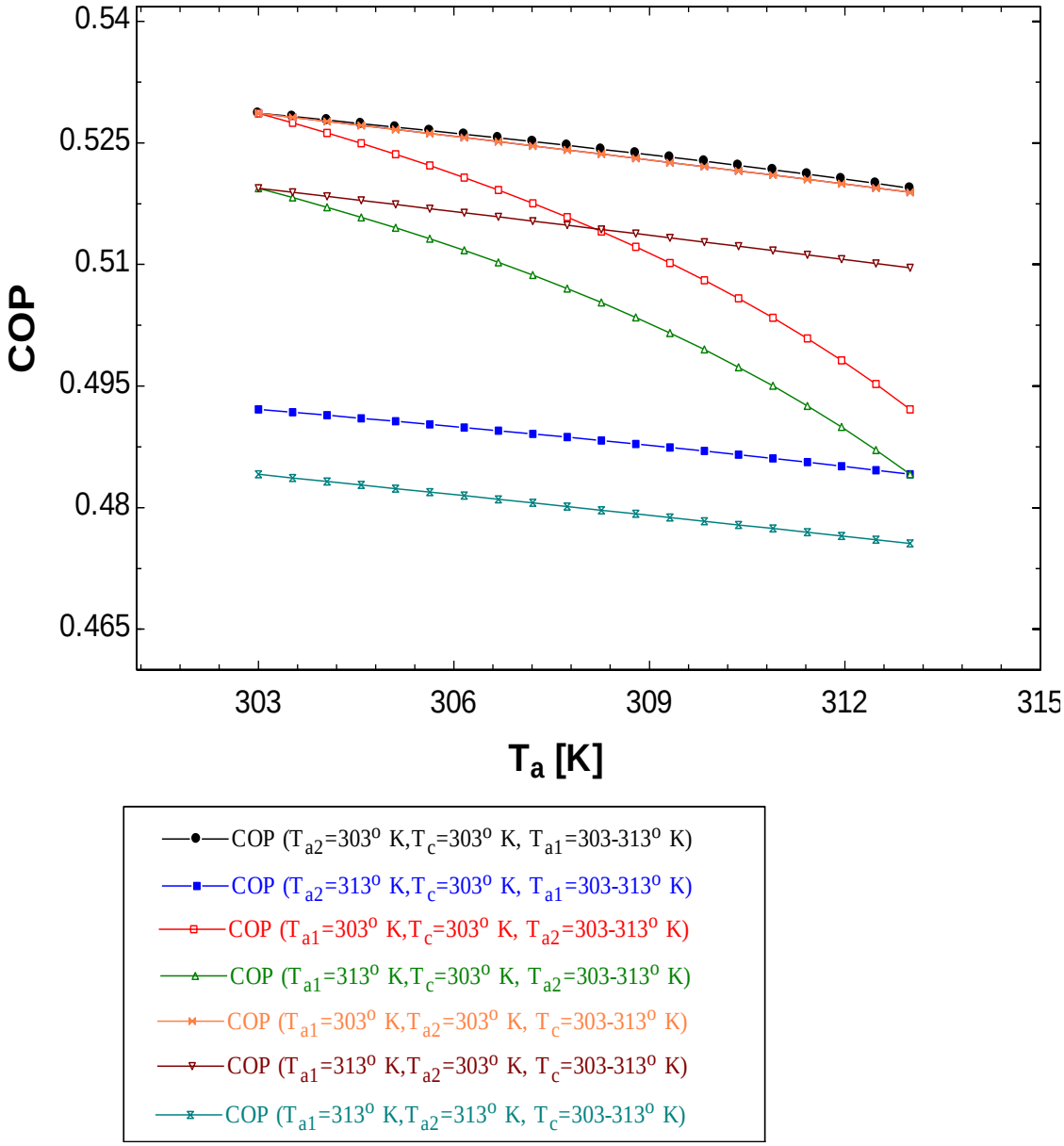

Fig.4.17 Variation of COP of the system with the difference in condenser, absorber-1 and absorber-2 temperature

4.2.10 Effect of ammonia mass fraction (X_r) on the COP of system

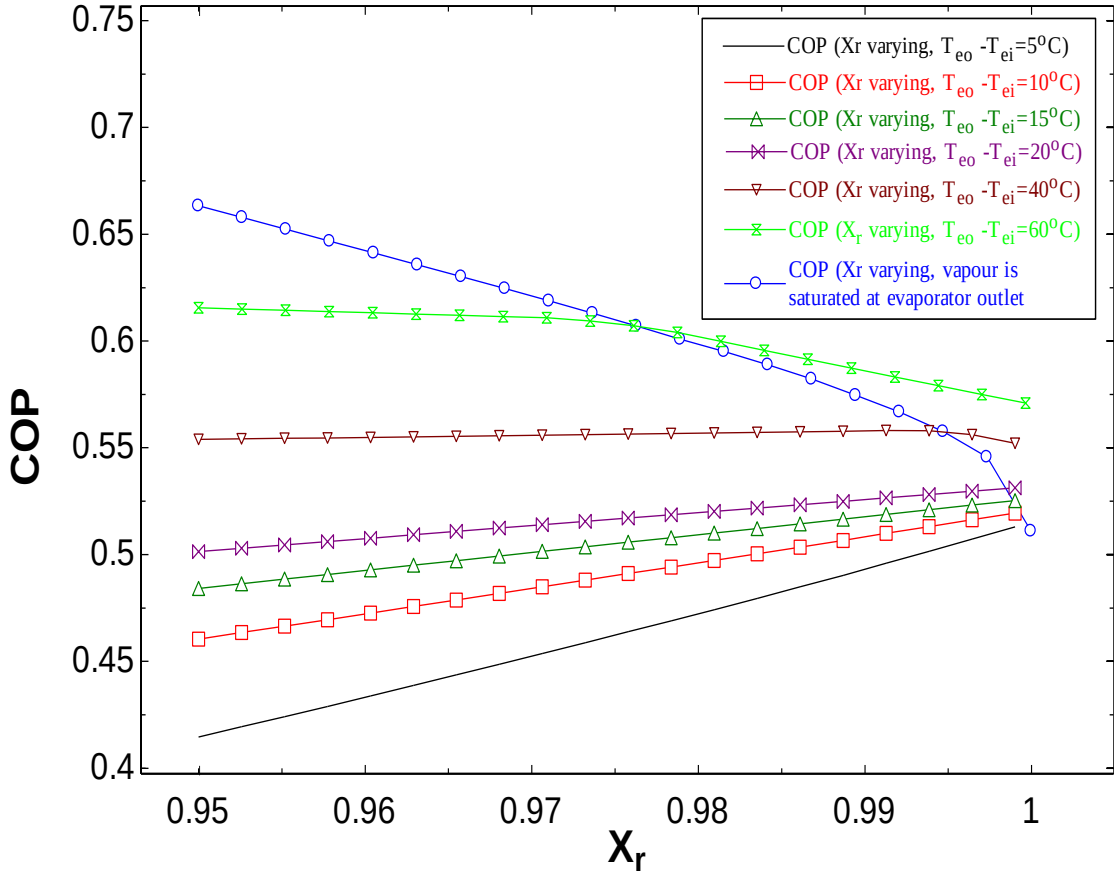

Fig.4.18 Variation of COP of system with ammonia mass fraction (X_r) at different temperature difference between evaporator-1 &2 exit and inlet

Fig.4.18 shows the effect of variation in ammonia mass fraction of vapour coming out from rectifier on the coefficient of performance (COP) of system at varying temperature difference between both evaporator outlet and inlet i.e. $(T_{eo} - T_{ei})_{1,2}$. At temperature difference of $(T_{eo} - T_{ei} = 5^oC)$ between both evaporator outlet and inlet, the COP of the system increase when X_r varies from 0.95-1 and it will remain almost constant at $(T_{eo} - T_{ei} = 40^oC)$ temperature difference but when the temperature difference $(T_{eo} - T_{ei})$ increase after 40^oC the COP variation decreases when X_r varies from 0.95-1.0 as shown in Fig. 17.

4.2.11 Effect of ammonia mass fraction on the evaporator inlet and outlet temperature

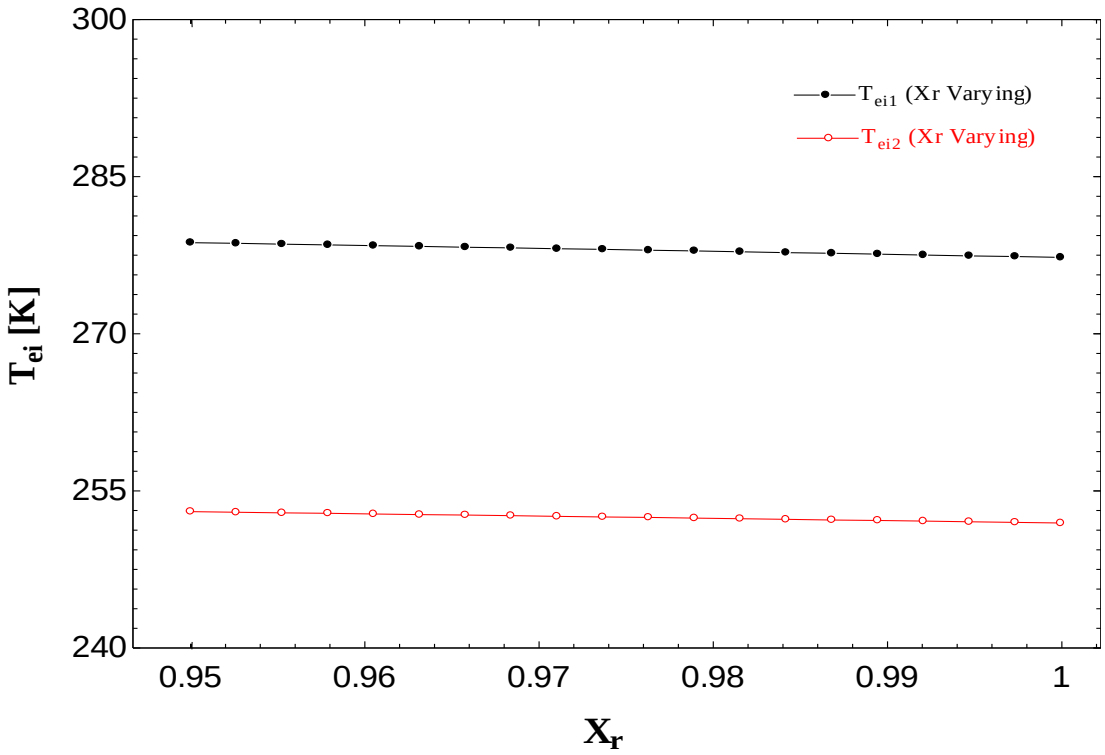

Fig.4.19 Variation of T_{ei} with ammonia mass fraction (X_r)

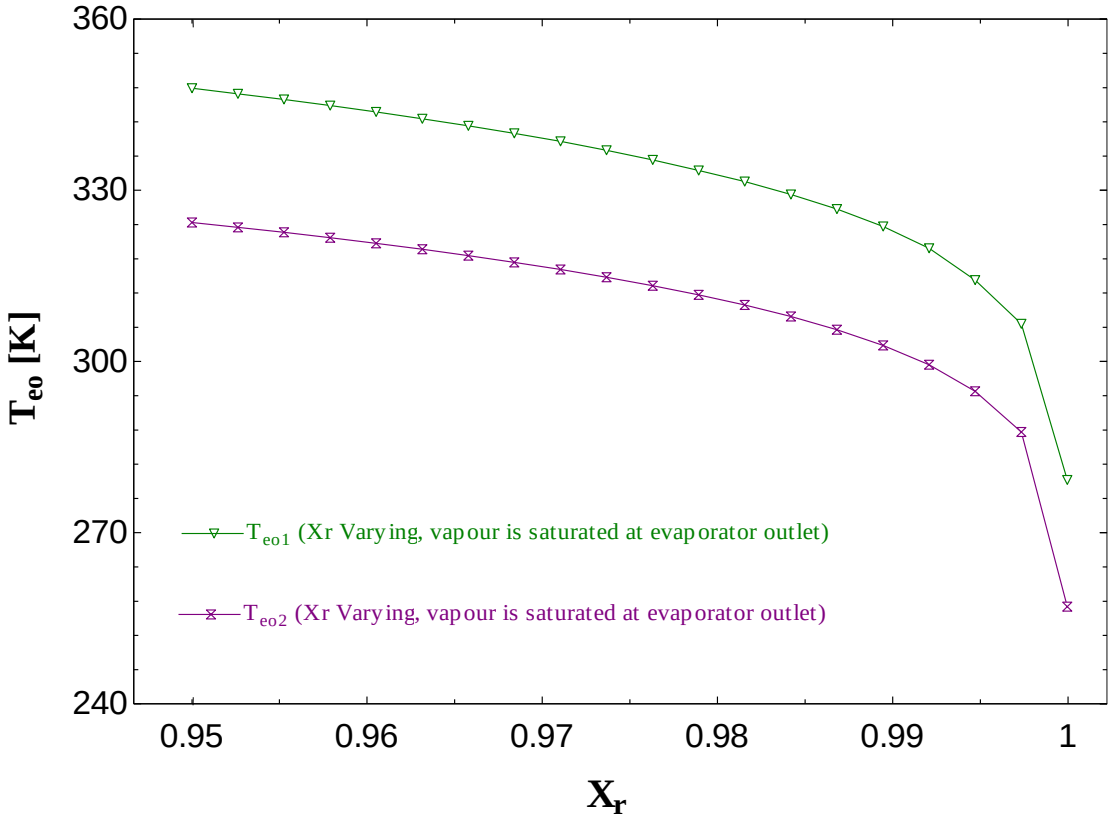

Fig.4.20 Variation of T_{eo} with ammonia mass fraction (X_r)

Fig.4.19 to 4.20 shows the effect of ammonia mass fraction (X_r) coming out from the rectifier on the COP of the system. The inlet temperature of evaporator-1 and evaporator-2 remains unchanged as the X_r varies from the 0.95 to 1 as shown in Fig. 18 because it will not affect the amount of pressure drop in expansion valve and hence temperature remains almost constant at evaporator inlet as X_r varies. However, the temperature at the outlet of both the evaporator is higher when dry saturated vapour is present at outlet in comparison to when wet vapour is present at outlet because to evaporate all the traces of water, the temperature of evaporator should have to increase as water has higher boiling point than ammonia. But the temperature at the exit of evaporator-1 and evaporator-2 decreases as X_r increases from 0.95 to 1 when saturated vapor is coming out from the evaporator outlet. This is due to fact that as X_r increases, the traces of water decrease in ammonia so to evaporates all water, small increase in temperature is sufficient to evaporate all traces of water.

4.3 Exergy analysis

4.3.1 Effect of generator-1 and generator-2 temperature on the exergetic efficiency

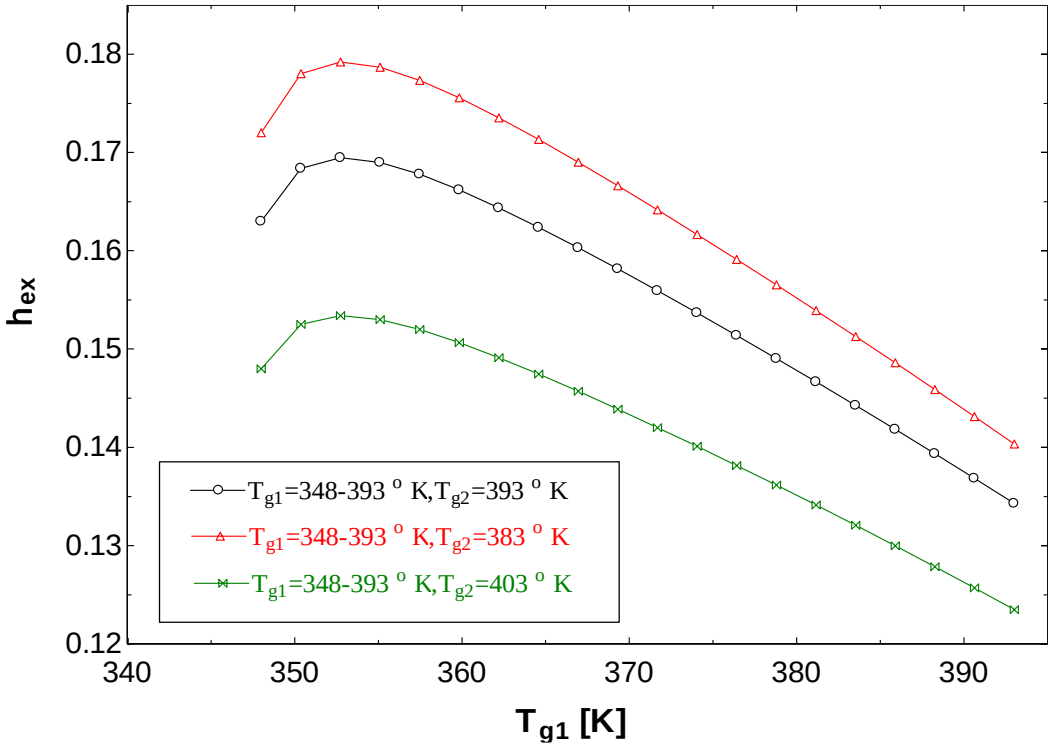

Fig.4.21 Variation of η_{ex} with the T_{g1} at different T_{g2}

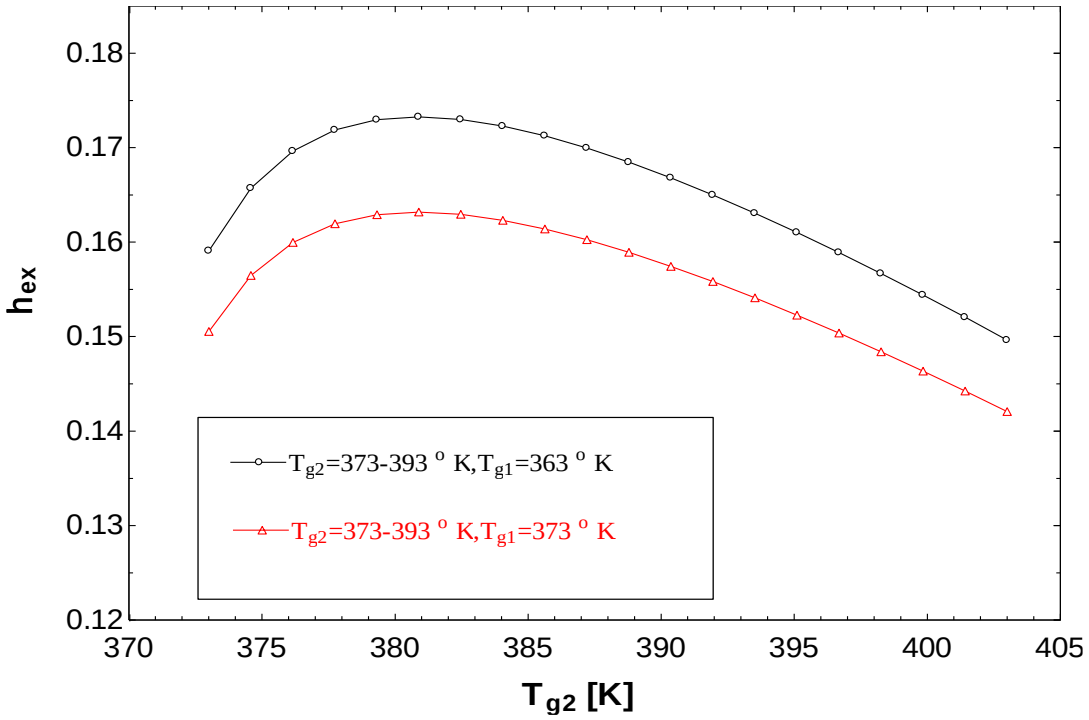

Fig.4.22 Variation of η_{ex} with the T_{g2} at different T_{g1}

Fig.4.21 to 4.22 shows the effect of generator-1 temperature on the exergetic efficiency of the system. It is observed that at constant temperature of generator-2, exergetic efficiency increases with increase in temperature of generator-1 initialy reaching maximum value at approximately 358^{o} K and then it decreases with further increase in generator-1 temperature and also the similar trend is observed with the generator-2 temperature at constant generator-1 temperature. As discuss in detail in section 4.2.1, the effects of increasing the generator temperature have three aspects. Firstly, on increasing the generator temperature more ammonia vapours generated. Secondly, this decreases the SCR due to decrease in the ammonia mass fraction of weak solution , which decreases the heat duty in the generator and the absorber so that exergy of the fuel ($\dot{E}F$) decreases, so exergetic efficiency increases. Thirdly, on increasing the generator temperature but at constant cooling load on the evaporator-1&2, the weak soution and ammonia vapours exiting from the generator in high and low pressure circuit increase, this increases the temperature of absorber-1, absorber-2, and the condenser which brings higher irreversibility in these components at high generator temperature. Therefore increasing the generator temperature initialy increase the COP due to less irreversibility but at high temperature the positive aspects of increase in COP is offset by degradation in COP due to high irreversibility in the components in each circuit so the net effect is the decrease in the exergetic efficiency (η_{ex}).

4.3.2 Effect of evaporator-1 and evaporator-2 inlet temperature on the exergetic efficiency of system

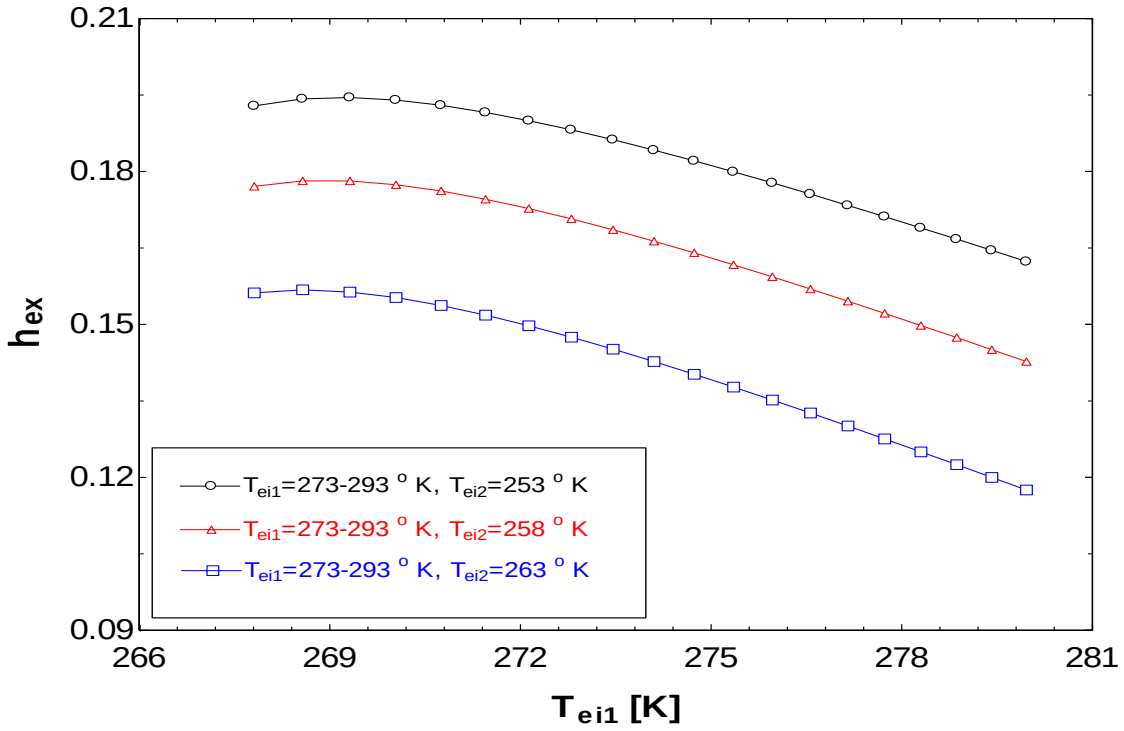

Fig.4.23. Variation of η_{ex} with the T_{ei1} at different T_{ei2}

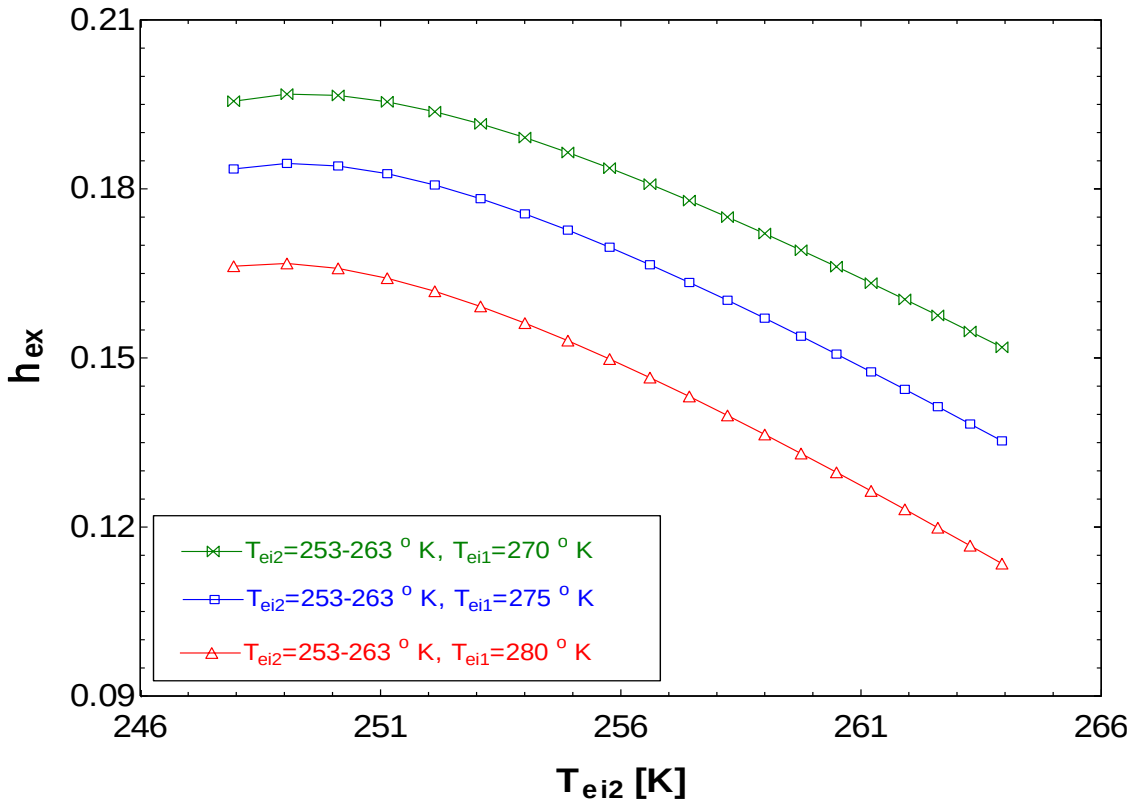

Fig.4.24 Variation of η_{ex} with the T_{ei2} at different T_{ei1}

Fig.4.23 & 4.24 shows the effect of T_{ei1} and T_{ei2} on the η_{ex} of the system. The COP of system increases with increase in evaporator temperature as discuss above in section 4.2.3. but in case of exergetic efficiency (η_{ex}) It is observed that initially the exergetic efficiency is almost constant for some temperature range then it decreases on increasing the inlet temperature of both of the evaporator. Above figure also depicts that when the temperature in the either of the evaporator which is kept constant is increases and other vary, then the value of the η_{ex} of the system decreases as shown in Fig.4.23 & 4.24.

The reason for decrease in η_{ex} is observed from equation (101). As the evaporator temperature increases the exergy of product ($\dot{E}P$) decreases because of decrease in the value of ratio of surrounding temperature and average temperature of evaporator-1&2. Since the exergy of fuel ($\dot{E}F$) is constant therefore η_{ex} of the system decreases.

4.3.3 Effect of absorber-1 and absorber-2 temperature on the COP of system

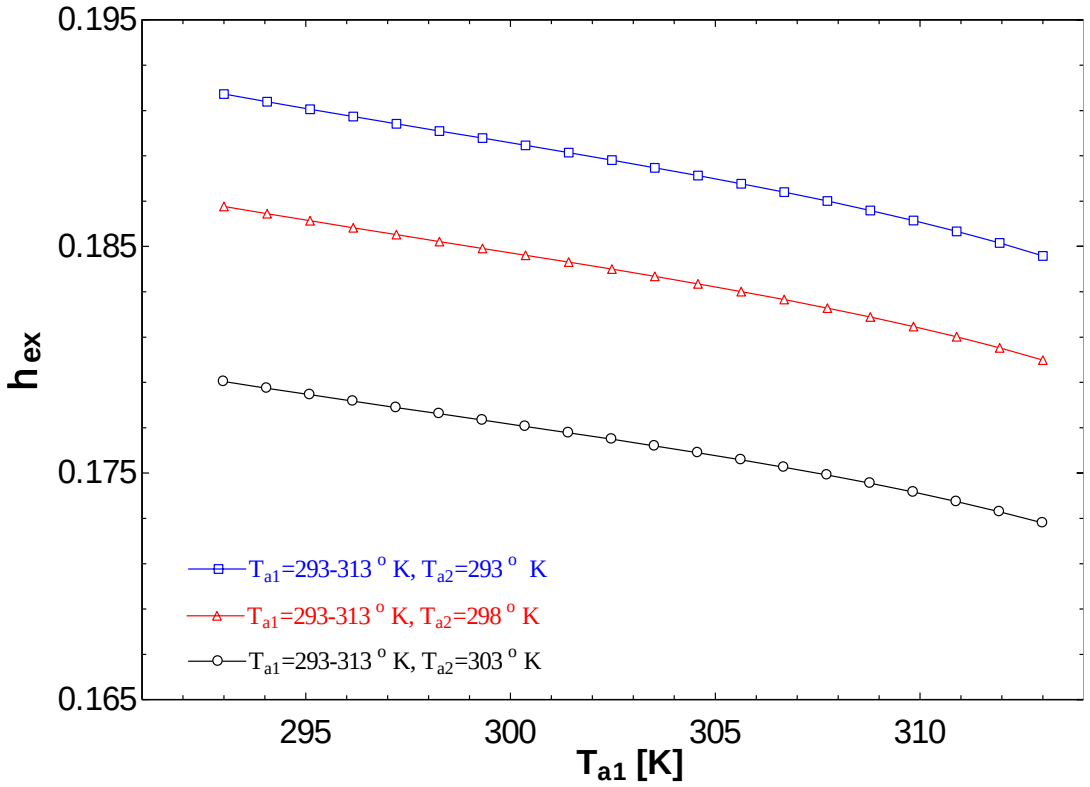

Fig.4.25 Variation of η_{ex} with T_{a1} at different T_{a2}

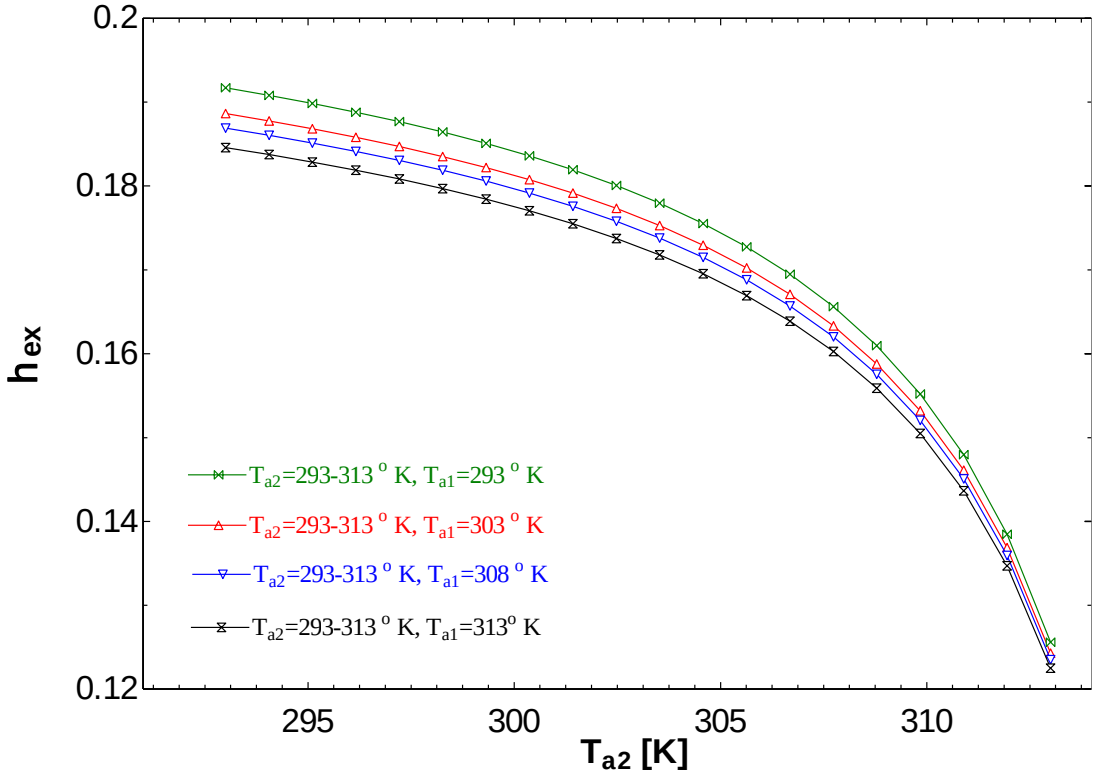

Fig.4.26 Variation of η_{ex} with T_{a2} at different T_{a1}

Fig. 4.25 & 4.26 shows the effect of the absorber-1 and absorber-2 temperature on the η_{ex} of the cycle. It is to be observed that at constant temperature of $293°$ K in absorber-2 and the absorber-1 temperature varied from $293° \text{ K} - 313° \text{ K}$, the η_{ex} of the cycle decreases similarly as the absorber-2 temperature in the same range, the η_{ex} of the cycle decreases but the decrement in the η_{ex} is more in the later case. Also the curve of η_{ex} shifts downward when the constant temperature in absorber-2 increases to $303°$ K as shown in Fig.4.25 similarly when the constant temperature in absorber-1 increases to $313°$ K as shown in Fig.4.26.

The reason for decreasing of η_{ex} with the either of the absorber temperature is due to decrease in ammonia mass fraction of the strong solution in the particular circuit which increase the solution circulation ratio (SCR) of the particular circuit due to which heat duty in the absorber and generator of that circuit increases which also increases the exergy of the generator so exergetic efficiency of the cycle decreases. Also the decrease in η_{ex} due to increase in the constant absorber temperature is due to increase in irreversibility in the absorber and generator of that circuit which will decrease the overall exergetic efficiency.

4.3.4 Effect of solution heat exchanger on the exergetic efficiency of system

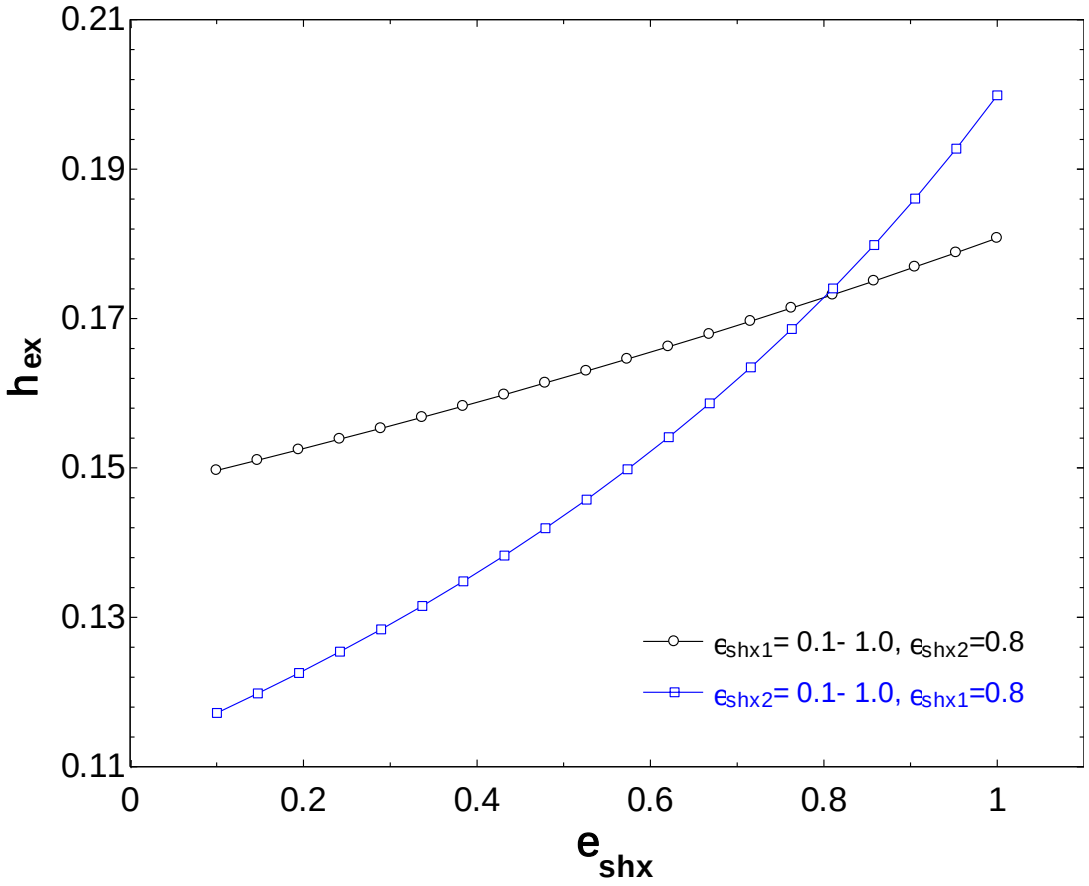

Fig.4.27 Variation of η_{ex} with ϵ_{shx-1} and ϵ_{shx-2}

Fig.4.27 represents the effect of solution heat exchanger effectiveness (ϵ_{shx1} & ϵ_{shx2}) on the exergetic efficiency of the DE VARS cycle. η_{ex} of the cycle increases with increase in the effectiveness of each of the solution heat exchanger. It is observed that the effectiveness of solution heat exchanger '2' (ϵ_{shx2}) has a greater effect on exergetic efficiency of the DE VARS than the effectiveness of solution heat exchanger '1' (ϵ_{shx2}). The value of exergetic efficiency of the system increase by about 16.66 % at $\epsilon_{shx2} = 0.8$ when the effectiveness of ϵ_{shx1} is increased from 0.1 to 1 whereas this value increases by 86.3 % at $\epsilon_{shx1} = 0.8$ when the effectiveness of ϵ_{shx1} is increased from 0.1 to 1.

The increase in exergetic efficiency of the cycle with increase in ϵ_{shx} is due to recovering in the waste heat of the weak solution coming out of generator which decrease heat duty of generator and hence increases the exergetic efficiency. The effect of ϵ_{shx2} is more on η_{ex}, this is due to the higher temperature of generator-2 so more heat is recovered in low pressure circuit.

4.3.5 Effect of generator-1 and generator-2 temperature on the exergy destruction in the system

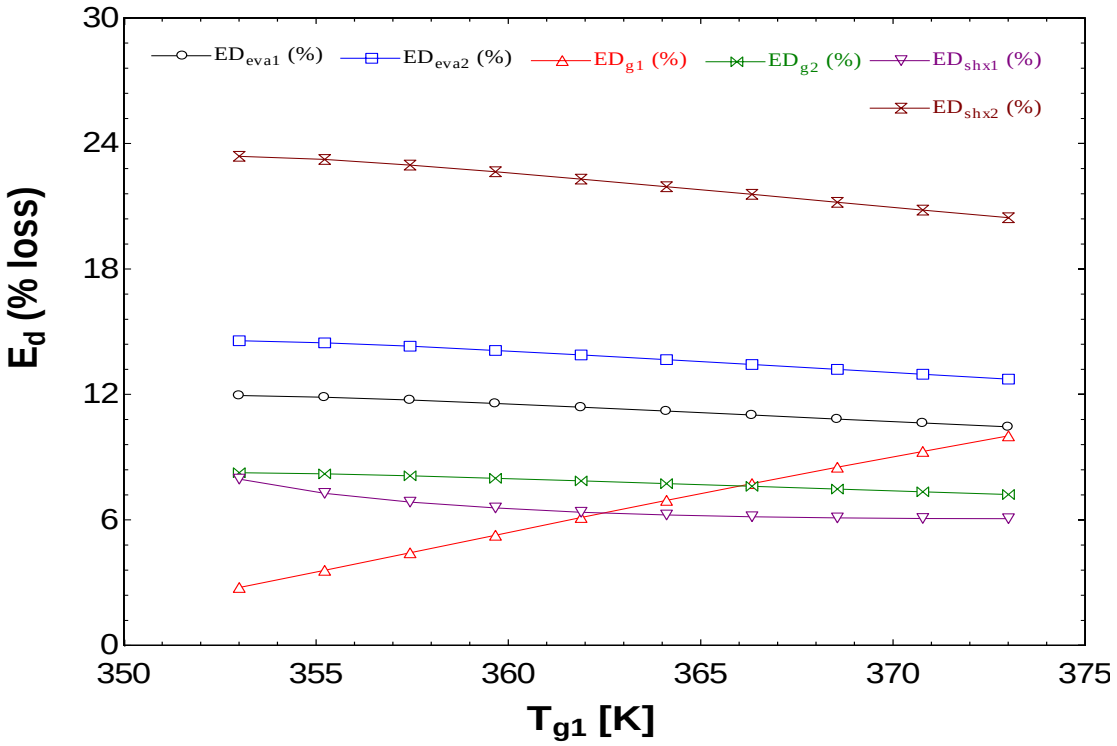

Fig.4.28 Effect of T_{g1} on the exergy destruction in evaporator-1&2, generator-1&2, SHX-1&2

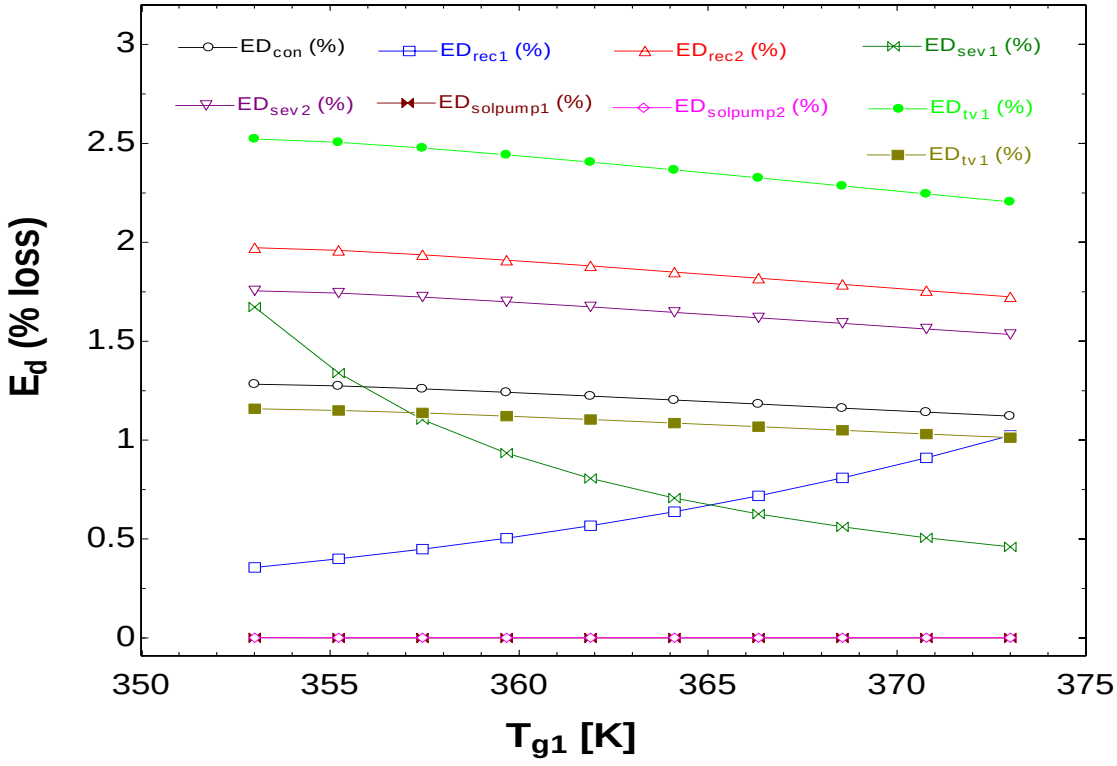

Fig.4.29 Effect of T_{g1} on the exergy destruction in rectifier-1&2, throttle valve-1&2, SEV-1&2, solution pump-1&2 and condenser

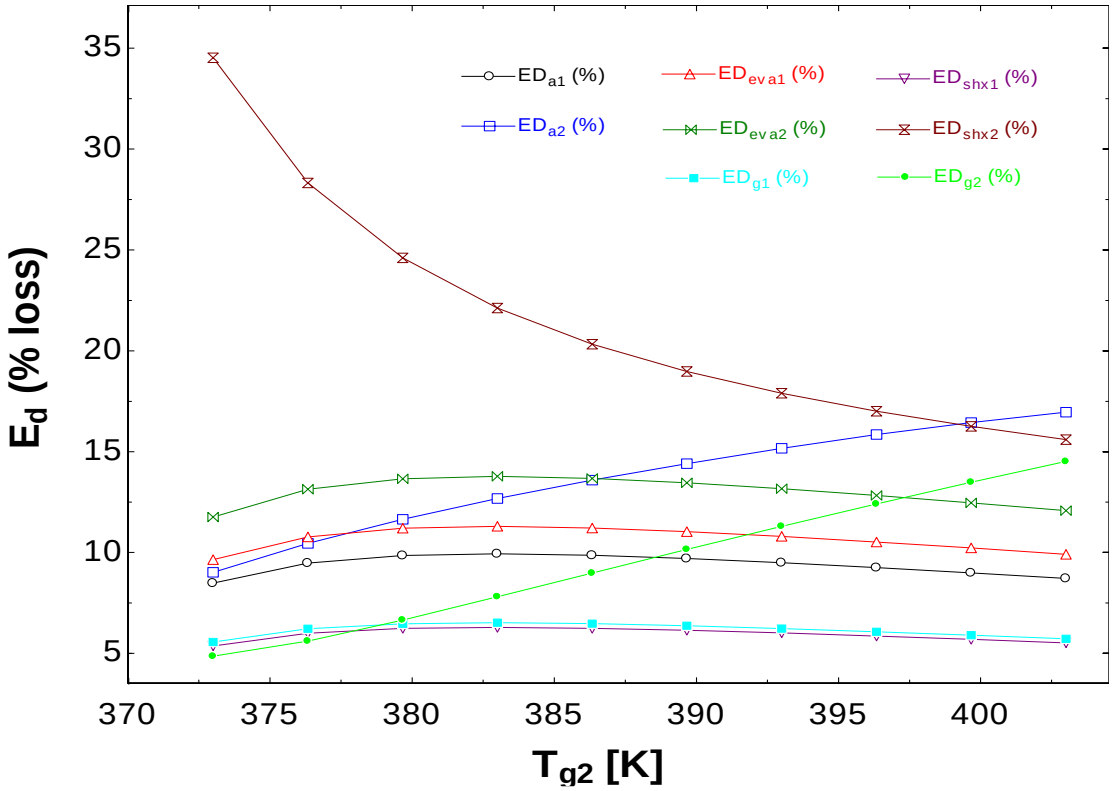

Fig.4.30 Effect of T_{g2} on the exergy destruction in evaporator-1&2, generator-1&2, SHX-1&2

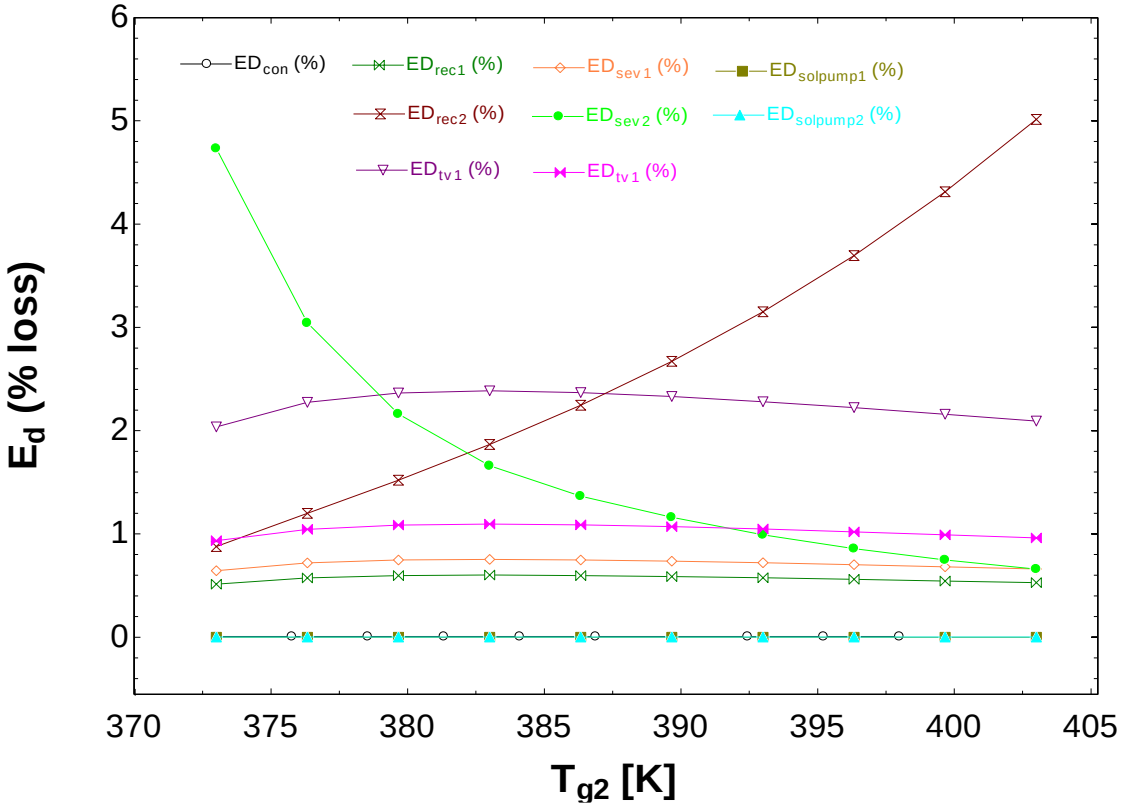

Fig.4.31 Effect of T_{g2} on the exergy destruction in rectifier-1&2, throttle valve-1&2, SEV-1&2, solution pump-1&2 and condenser

Fig.4.28 to fig.4.31 shows the effect of the temperature of generator-1&2 on the percentage exergy destruction in the components of the system. It is observed from the Fig.4.28 & 4.29 that at $T_{g2} = 383°$ K, if the temperature of generator-1 varies from 353° K to 373° K , the exergy destruction (%) in the components of high pressure circuit increases (i.e. 5% in generator-1, 1% rectifier-1 and absorber-1) with slightly decrease in $\dot{E}_D$(%) of other components Similarly it is observed from Fig.4.30 & 4.31, that at $T_{g1} = 363°$ K, if the temperature of generator-2 increases from 373° K to 403° K, exergy destruction in the components of low pressure circuit increases (i.e. 7 % in absorber-2, 10 % in generator-2 and 5 % in rectifier-2) with slightly decrease in exergy destruction of the other components.

The reason for the increase in the exergy destruction (%) in the components of corresponding circuit with increase in temperature of generator-1&2 is that on increasing generator temperature, the ammonia mass fraction of weak solution decreases in that particular circuit, which increases the solution circulation ratio in that circuit due to which circulation losses increases and the effect of increasing the generator temperator also increases absorber temperature so due to this effect the exergy destruction in generator and absorber of the corresponding circuit increases. The increase in exergy destruction of the rectifier is due to the increase in the temperature of the vapour going to the rectifier but the outlet temperature is almost constant so more losses occur in the rectifier of the corresponding circuit. Therefore exergy destruction is increases due to increase in generator temperaature.

The decrease in exergy destruction in other components is due to increase in the total exergy destruction due to increase in the generator temperature but the $\dot{E}_D$ (kW) in the particular component is same so that percentage exergy destruction decreases in the other components because of increase in denominator part.

4.3.6 Effect of ammonia mass fraction (X_r) on the exergetic efficiency of system

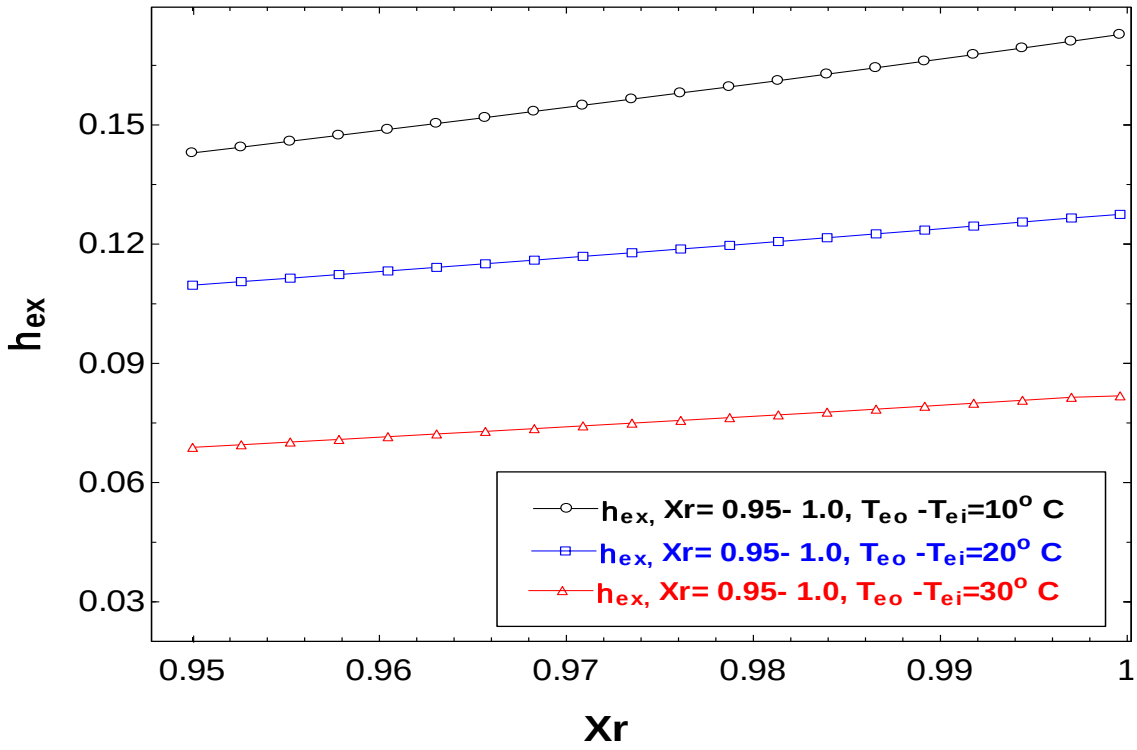

Fig.4.32 variation of η_{ex} with the ammonia mass fraction (X_r) at different temperature difference between evaporator exit and inlet

Fig.4.32 shows the effect of ammonia mass fraction coming (X_r) coming out from rectifier on the exergetic efficiency of the system. The value of η_{ex} increases by 16.66 % at temperature difference in both the evaporator is $10°\,C$ with the increase in the X_r from 0.95 to 0.99963. It is also observed that if the temperature difference between outlet and inlet in both of the evaporator increases, the exergetic efficiency of the cycle decreases. The increase in the η_{ex} is due to the increase in the rate of heat transfer to evaporator at constant mass flow rate of refrigerant mixture because of the increase in the ammonia vapour in the refrigerant mixture which provides useful refrigeration effect which increase exergy of the fuel ($\dot{E}F$) and thus increase in the exergetic efficiency. The decrease in η_{ex} with the increase in $(T_{eo} - T_{ei})$ is due to the increase in evaporator outlet temperature which will increase temperature of absorber which will increase irreversibility as discussed in section 4.3.3 and hence exergetic efficiency of the cycle decreases.

4.3.7 Effect of surrounding temperature (T_o) on the COP of system

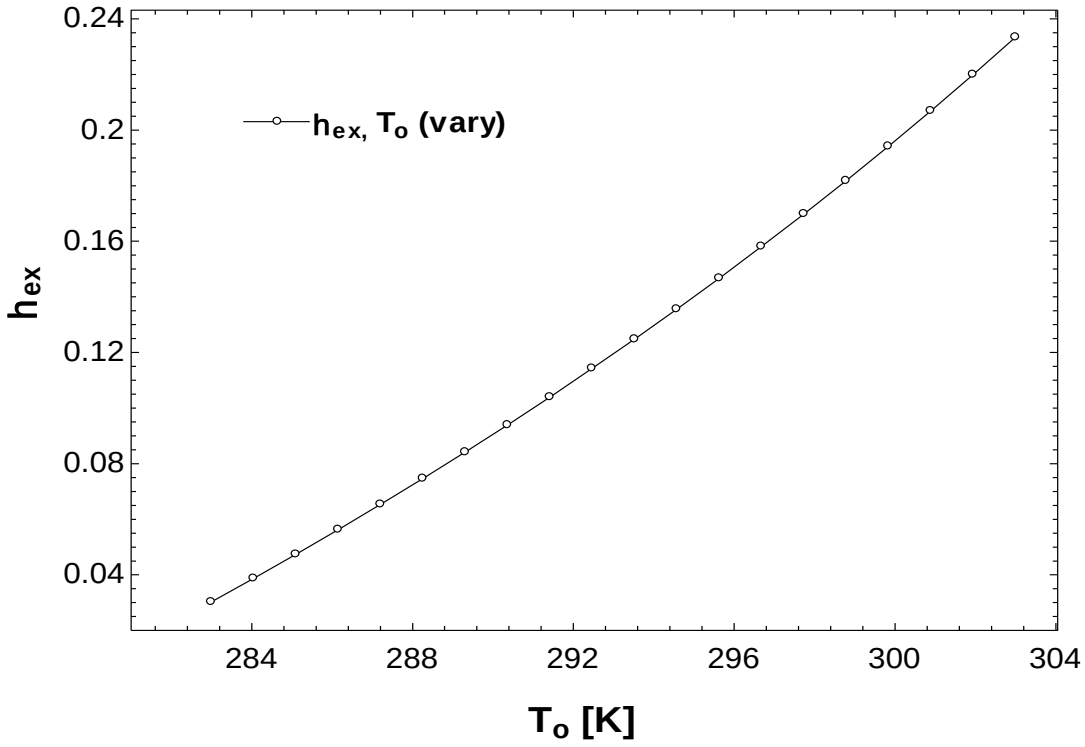

Fig.4.33 variation of η_{ex} with surrounding temperature (T_o)

Fig.4.33 shows the effect of the surrounding temperature (T_o) on the exergetic efficiency of the system. The value of the exergetic efficiency of the cycle increases from 4 % to 22 % when the value of the surrounding temperature (T_o) increases from 283° K to 303° K. this is because of decrease in irreversibility in the generator due to decrease to decrease in finite temperature difference between generator-1, generator-2 and the surrounding but there is also an increase in irreversibility in the evaporator due to increase in temperature difference between evaporator-1 & 2 and surroundings because heat duty in the generator is more than the evaporator so the net effect is the increase in the exergetic efficiency of the cycle.

4.3.8 Effect of generator-1 and generator-2 temperature on the thermal exergy loss of the system

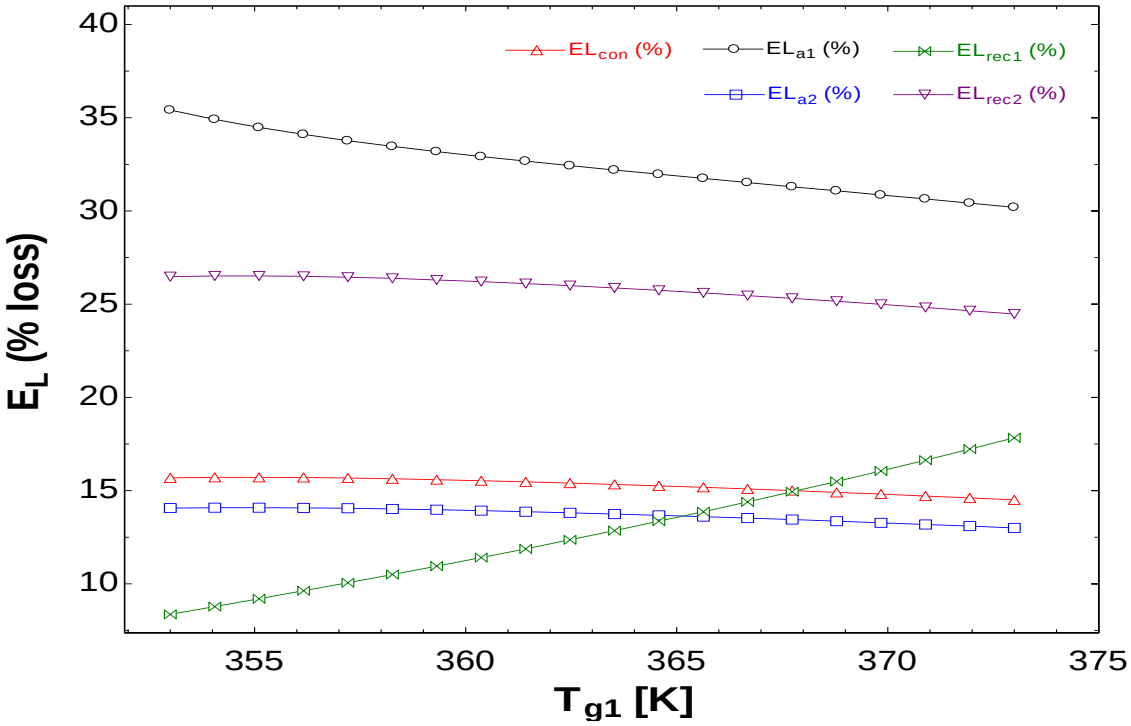

Fig.4.34 Variation of thermal exergy loss with T_{g1} in absorber-1&2, rectifier-1&2 and condenser

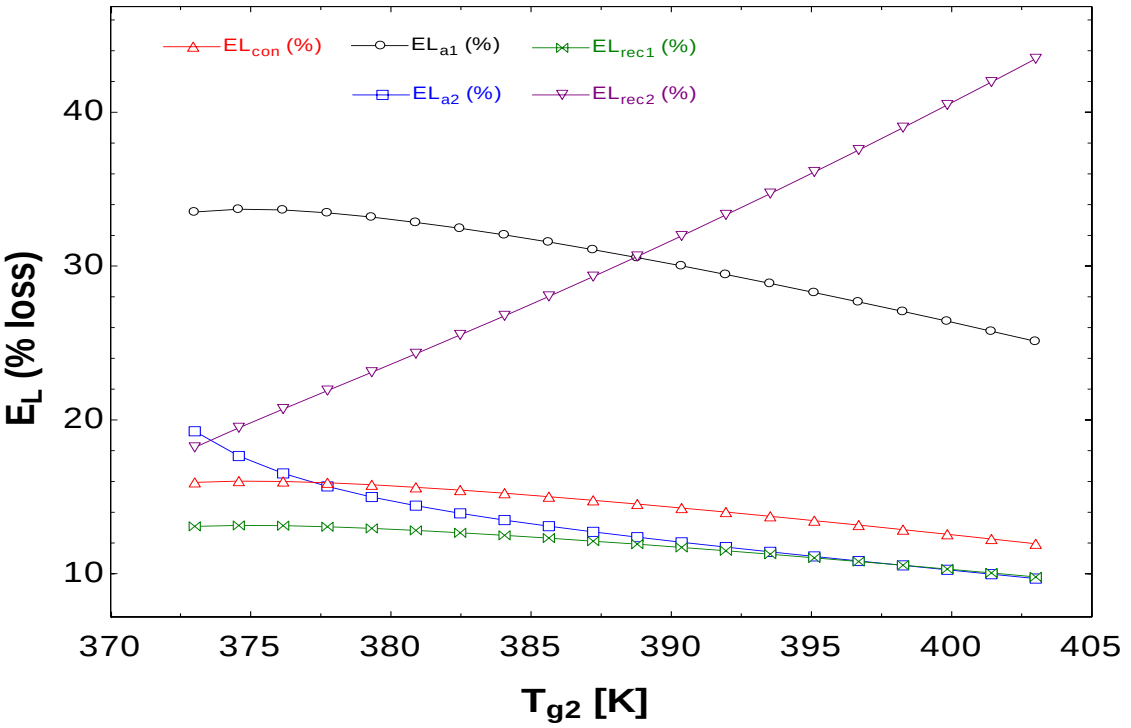

Fig.4.35 Variation of thermal exergy loss with T_{g2} in absorber-1&2, rectifier-1&2 and condenser

Fig.4.34 and 4.35 shows the effect of the generator-1&2 on the thermal exergy loss ($\dot{E}_L$) as defined in equation (61). It is observed that the thermal exergy loss in the rectifier-1 only increases by 11% when temperature in generator-1 increases from 353° K to 373° K without significantly affecting the thermal exergy loss in other components. Similarly the thermal exergy loss in the rectifier-2 increases by 31% when temperature in generator-1 increases from 373° K to 403° K without significantly affecting the thermal exergy loss in other components.

The increase in exergy loss only in the rectifier of corresponding circuit is due to the increase in the amount of ammonia-water vapour going to rectifier because at high temperature, more ammonia-water vapour is generated that is to be rectified by extracting heat out of the rectifier and hence increases thermal exergy destruction. The slightly decrease in thermal exergy loss (%) is due to increase in total thermal exergy destruction as discussed in section 4.3.5.

4.3.9 Effect of temperature of various components on the total loss due to irreversibility in the system

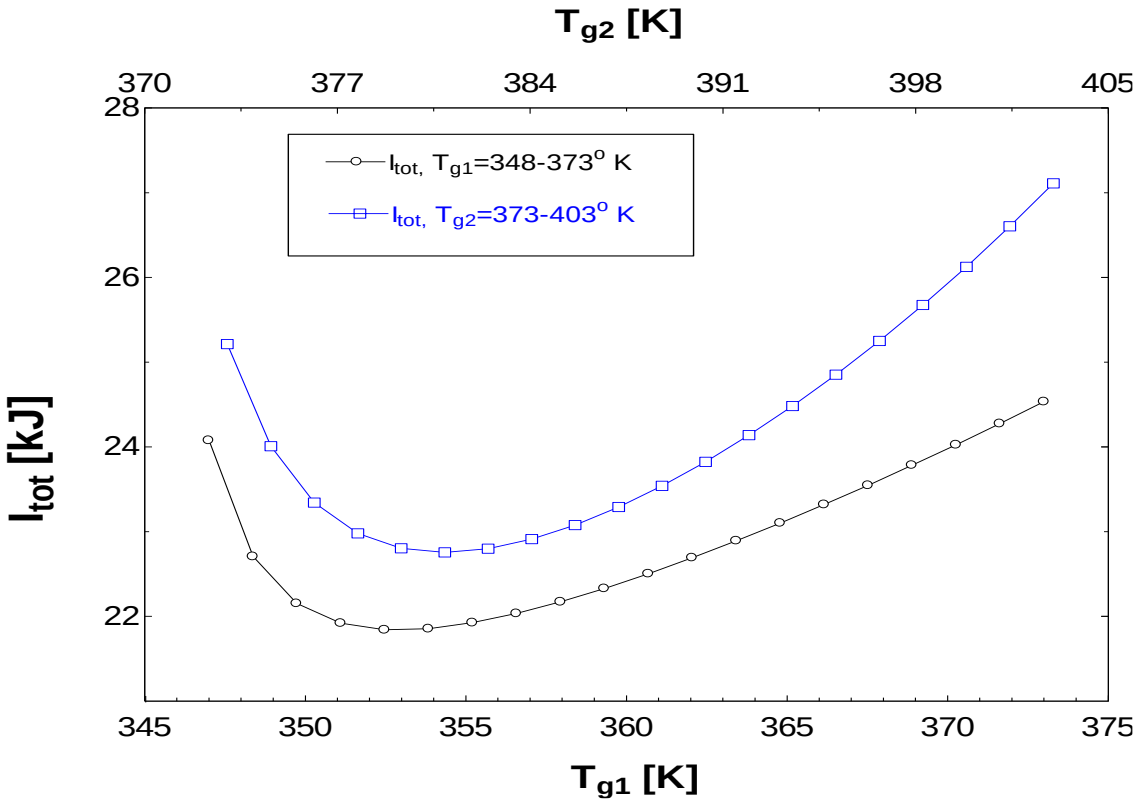

Fig.4.36 Variation of I_{tot} with T_{g1} and T_{g2}

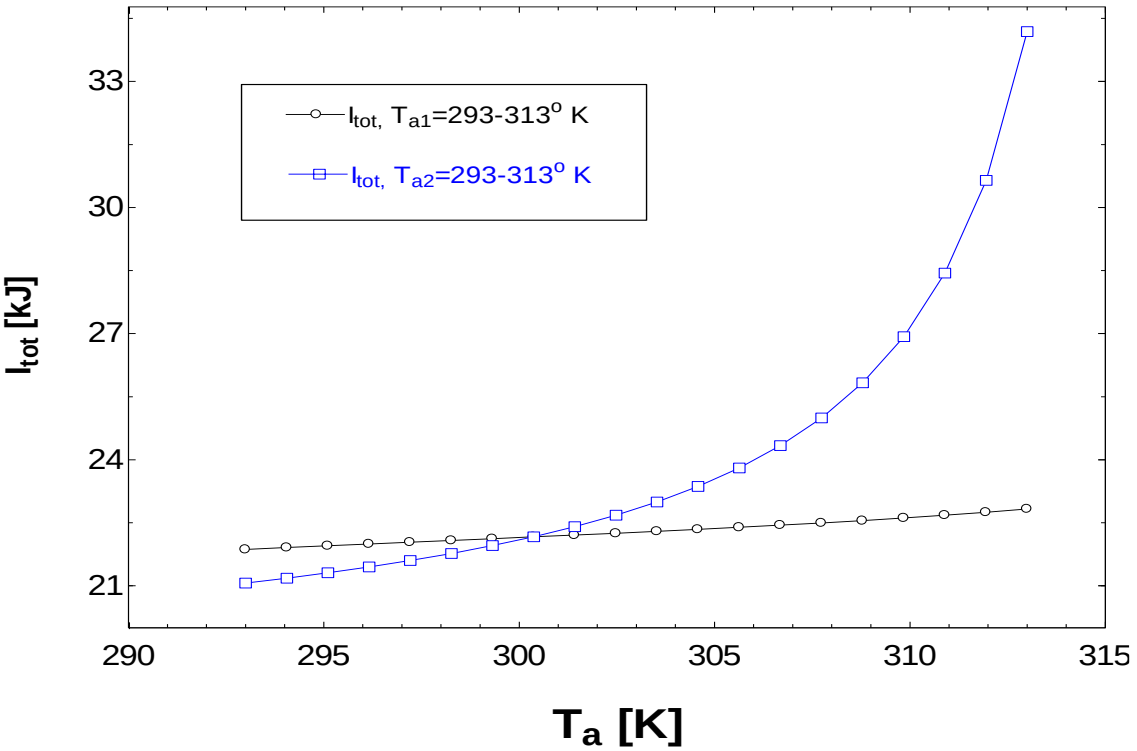

Fig.4.37 Variation of I_{tot} with T_{a1} and T_{a2}

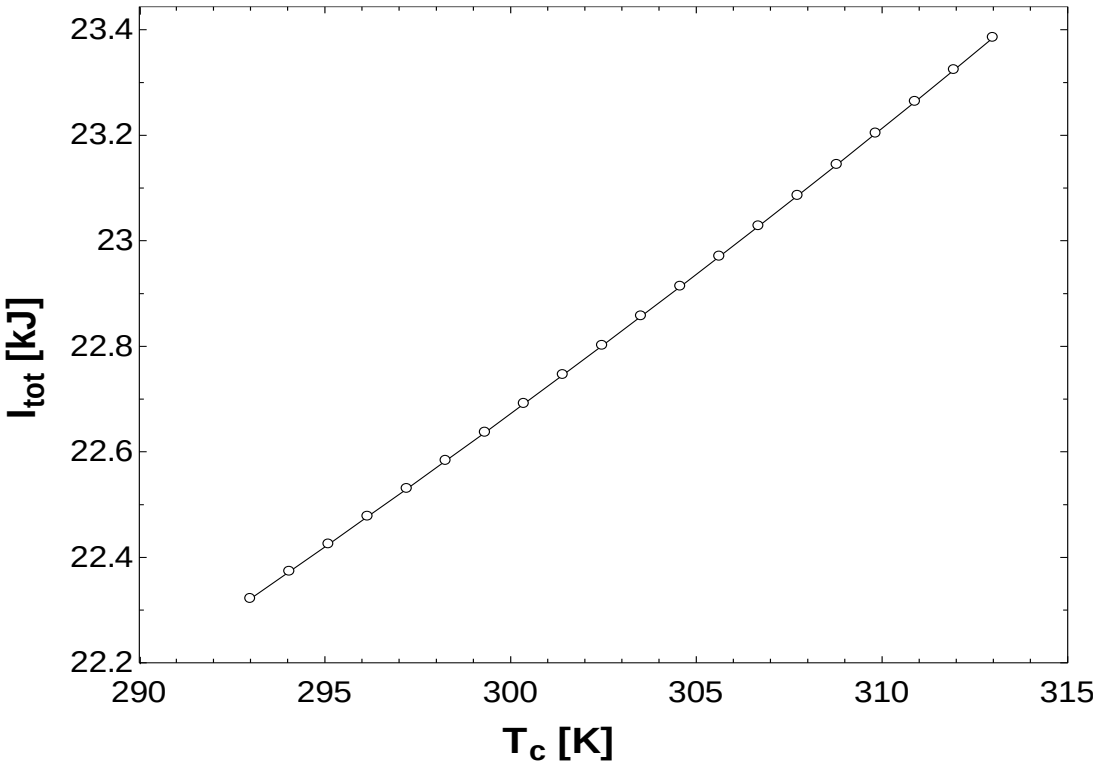

Fig.4.38 Variation of I_{tot} with T_c

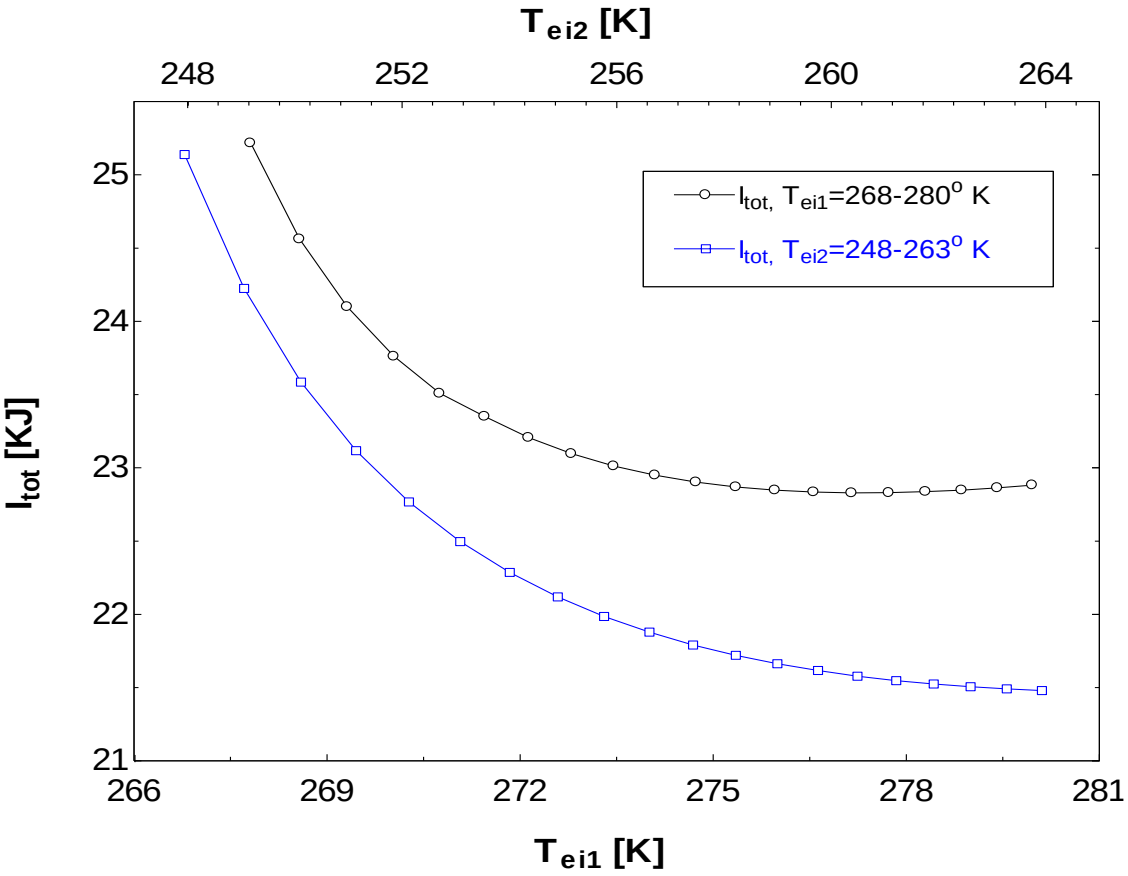

Fig.4.39 Variation of I_{tot} with T_{ei1} and T_{ei2}

Fig.4.36 to 4.39 represents the effects of temperature in various components like generator-1 & 2, absorber-1 & 2, evaporator-1 & 2 and the condenser etc on the total irreversibility of the cycle. The value of loss due to irreversibility in the system decreases initialy and then increases when the temperature in either of the generator increases as shown in fig.4.36. The reason for the same is discussed in detail in the section 4.3.1. The value of loss due to irreversibility in the absorber-1 increases by 4.5 % and 57.14 % when the temperature in either of the absorber varies from 293° K to 313° K. The reason for the same is discussed in detail in section 4.3.3. It is also observed from fig.4.38 that the value of irreversibility loss in the condenser is linearly increases by 4.4 % when the condenser temperature varies from 293° K to 313° K. this is because of increase in corresponding generator pressure with increase in condenser temperature which correspondingly increase generator temperature which increase irreversibility loss as discussed in section 4.3.1. The value of irreversibility loss decreases by 8 % and 14% when the inlet temperature at the evaporator-1 varies from 268° K to 280° K and 248° K to 263° K respectively.

4.3.10 Exergy destruction in components

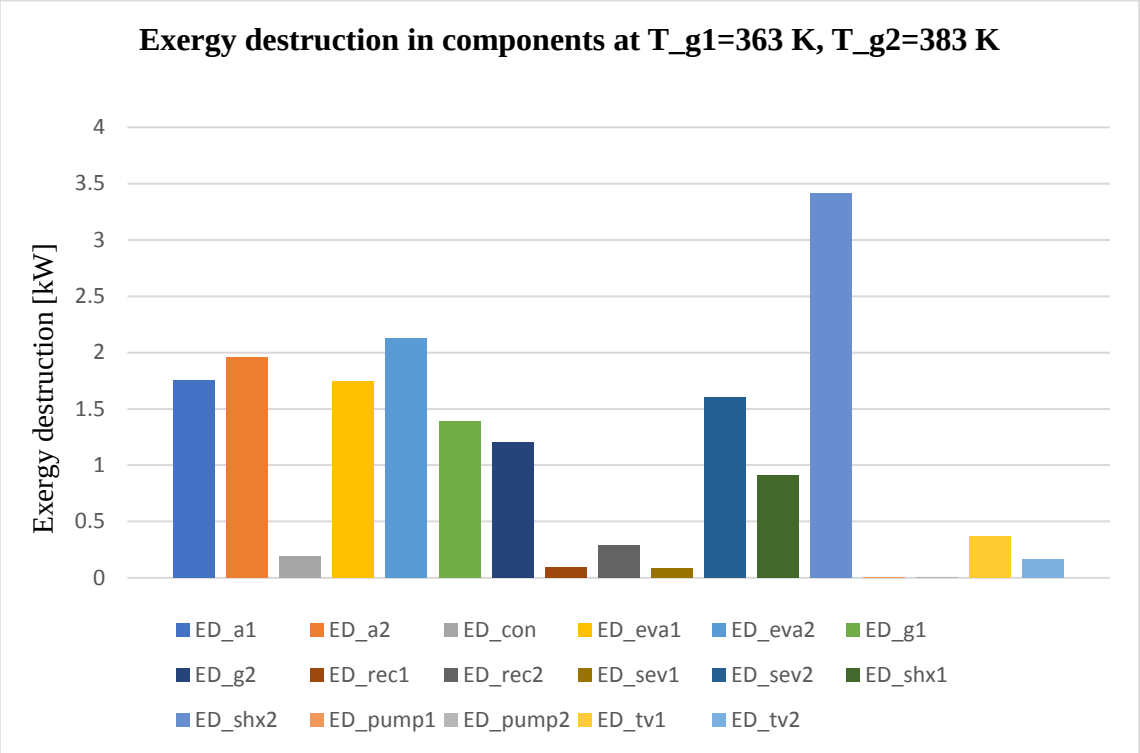

Fig.4.40 Exergy destruction in components at $T_{g1} = 363$ K, $T_{g2} = 383$ K

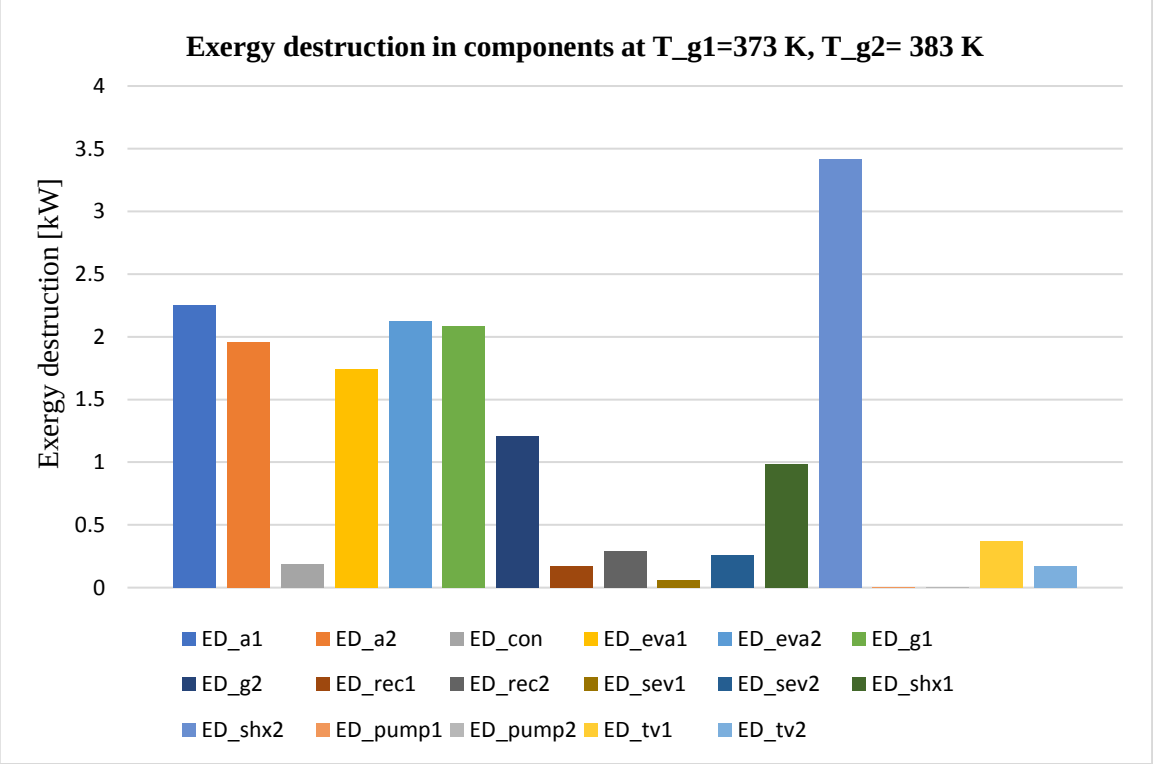

Fig.4.41 Exergy destruction in components at $T_{g1} = 373$ K, $T_{g2} = 383$ K

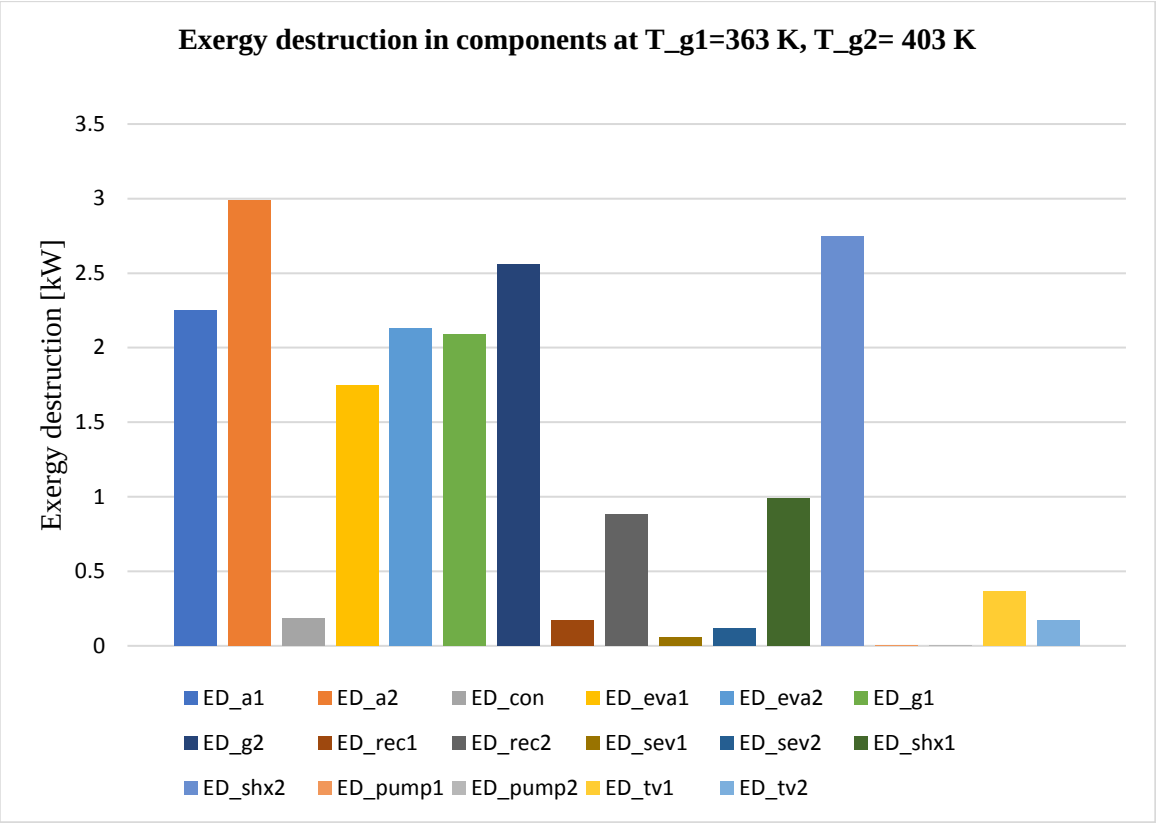

Fig.4.42 Exergy destruction in components at $T_{g1} = 363$ K, $T_{g2} = 403$ K

Fig.4.40 to 4.42 shows the exergy destruction in the components at different temperature conditions. At $T_{g1} = 363$ K, $T_{g2} = 383$ K, the exergy destruction in the components of system shows in Fig.4.40, in which exergy destruction mainly occurs in absorber-1&2, evaporator-1&2, generatoe-1&2 and SHX-1&2, of which exergy destruction in solution heat exchanger '2' is highest. If the temperature of generator-1 increases to 373 K at constant T_{g2} then the exergy destruction in the components of high pressure circuit have been increased not affecting the exergy destruction in the components of low pressure circuit as shown in fig.4.41 similarly if the temperature in the generator-2 increases to 403 K at constant T_{g1}, then the exergy destruction in the low pressure circuit have been increased not affecting the exergy destruction in the components of high pressure circuit as shown in fig.4.42.

The reason for increasing of exergy destruction with increase in temperature of generator is due to the increase in the temperature of corresponding circuit and increasing mass flow rates at constant cooling load which brings more irreversibility in the corresponding circuit therefore exergy destruction in the circuit increases.

4.3.14 Thermal Exergy loss in components

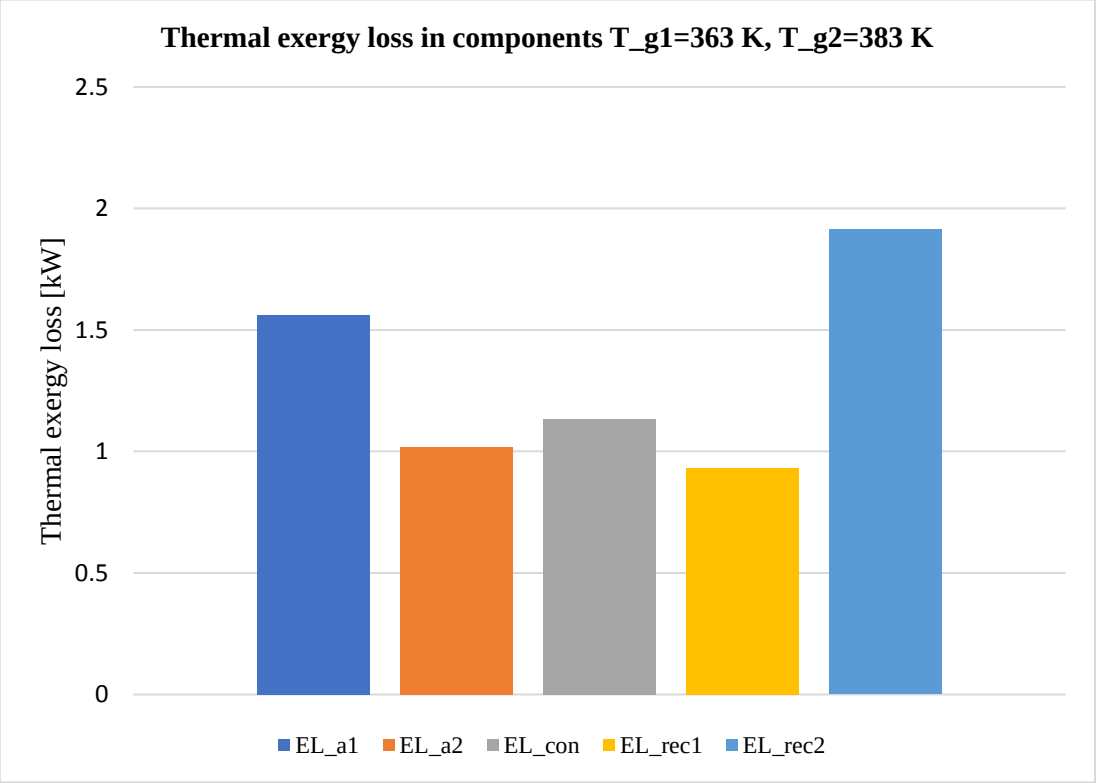

Fig.4.43 Thermal exergy loss in components at $T_{g1} = 363$ K, $T_{g2} = 383$ K

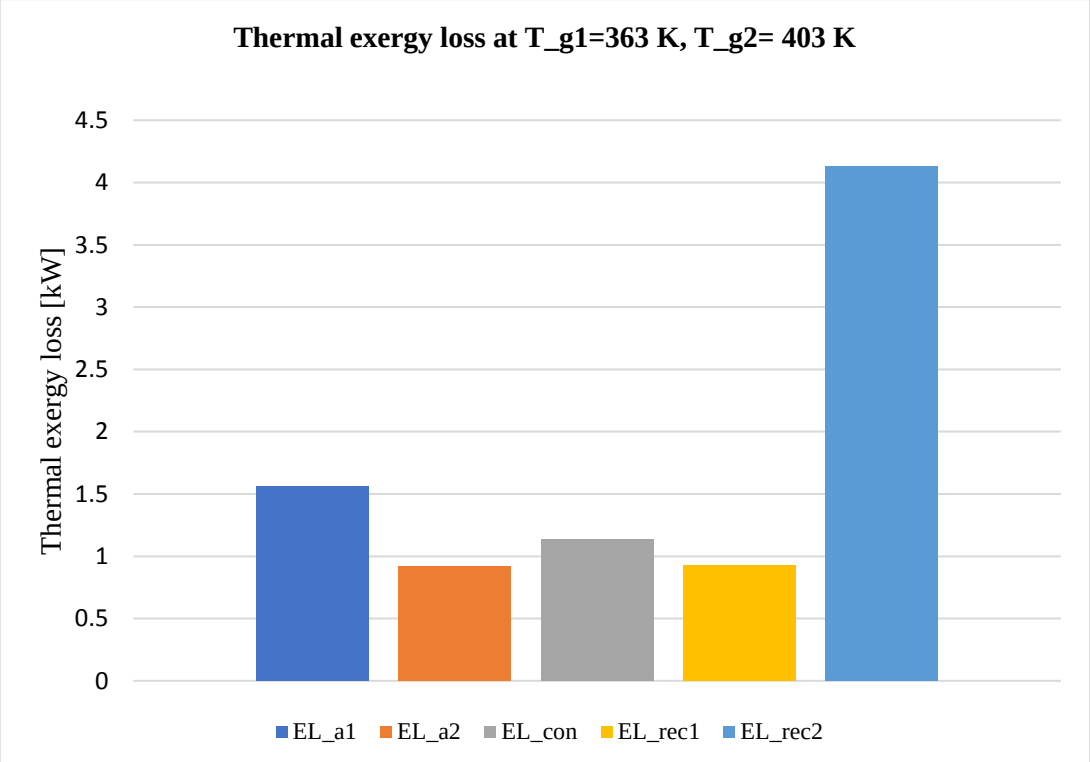

Fig.4.44 Thermal exergy loss in components at $T_{g1} = 363$ K, $T_{g2} = 403$ K

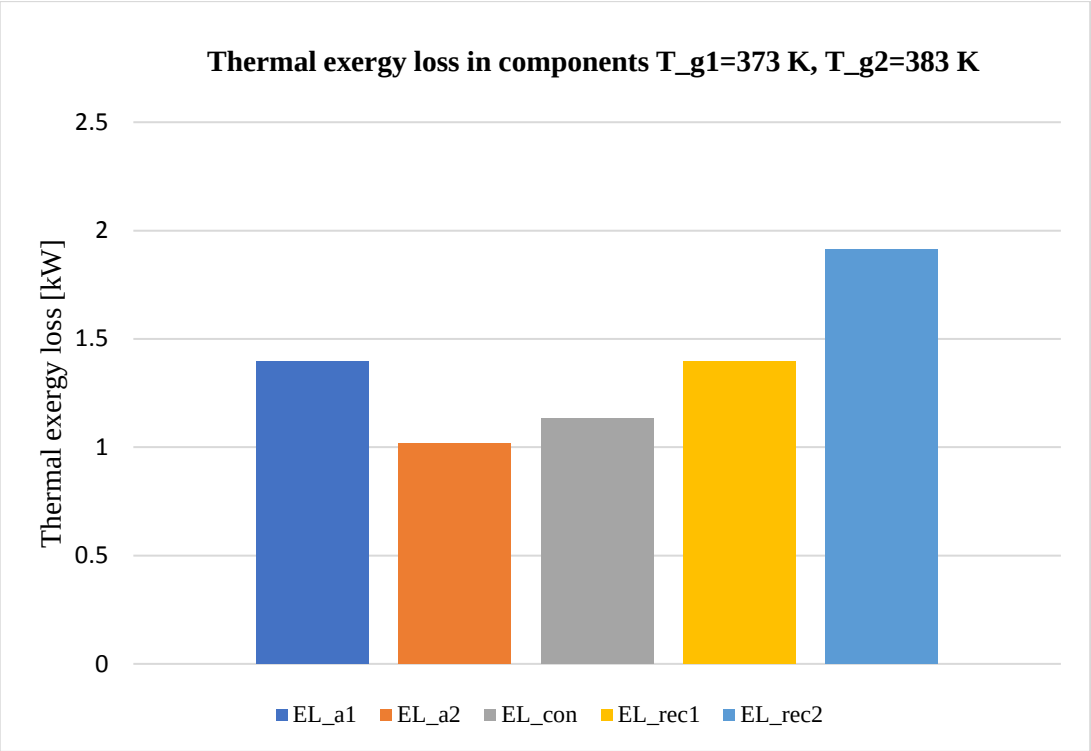

Fig.4.45 Thermal exergy loss in components at $T_{g1} = 373\ K, T_{g2} = 383\ K$

Fig.4.43 to 4.45 shows the thermal exergy loss in the components at different generator-1 & 2 temperature. Thermal exergy loss occurs due to the heat interaction between the components and surrounding which takes place because of temperature difference between the control volume and the surroundings where system boundary does not include immediate surrounding, hence the thermal exergy loss occurs only in absorber-1 & 2, rectifier-1 & 2 and condenser. At optimum conditions of $T_{g1} = 363\ K, T_{g2} = 383\ K$, the thermal exergy loss graph shown in fig. 43, in which thermal exergy loss ($\dot{E}_L$) value is highest in rectifier-2 (1.9 kW) followed by absorber-1 (1.4 kW), condenser (1.1 kW), absorber-2 and recrifier-1. If the temperature of generator-2 increases keeping temperature of generator-1 constant (i.e. at $T_{g1} = 363\ K, T_{g2} = 403\ K$), the $\dot{E}_L$ in rectifier-2 sharply increases to 4.1 kW with negligible effect in the other components as shown in Fig.4.43. This is because of increase in refrigerant mixture containing more water vapours coming out from generator-2 which has to be rectified in rectifier-2, so more heat is rejected out from the rectifier-2 which correspondingly increases thermal exergy loss from the rectifier-2 similarly if the temperature of generator-1 increases keeping temperature of generator-2 constant (i.e. at $T_{g1} = 373\ K, T_{g2} = 383\ K$), the $\dot{E}_L$ in rectifier-1 increases as shown in Fig.4.45.

CHAPTER- 5
CONCLUSIONS AND RECOMMENDATIONS

5.1 Conclusions

A program has been developed in the EES software to predict the performance of double evaporator ammonia-water vapour absorption refrigeration system using energy and exergy analysis. The conclusions drawn from the results are illustrated as below

1. It is observed that the increase in temperature of both the generator increases the COP of the system up to an optimum generator temperature of 90^{o}C in generator-1 and 115^{o}C in generator-2, and with further increase in temperature of both generator the COP of system decreases.
2. Similar trend in the variation of exergetic efficiency with generator-1 and generator-2 temperature is observed as that of COP but the maximum value of exergetic efficiency is obtained at a temperature of 80^{o}C and 105^{o}C in generator-1 and generator-2 respectively.
3. The COP of double evaporator VAR system at constant cooling load of 20 TR (in which 10 TR in each of the evaporator-1 and evaporator-2) is nearly 11.11% greater than simple VARS operated at 20 TR cooling load. It is also shown that the increase in evaporator temperature increases the COP of the system, the conclusion drawn from here is that if cooling load is available at high temperature as well as at low temperature then performance is increased by using two or more evaporator instead of using single evaporator at low temperature.
4. It is also observed that the increase in the temperature of both the absorber i.e. abrorber-1 and absorber-2, the performance of the system decreases and effect of absorber-2 is more on the variation of COP of the system than the absorber-1 and condenser.
5. It is also observed that increase in effectiveness of heat exchanger increases the performance of the system but effect of heat exchanger-2 is more than the heat exchanger-1.
6. It is also observed that the COP of the system increases when ammonia mass fraction coming out from evaporator increases at constant temperature difference

up to 40^{o}C between evaporator outlet and inlet i.e. ($T_{eo} - T_{ei} = 40^{o}$C), with further increase in temperature difference the COP of the system decreases.

7. It is also shown that variation in ammonia mass fraction (X_r) has no affect on the inlet temperature of evaporator but it affects the outlet temperature of evaporator in a manner that outlet temperature decreases when ammonia mass fraction (X_r) increases.
8. The exergy destruction mainly occurs in solution heat exchanger (SHX-2), abrorber-1&2, generator-1&2, evaporator-1&2 of which exergy destruction in the SHX-2 is highest.
9. It is also concluded that the variation in temperature of absorber-2 has the maximum effect on the COP is observed than the temperature in absorber-1 and condenser and the effect of change in the temperature of absorber-1 and condenser is almost same on the COP of system.

5.2 Limitations and recommendations for future work

Following are the limitations of the DE VAR system

1. The addition of extra components in the system increases its cost and complexity.
2. The addition of extra components in the system increases the irreversibility in the system.
3. This model is not successful for commercial purposes so continuous improvement of the design is required to reduce its cost and complexity.
4. The results obtained at specified conditions in this system and valid for certain assumptions considered, outside that conditions the results are not valid.

Since there are some of the limitations of the system but it has been recommended in certain areas where it gives better results which are given below:

- In certain industries which requires cooling load at different temperature for the processing or manufacturing of product, storing of product or raw materials and for comfort of peoples working there requires these types of systems which not only saves additional cost but also use waste heat from the plant to utilise as a input for the system.

REFERENCES

[1] Meng Wang, Tim M. Becker, Bob A. Schouten, Thijs J.H. Vlugt, Carlos A. Infante Ferreira, Ammonia/ionic liquid-based double-effect vapor absorption refrigeration cycles driven by waste heat for cooling in fishing vessels, Energy Conversion and Management 174 (2018) 824–843

[2] Yuanyuan Liang, Shuhong Li, Xiaoyang Yue, Xiaosong Zhang, Analysis of $NH_3-H_2O-LiBr$ absorption refrigeration integrated with an electrodialysis device, Applied Thermal Engineering 115 (2017) 134–140

[3] Vikul Vasudeva, Raja Sekhar Dondapatib, Experimental and Exergy Analysis of Ammonia/Water Absorption System using Ethylene Glycol $[C_2H_4(OH)_2]$ in the Evaporator, Energy Procedia 109 (2017) 401 – 408

[4] Marcello Aprile, Rossano Scoccia, Tommaso Toppi, Marco Guerra, Mario Motta, Modelling and experimental analysis of a GAX NH_3-H_2O gas-driven absorption heat pump, international journal of refrigeration 66 (2016) 145–155

[5] Sumit K. Swarnkar, S. Srinivasa Murthy, Ramesh L. Gardas, G. Venkatarathnam, Performance of a vapour absorption refrigeration system operating with ionic liquid-ammonia combination with water as cosolvent, Applied Thermal Engineering 72 (2014) 250-257

[6] Teng Jia, Enqian Dai, Yanjun Dai, Thermodynamic analysis and optimization of a balanced-type single-stage NH_3-H_2O absorption-resorption heat pump cycle for residential heating application, j. energy 2019.01.002

[7] C.P. Jawahar, B. Raj, R. Saravanan, Thermodynamic studies on NH_3-H_2O absorption cooling system using pinch point approach, international journal of refrigeration 33 (2010) 1377 -1385

[8] I. Horuz, A comparison between NH_3-H_2O and Li-Br & H_2O solution in vapor absorption refrigeration system, Int. comm. Heat mass transfer, vol. 25, No. 5, (1998) 711-721

[9] Tommaso Toppi, Marcello Aprile, Marco Guerra, Mario Motta, Numerical investigation on semi-GAX NH_3-H_2O absorption cycles, international journal of refrigeration 66 (2016) 169–180

[10] Wei Wu, Baolong Wang, Sheng Shang, Wenxing Shi, Xianting Li, Experimental investigation on NH_3-H_2O compression-assisted absorption heat pump (CAHP) for low temperature heating in colder conditions, international journal of refrigeration 67 (2016) 109–124

[11] Dixit, M., Arora, A., & Kaushik, S. C. (2015), Thermodynamic analysis of GAX and hybrid GAX aqua-ammonia vapor absorption refrigeration systems. International Journal of Hydrogen Energy, 40(46), 16256-16265

[12] Arora, A., & Kaushik, S. C. (2009), Theoretical analysis of $LiBr/H_2O$ absorption refrigeration systems. International Journal of Energy Research, 33(15), 1321-1340

[13] Keith E. Herold, Reinhard Radermacher, Sanford A. Klein, Absorption Chillers and heat pumps, CRC press (2016)

[14] Klein S.A., Alvarado F., 2007, Engineering Equation Solver (EES). WI: F-chart software.

[15] Patek, J., & Klomfar, J. (1995). Simple functions for fast calculations of selected thermodynamic properties of the ammonia-water system. International Journal of refrigeration, 18(4), 228-234.